

A DETAILED GRAVITY INVESTIGATION OF
THE KWELLO ANOMALY IN THE NORTH
CENTRAL AREA OF NIGERIA

BY

AKAOL TSA, CASMIR ZANDERS
B.Sc (Hons) MATHEMATICS

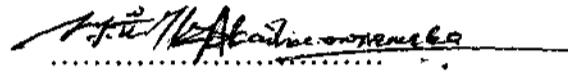
A THESIS SUBMITTED TO THE POSTGRADUATE
SCHOOL, AHMADU BELLO UNIVERSITY, ZARIA
IN PARTIAL FULFILMENT OF THE
REQUIREMENTS FOR THE AWARD OF THE
DEGREE OF MASTER OF SCIENCE, APPLIED
GEOPHYSICS.

DEPARTMENT OF PHYSICS
FACULTY OF SCIENCE
AHMADU BELLO UNIVERSITY, ZARIA
NIGERIA

MAY, 1997

DECLARATION

I hereby declare that, this thesis is an original work carried out by me (the author) under the Supervision of Dr. I.B. Osazuwa and Dr. M.N. Umego. To the best of my knowledge no part thereof has been submitted elsewhere for the award of any degree. The works of others have been duly referenced and acknowledged.

A handwritten signature in black ink, appearing to read 'C. Z. Akaolisa', is written over a horizontal dotted line.

C. Z. AKAOLISA

AUTHOR.

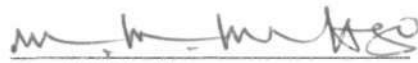
CERTIFICATION

This thesis entitled: A detailed gravity investigation of the Kwello anomaly in the North-central area of Nigeria, By Akaolisa Casmir Zanders, meets the regulations governing the award of the degree of Master of Science, Applied Geophysics of Ahmadu Bello University and is approved for its contribution to knowledge and literary presentation.



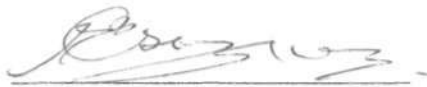
Prof. I.B. Osazuwa
Chairman, Supervisory Committee

14th Sept, 1997
Date



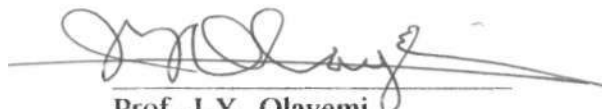
Dr. M.N. Umego
Member, Supervisory Committee

14/9/97
Date



Prof. I.B. Osazuwa
Head of Department

14th Sept. 1997
Date



Prof. J.Y. Olayemi
Dean, Postgraduate School

18/5/98
Date

DEDICATION

This Work is Dedicated to the Helpless

and to

Uchenna, My Pearl

ACKNOWLEDGEMENTS

I thank God Almighty for his guidance, protection and care, and for his help even when the completion of this work seem not possible.

I sincerely thank my Supervisor Prof. I. B. Osazuwa for suggesting the project and without whose patient guidance, assistance and useful suggestions, the completion of this work would not have been possible. His Keen interest in the work and supervision and allowing me use of his personal computer for all my analysis are highly appreciated.

I equally thank Dr. M.N. Umego for his wonderful contributions and suggestions. My profound gratitude goes to Prof. S.B. Ojo, the former Head of Department, for his usual encouragement. Thanks are also due to Mr. Alagbe of the Geology Department who assisted in the rock identification, reading through and making useful comments on the draft of the chapter on Geology.

I owe a debt of gratitude to my Pearl, Uchenna, whose invaluable assistance during this period would forever be remembered. I sincerely thank Mr Julian Ndunelo, S.C.O.A workshop manager, Kaduna, who made the repairs on the field vehicle affordable by me and hence making the field trip possible. Thanks also to the International Programme in the Physical Sciences (IPPS) of Uppsala University Sweden, for the facilities provided to the geophysics group of this department, which made the completion of this work possible, and also for the grants made available to me for the final production of this thesis.

I wish to thank my colleagues especially Mohammed Anka and Salisu Abdullahi and all staff of Physics Department who by one way or the other have contributed in no small way to the success of this work, especially Dr Kangkolo Roland who assisted me with some of the computer programs that I used. Also I thank Peace Nnorom for Wordprocessing the manuscript.

Finally, I thank those whose names could not be mentioned here due to space constraint for their invaluable contributions, I pray that God will continue to bless them abundantly, Amen.

ABSTRACT

A detailed gravity survey of the Kwello area of the Basement Complex of Northwestern Nigeria has been carried out to determine the structure and probable mode of emplacement of the causative body of the Kwello Bouguer gravity anomaly. Two hundred and sixty seven gravity stations were occupied at 2 km intervals using a LaCoste and Romberg Model G gravimeter for relative gravity measurements and two Wallace and Tiernan aneroid altimeters for the elevation determination. Density measurements of two hundred and twenty nine rock samples were carried out.

Results of gravity measurements in the Kwello area show that the area is characterized by negative Bouguer anomaly values ranging in amplitudes from -30 mGal to -58 mGal. Free-air anomalies distributed about a mean of +28 mGal seem to suggest that the area is isostatically compensated. Interpretation of the Bouguer anomaly field shows that the area is characterized by prominent residual anomalies of -8 mGal to +12 mGal amplitude. The residual anomalies were enhanced by the second vertical derivatives and the lithologies with contrasting densities in the area were delineated by the zero contours of the second derivative map. A residual gravity high of +12 mGal amplitude correlate well with mapped schist body in the area, while residual gravity lows are correlated to the granite bodies in the area. A N - Streuding regional anomaly with an E - W gradient of the order of 0.18 mGal/km is obtained from a first order polynomial fitting to an upward continued Bouguer anomaly data.

A $2^{1/2}$ - Dimensional modelling of the residual anomaly reveals that the thickness of the schist vary between 1 to 5 km with inward dipping walls of dips 60° and the

granite bodies have a depth extent of about 6 km with an outward dipping wall of dip 48° . The sharp contacts of the bodies indicate that the contacts are possibly faulted. The general configuration of the modelled bodies and the pattern of the gravity anomalies suggest that the Older Granites make sharp contact with the country rocks and were magmatically emplaced into the Basement Complex.

The Bouguer gravity high over the schists in the Kwello area have a maximum amplitude of only -30 mGal. These values are thought to be too low to indicate the existence of more mafic rocks at depth. The schists in the Kwello area are therefore believed to have evolved in an ensialic environment.

TABLE OF CONTENTS

	<u>Page</u>
DECLARATION	ii
CERTIFICATION	iii
DEDICATION	iv
ACKNOWLEDGEMENT	v
ABSTRACT	vii
TABLE OF CONTENTS	ix
LIST OF TABLES	xii
LIST OF FIGURES	xiii
ABBREVIATIONS	xv
<u>CHAPTER ONE</u>	
1.0 INTRODUCTION	1
1.1 General	1
1.2 Previous Work in the Area	3
1.3 Objective and Scope	3
1.4 Data Collection	4
<u>CHAPTER TWO</u>	
2.0 GEOLOGY OF THE STUDY AREA	6
2.1 General Geology	6
2.2 Rock Types in the Study Area	10
2.2.1 Migmatites and Gneiss Complex	10
2.2.2 Quartzites	11

	<u>Page</u>
2.2.3 Granites and Granodiorites	12
2.2.4 Schist	12
2.3 Structural Aspects	14
2.3.1 Rock Contacts	14
2.3.2 Folding	14
2.3.3 Fractures	15
2.4 Economic Geology and Mineralogy	16

CHAPTER THREE

3.0 FIELD PROCEDURES, DATA REDUCTIONS AND CORRECTIONS	17
3.1 General Work Plan	17
3.1.1 Instrumentation	17
3.2 Field Work	21
3.3 Data Reduction	24
3.3.1 Altimeter Data	24
3.3.2 Gravity Data	24
3.4 Sources of Error in the Bouguer Anomaly	28
3.5 Density Determination	30
3.5.1 Densities Acceptable for Models	36

CHAPTER FOUR

4.0 GRAVITY FIELD DETERMINATION AND MAP PRODUCTION	37
4.1 Gravity Field	37
4.1.1 Introduction	37

	<u>Page</u>
4.1.2 Upward Continuation Field	38
4.1.3 Downward Continuation Field	41
4.1.4 Second Vertical Derivatives	42
4.2 Anomaly Map Production	44
4.2.1 Gridding	44
4.2.2 Bouguer Anomaly Map	44
4.2.3 Free - Air Anomaly And Topographic Maps	47
4.2.4 The Regional Anomaly Field	47
4.2.5 The Residual Anomaly Field	53

CHAPTER FIVE

5.0 INTERPRETATION OF BOUGUER AND RESIDUAL ANOMALIES 56

5.1 Introduction	56
5.2 Qualitative Interpretation	56
5.2.1 The Bouguer Anomaly Map	56
5.2.2 The Free - Air Anomaly Field	58
5.2.3 Residual Anomaly Field	59
5.2.4 The Upward Continuation Field	61
5.2.5 The Downward Continuation Field	61
5.2.6 The Second Vertical Derivative Field	70
5.3 Quantitative Interpretation of the Residual Anomalies	70
5.3.1 Profile A - A'	73

	Page
5.3.2 Profile B - B'	79
5.3.3 Profile C - C'	82
5.3.4 Profile D - D'	86
 <u>CHAPTER SIX</u>	
6.0 CONCLUSION	90
6.1 General Discussions	90
6.1.1 The Schists	90
6.1.2 The Granites	91
6.2 Summary of Results and Conclusions	93
6.3 Recommendations	94
REFERENCES	96

LIST OF TABLES

	Page
Table 2.1	Sequence of Events in the Basement Complex 8
Table 2.2	General Chronological Sequence of Rock Types in the Study Area 10
Table 3.1	Summary of Rock Densities in Survey Area Based on Laboratory Measurements 32

LIST OF FIGURES

	<u>Page</u>
Fig 1.1	Simplified Geological Map of Nigeria Showing The Study Area. 2
Fig 2.1	Geological Map of Kwello Area 7
Fig 3.1	Altimeter Drift Curves 19
Fig 3.2	Gravimeter Drift Curves 20
Fig 3.3	Station Distribution Map 22
Fig 3.4	Histograms of Rock Densities Based on Laboratory Measurements 33
Fig 3.5	Histograms of Rock Densities Based on Laboratory Measurements 34
Fig 4.1	Grid Superimposed on Data Points 45
Fig 4.2	Bouguer Anomaly Map of Kwello Area 46
Fig 4.3	Free-air Anomaly Map of Kwello Area 48
Fig 4.4	Contour Map of Observed Elevation in the Study Area 49
Fig 4.5	Regional Anomaly of Kwello 51
Fig 4.6	Regional Anomaly of Kwello Area from Upward Continued Data 52
Fig 4.7	Residual Anomaly of Kwello Area 54
Fig 5.1	Bouguer Anomaly Map of Kwello Area Superimposed over the Geologic Map 57
Fig 5.2	Residual Anomaly Map of Kwello Superimposed over the Geologic Map 60

	<u>Page</u>
Fig 5.3	Bouguer Anomaly Upward Continued By 0.5 Grid Units 62
Fig 5.4	Bouguer Anomaly Upward Continued By 1.0 Grid Units 63
Fig 5.5	Bouguer Anomaly Upward Continued By 1.5 Grid Units 64
Fig 5.6	Bouguer Anomaly Upward Continued By 2.0 Grid Units 65
Fig 5.7	Bouguer Anomaly Upward Continued By 2.5 Grid Units 66
Fig 5.8	Bouguer Anomaly Upward Continued By 3.0 Grid Units 67
Fig 5.9	Bouguer Anomaly Downward Continued By 0.5 Grid Units 68
Fig 5.10	Bouguer Anomaly Downward Continued By 1.0 Grid Units 69
Fig 5.11	The Second Vertical Derivative Map (General) 71
Fig 5.12	The Second Vertical Derivative Map (Zero Contours) 72
Fig 5.13	Bouguer, Regional and Residual Anomalies along profiles A-A' and B-B' 74
Fig 5.14	Bouguer Anomaly, First Regional Field and the corresponding Residual Anomalies along profile C-C' 75
Fig 5.15	Bouguer Anomaly, Second Regional Field and the corresponding Residual Anomalies along profile D-D' 76
Fig 5.16	2½-Dimensional Model of Profile A-A' assuming the intrusive granite body is of magmatic origin 77
Fig 5.17	2½-Dimensional Model of Profile A-A' assuming the intrusive granite body evolved through the process of granitization 78
Fig 5.18	2½-Dimensional Model of Profile B-B' without a compensating granitic body 80

	<u>Page</u>
Fig 5.19	2½-Dimensional Model of Profile B-B' with a compensating granitic body 81
Fig 5.20	2½-Dimensional Model of Profile C-C' 83
Fig 5.21	2½-Dimensional Model of Profile C-C' based on the modified regional fit 84
Fig 5.22	2½-Dimensional Model of Profile D-D' 87
Fig 5.23	2½-Dimensional Model of Profile D-D' based on the modified regional fit 88

ABBREVIATIONS

m	meter
km	kilometer
N	North
S	South
NE	Northeast
NW	Northwest
SE	Southeast
SW	Southwest
SSW	Southsouthwest
NNE	Northnortheast
kg	kilogram
G.S.N.	Geological Survey of Nigeria
m.y.a.	Million years ago
m.s.l.	Mean Sea Level

CHAPTER ONE

1.0 INTRODUCTION

1.1 GENERAL

The area covered by this survey lies between latitudes 10°56'N and 11°32'N and longitudes 6°42'E and 7°30'E, and covers an area of about 5935.41 km² (Figure 1.1) On a scale of 1:100,000, it forms parts of sheets 100 (kwiambana), 101 (Maska), 122 (Kushaka) and 123 (Kaduna). The area falls within the aridic savanna climatic belt of Northern Nigeria where the rainfall is between the months of April and September with a mean annual precipitation varying from 1000 to 1250 mm. The mean annual temperature is 27°C but during the harmattan period of November through January, temperatures can fall as low as about 13°C. The months of February through April are usually very hot. Weathering processes throughout the year are very intense and the soils are generally sandy. The drainage pattern is dendritic while the height range is 568 to 711 m above sea level.

The area became of interest when an anomalous gravity high of amplitude ranging from -40 mGal to -30 mGal was observed from a regional gravity survey of Kaduna and Katsina states which was carried out and reported by Osazuwa *et al* (1994). A follow-up detailed gravity survey and interpretation became necessary and hence the need for this project. This survey is equally of some significance since virtually no detailed geophysical work has been done in the area despite the fact that the area is often associated with gold mineralization.

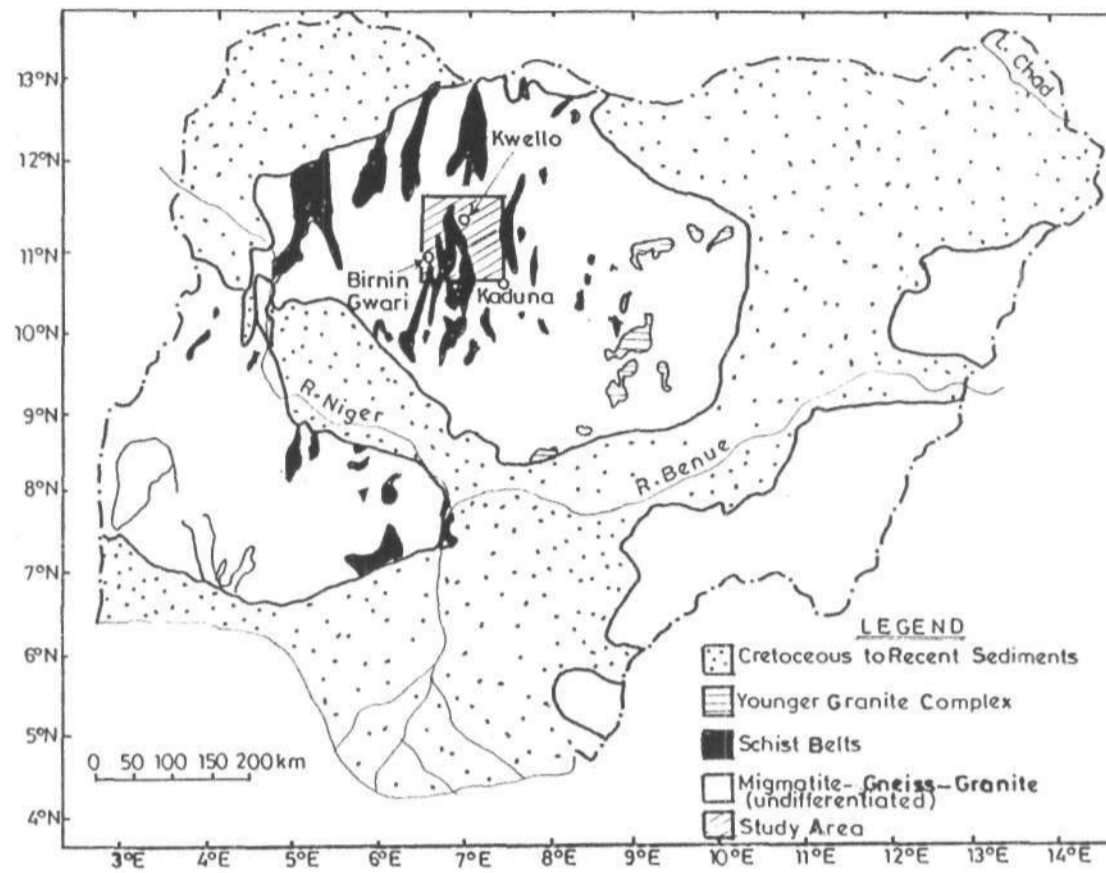


FIGURE.11: SIMPLIFIED GEOLOGICAL MAP OF NIGERIA SHOWING THE STUDY AREA

1.2 PREVIOUS WORK IN THE AREA

The most important geophysical work in the survey area was the regional gravity survey of Kaduna and Katsina states carried out by Osazuwa et al (1994). The region is characterized by Bouguer gravity highs (referred to as Kwello anomaly) with relative amplitudes ranging between -56 mGal to -30 mGal. A gravity survey carried out by Udensi (1984) in the south of the area around Minna, revealed a prominent residual gravity low of -21 mGal relative to a NE - SW trending regional anomaly. Three dimensional modelling of the residual gravity indicates that the Older Granite suite extends to a depth of 5 km and that the walls of the suite may be inward dipping.

Ananaba (1983) carried out a gravity survey along two profiles, one from Kontagora to Yelwa and the other from northern end of the Kainji lake to a distance of 52 km in the northeast direction. The survey suggests that the area had possibly been subjected to about 4km tectonic uplift of the mantle in response to isostasy with consequent thinning of the crust and also revealed the existence of a major gravity high corresponding to an area where gold mineralization is being suspected by the Geological Survey of Nigeria. Ananaba (1983) proposed that a more detailed ground geophysical study be carried out in the area.

1.3 OBJECTIVE AND SCOPE

The present survey is designed to be a follow-up to the regional gravity survey of Kaduna and Katsina States, (Osazuwa *et al*, 1994). The main objectives of this survey are:

- (i) To determine the lateral and depth extent of the causative body of the kwello anomaly.

- (ii) To infer any other subsurface structures within the survey area.
- (iii) To obtain information on the structural relationship between the schists and the granitic intrusion.
- (iv) To investigate and propose a mode of emplacement for the intrusions.

1.4 DATA COLLECTION

The field work was carried out in May 1995. An additional one week field trip was undertaken in November 1995 mainly to fill up the gaps with scanty field data, and also to collect rock samples. Two hundred and sixty seven gravity stations at 2 km, and occasionally 1 km intervals, were established on available motorable roads and tracks in the area. In order to ensure a standard reference for this survey, all the observed gravity values were tied to the Primary Gravity Network for Nigeria base station number 101802 (GMSC 9) at Government Secondary School, Funtua. The base, which was established by Osazuwa (1985) has an absolute gravity value of 978048.326 ± 0.001 mGal.

In order to ensure an absolute precision of 0.01 mGal in the field measurements, a LaCoste and Romberg gravimeter was used. Besides the gravimeter is noted for its ruggedness and low drift rate during field observations.

The gravity method of investigation was chosen for this survey firstly, because the subsurface shape of structures can be readily determined from the gravity anomalies they produce if the density contrast between the structures and their host rocks is known. Secondly, the survey area is fairly large, about 6000 km² and the gravity method lends itself as one of the cheap methods for covering large areas.

The seismic method was not used in this work due to the huge cost involved and non-availability of the seismic equipment.

CHAPTER TWO

2.0 GEOLOGY OF THE STUDY AREA

2.1 GENERAL GEOLOGY

The survey area Figure 2.1 is underlain by rocks of the Basement Complex of Northern Nigeria which was first described by Falconer (1911). The Nigerian Basement Complex form a part of the Pan African Mobile Belt and lies to the east of the West African Cratons and South of Tuareg Shield. Unlike the Cratons, (example the Taoudeni Basin), which are areas of high geolo-gical stability unaffected by the Pan African events, the Basement Complex within the Pan African Mobile Belts are areas affected by Tectono-Metamorphic and orogenic movement during the Pan-African age (Dallameyer *et al.*,1991). In the North - central part of Nigeria, the basement is intruded by the Mesozoic to Cenozoic calc-alkaline ring complexes consisting mainly of young granitic and volcanic rocks. The sequence of events that gave rise to the present Basement Complex can be summarized in Table 2.1.

Rahaman (1988), Ajibade (1976) and McCurry (1976) have classified the rocks of the Basement Complex of Northern Nigeria. Rahaman (1988) grouped the rocks into six major types viz:

- i) Migmatites - gneiss - quartzite complex.
- ii) Slightly migmatized to non - migmatized meta-sedimentary and meta-igneous rocks which are often referred to as Younger Metasediments, Schist Belts (McCurry, 1976) or Newer Metasediments (Oyawoye 1964).
- iii) Charnockitic, gabbroic and dioritic rocks.

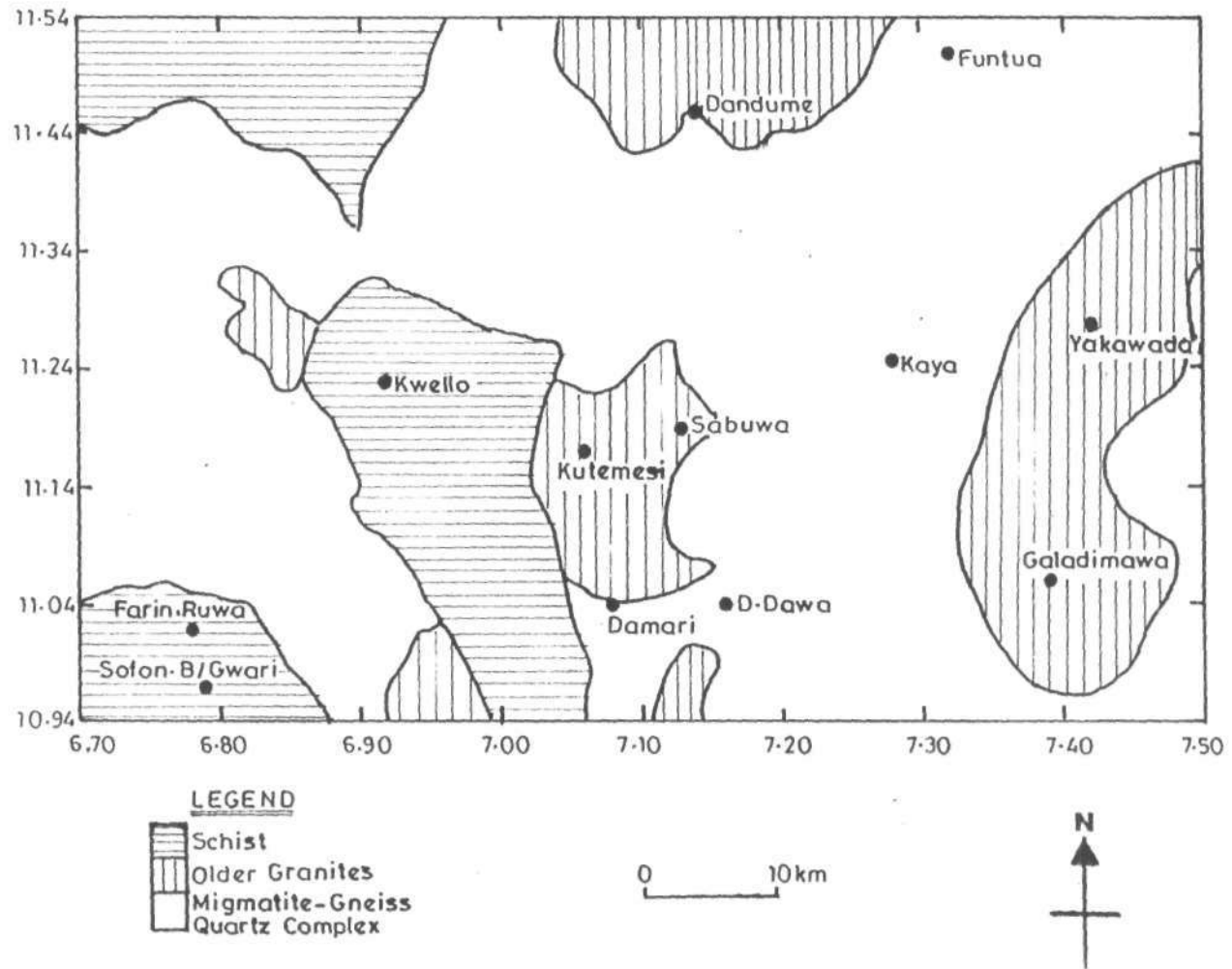


FIGURE.2.1:GEOLOGICAL MAP OF KWELLO AREA (From Geol map of Nig. 1984 with more information from Adekoya, 1988, and G.S.N. Kaduna)

Table 2.1: *Sequence of Events of the Basement Complex: (After Grant et al., 1969)*

AGE	STRATIGRAPHIC CLASSIFICATION	ACTIVITY
500±40 m.y.a	Mid-Cambrian	Uplift cooling, fracturing, faulting and high level inorganic activity
540-650 m.y.a	Lower-Cambrian	Granite Intrusion and Aplite development.
650-850 m.y.a	Pan-African	Orogenic deformation, Metamorphism Migmatization and Reactivation of existing rocks.
800-1000 m.y.a	Katagan	Geosynclinal deposition and Intrusion of Hypersthene bearing rocks.
1900±250 m.y.a	Eburnean	Granite Intrusion, Orogenesis, Folding Metamorphism and Reactivation of Pre-existing rocks.
2500 > 2800 m.y.a	Birimian	Initiation of crustal forming processes. Geosynclinal deposition, Crustal growth by sedimentation and Orogenesis

- iv) Members of the Older granite suite which include both the migmatite gneiss complex and the schist belts.
- v) Metamorphosed to unmetamorphosed calc-alkaline volcanics and hypabyssal rocks [McCurry 1976, McCurry and Wright, 1971].
- vi) Unmetamorphosed dolerite dyke, basic dykes and syenite dykes etc.

According to Rahaman (1988) the first group is the most widespread and occupies about 30% of total surface area of Nigeria. It is a heterogenous rock group and comprises largely of migmatitic and granitic gneisses, basic schists and gneisses and relics of metasedimentary calcareous quartzitic and granitic rocks. The gneisses were

considered to be of a sedimentary origin (Rahaman, 1988). The slightly migmatized to non-migmatized meta-sedimentary and meta-igneous rocks constitute the schist - belts of Nigeria. They show lithologic similarities to schists belts from other parts of the world (Anhausseuer *et al*, 1969) which are known to harbour important economic mineral deposits.

The rocks are the result of at least two major orogenic cycles (Wright and McCurry, 1971) which correspond to the Birimian and the Pan-African (Grant *et al*, 1969). The first deformation is characterized by intense deformation and isoclinal folding was accompanied by regional metamorphism, which was further followed by extensive migmatization. The second deformation, which is referred to as Pan-African Orogeny, was accompanied by a regional metamorphism, migmatization and extensive granitization and gneissification which produced potassic syntectonic granites and homogeneous gneisses (Abaa, 1983). Late tectonic emplacement of granites and granodiorites and associated contact metamorphism accompanied the end stages of this deformation. The end of the orogeny was marked by cooling, faulting and fracturing (Jacobson *et al*, 1963). Other rock types are mainly feldspathic quartzites, schists, basic and calcareous rocks (Abaa, 1983).

The generalized chronological sequence of the various rock types found in the Nigerian Basement Complex is shown in Table 2.2.

the main feldspar appears to be plagioclase while biotite and hornblende are in greater quantity than the felsic minerals (McCurry, 1970). The gradual change from gneiss to migmatite is very subtle and units cannot be separated on geological maps. The migmatites include rocks of varying lithology, texture and structure showing differing degrees of granitisation and migmatisation. Truswell and Cope (1963) distinguished between embrechitic migmatites, in which structural features of the original crystalline rocks are wholly or partly preserved, and anatectic migmatites in which original structures have been nearly or completely obliterated so that these rocks approach granite in composition.

2.2.2 Quartzites

These occur as elongated bodies which may sometimes be of several kilometers long before appearing to wedge out or disappear under superficial cover (McCurry, 1970). They are classified into massive pseudo-conglomerates and schistose quartzite. They are closely associated and difficult to be separated into different units. They are interbedded with biotite gneiss and migmatites. Marble have been reportedly found to be interbedded with quartzites and sillemantite is found in some places surrounded by some quartzites.

Quartzites are more resistant to weathering and as such, they form well marked ridges in morphology and they usually trend north-south or northeast-southwest. The rocks are brownish and whitish but in some places fragments of darker material are present. The minerals present are muscovite, iron oxide and tourmaline, (McCurry, 1970).

2.2.3 Granites and Granodiorites

These rock types have been through at least two tectonometamorphic cycles (Eburnean orogeny and Pan-African Orogeny) and subsequent metamorphism, migmatization and granitization which has extensively modified the original rocks so that they generally occur as relict raft and xenoliths in migmatites and granites.

The granite and granodiorites occur in the form of elliptical plutons, inselbergs and whalebacks. The granite types based on texture are Coarse porphyritic granites, medium-coarse grained granites and equiangular fine-medium grained granites. The granodiorites are generally medium to coarse grained with a gneissose texture. Some of the granites exhibit some flow structures and contain rotated xenoliths indicating some movement of the granitic material (Webb, 1972).

2.2.4 Schists

Schists constitute a fairly large part of the study area and form north-south trending belts. They are low grade metamorphic rocks underlain by pre-Pan-African basement of gneisses and migmatites. The three main schists occurring are Muscovites, Garnet-mica schists or Phyllites and Quartz-biotite schists, interbedded with thin quartzites (McCurry 1970). There also exist carbonaceous schists. The garnet-mica schists are

extensive and characterized by clear mineralogical binding involving alternation of mafic and quartzo-feldspatic mineral. McCurry (1970), Oyawoye (1964) and McCurry (1976) had earlier suggested that the schists are restricted to the west of the longitude through Kaduna and 8°E respectively. However, recent mappings have revealed significant occurrences of schists further east (Okezie 1974, Adegoke 1979, and Rahaman *et al.*, 1981).

The schists belts are composed predominantly of pelitic - semipelitic rocks, psammites, polymict conglomerates, calcareous rocks and mafic to ultramafic igneous rocks. Turner (1964) and Ajibade (1980) reported the occurrence of acidic and intermediate volcanic rocks interbedded with the Anka, Brinin-Gwari and Zungeru schist belts. Mafic to Ultramafic rocks commonly referred to as the amphibolite complex, constitute important components of some of the schist belts. Pan-African tectonics imposed the North-South structural trend and its magmatism led to the widespread emplacement of granites in the schists (Turner, 1983). Both garnet-mica and quartz-biotite schists braid into mica-schists. The rocks of the schists belts have been divided into lithostratigraphic units termed formations (Ajibade and Wright, 1988). These are:

- i) The Brinin Gwari Formation
- ii) The Kushaka Formation
- iii) The Zungeru - Psamite Formation
- iv) The Zuru Quartzite Formation
- v) The Wonaka Schist Formation
- vi) The Anka - Meta - Conglomerate Formation.

The formations in the schist belts can be traced over long distances. Fresh specimens are difficult to obtain and they are usually only exposed in river valleys where they are deeply weathered (McCurry, 1970). Ajibade (1980) suggested the possibility of the Kushaka formation being deposited on a continental crust where semi-pelitic meta-sediments are predominant. Truswell and Cope (1963) noted significant lateral variation which include phyllites, siltstones, carbonaceous siltstones, mica schists, banded iron rich rock, carbonaceous schists and amphibolites. Nwabufo-Ene and Mbonu, (1988) observed that the amphibolite belt probably represents a brief period of extensive basaltic volcanism with only a minor acid volcanic activity.

2.3 STRUCTURAL ASPECTS

2.3.1 Rock Contacts

The Nigerian basement complex is believed to be polycyclic and has undergone various tectonic events with differing intensities from Archean to late Proterozoic (Pan-African). The Nigerian Precambrian rocks are poorly exposed and the nature of the contacts e.g migmatite/gneiss - metasedimentary, migmatite/gneiss-granite, granite-metasedimentary are yet to be fully and accurately mapped (Oluyide, 1988). However, detailed work by some interested groups have thrown some light on the nature of the rock boundaries in the basement complex. For instance, the contacts between migmatites and gneiss are in most cases gradational (Oluyide, 1988). The contacts between the migmatite-gneiss complex and the metasedimentary series could be sharp or gradational, Ajibade *et al* (1979) have shown that the contacts are often sheared or represent thrust surfaces.

2.3.2 Folding

Field and laboratory studies indicate that the foliations present in the basement complex are essentially tectonic and metamorphic in origin. Primary sedimentary structures, including unconformities, according to Oluyide (1988), have most probably, been obliterated and are therefore difficult to recognise (Oluyide, 1988). Also the quartzites and meta-conglomerates which could be used as marker horizons, have themselves been deformed and rotated from their original disposition. The dominant foliation defined by alternating dark and light bands are prominent in the migmatite - gneiss complexes trend roughly North-South with variations between NW-SE and NE-

SW. The Precambrian schists, phyllites and quartzites of the metasedimentary series, have shown to have preserved four foliations representing four folding phases, (Grant 1978, Ajibade and Wright, 1988). Some of these folds are known to have overturned and are preserved as isolated mega-tight folds in the schists with their axes trending NNE-SSW direction (Muotoh *et al*, 1988).

Chukwu-Ike (1978) identified two fold trends roughly E-W and N-S in NW Nigeria. He considered the E-W trend, which he reported as being severely refolded along N-S axis, as the major and earliest basement folds. Truswell and Cope (1963) considered the deformation of the schist belts in the Kuseriki region to have preceded and accompanied the emplacement of the granites. McCurry (1970) identified two phases of deformation in Zaria region which she designated as F_E (Earlier folds) and F_L (Later folds).

2.3.3 Fractures

Fracture is a characteristic feature of the Nigerian Basement Complex tectonics. The major fracture directions are the N-S, NNE-SSW, NE-SW, NNW-SSE and NW-SE (McCurry, 1970, Oluyide, 1988) and to a lesser extent, the E-W trends (Oluyide 1988).

Evidence suggests that there are two contrasting structural styles in the Brinin-Gwari and Kushaka schist formations which form two elongated metasedimentary belts in the area (Grant, 1978). According to Grant (1978), the Brinin-Gwari Formation is simple monocyclic and, younger while Kushaka Formation is complex, polycyclic and, older. Grant, (1978) suggested that the Kushaka belt could have been infolded and metamorphosed during the Kibaran (1110mya) or even in the earlier Eburnean (2000

mya) and the Brinin-Gwari belt during the Pan-African. Ajibade and Wright, (1988) described the structural sequence in the Brinin-Gwari formation and compares the structures with those identified by Grant (1978) in the Kushaka formation. They observed that the Brinin-Gwari formation occurs as a narrow (3 - 10 km) N-S trending belts in the central part of the Kuseriki region.

2.4 ECONOMIC GEOLOGY AND MINERALOGY

The dominant economic mineral in the area is gold but a number of other minerals have been recorded including iron-ore, asbestos, chromite, talc, diamonds, manganese and kyanite (Woakes, 1988). Anhausseurs *et al.*, (1969), observed that the schist belts of Nigeria show lithologies similarities to schist belts from other parts of the world and are known to harbour important economic mineral deposits. Gold distribution is not haphazard but according to geological provinces largely defined by different orogenic cycles and tectono-structural boundaries (Chuku, 1988).

The distribution of gold in a variety of settings reflect the poly-cyclic characteristic of the basement rocks and effective exploration is linked to a better understanding of these problems (Woakes, 1988).

CHAPTER THREE**3.0 FIELD PROCEDURES, DATA REDUCTIONS AND CORRECTIONS****3.1 GENERAL WORK PLAN**

In order to set up an adequate gravity network in a gravimetric Survey, careful consideration must be given to logistics of the area under study, the instrumental factors and availability of field requirements. A logistic problem encountered during planning was the poor road network in the area. The Federal highways in the area are dilapidated. Although there are quite some smaller roads and tracks (mainly DFRRRI Roads), they are equally in very poor condition owing, in part, to the fact that they are largely untarred. Lack of current topographic maps of the area posed a great problem to the study. The available topographic maps were produced several years ago and did not reflect new roads in the area.

The choice of routes was governed by the available road network, the accessibility and motorability and the need for an even spatial distribution of stations over the study area. The field stations were located at intervals of 2 km and, in some cases, 1 km along motorable roads.

3.1.1 Instrumentation

The field work was carried out using a LaCoste and Romberg (LCR) model G geodetic gravity meter No G446 with a reading precision of 0.01 milligal and a drift rate of less than 1 milligal per month (according to the manufacturers). Two Wallace and Tiernan aneroid altimeters model No. FA181 were used for obtaining elevation measurements. A psychrometer was used, wet and dry bulbs thermometer readings were

taken at each station to correct the altimeter readings for humidity. A pre-fieldwork calibration of the gravimeter and the two altimeters was carried out using the first order gravity network for Nigeria stations at Funtua, Zaria, and Kaffin Maiyaki.

The altimeters drifts were computed and their calibration factors of 1.074855 and 1.052264 were obtained respectively for the altimeters A and B used for the fieldwork. Standard procedures as described in the gravimeter manual were employed to carry out routine checks and level adjustment and sensitivity of the gravimeter after which the instrument was observed for four days inside a room in the physics department. Six wallace and Tiernan aneroid altimeters were simultaneously observed with the gravity meter between the hours of 0500 and 2200 (local time). This was necessary to detect any malfunctioning instrument, identify any peculiarity in instrument behaviour as well as their drift characteristics (Osazuwa, 1992). This observation was repeated at the end of the field work for two days to confirm that the instruments still retained their earlier recorded behaviour and drift characteristics. Figures 3.1 and 3.2 show the plots of the instrumental responses during the two epochs of test observations. The figures represent the instrument drift curves due to tidal effect of sun and moon.

Two of the altimeters labelled A and B were chosen for the field work. The observation revealed a faulty altimeter (ALT E). Two functional altimeters (ALT A and ALT B) were selected because they gave better representation of the linear windows (Figures 3.1 (a and b)). The shift of the responses of the altimeters along the reading axis is ascribed to the difference in characteristic behaviour of each instrument (Osazuwa, 1992). The three major time-segments of the drift curve which are of interest are: 0500 - 0845, 1050 - 1400 and 1700 - 2100 hours. The response of the instruments during these periods above, indicates approximate linear drift characteristics within a

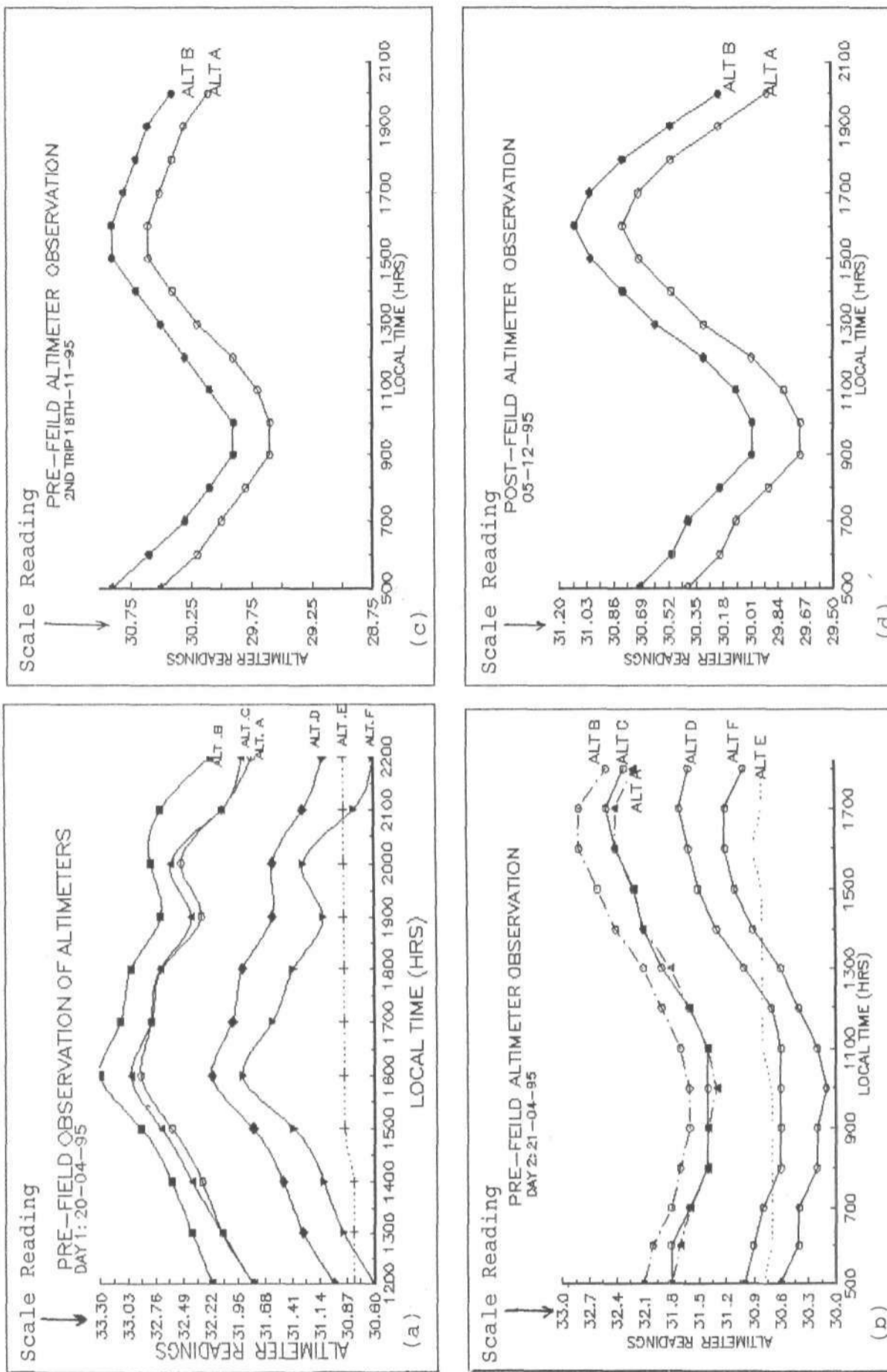


Figure 3.1: Altimeter Drift Curves

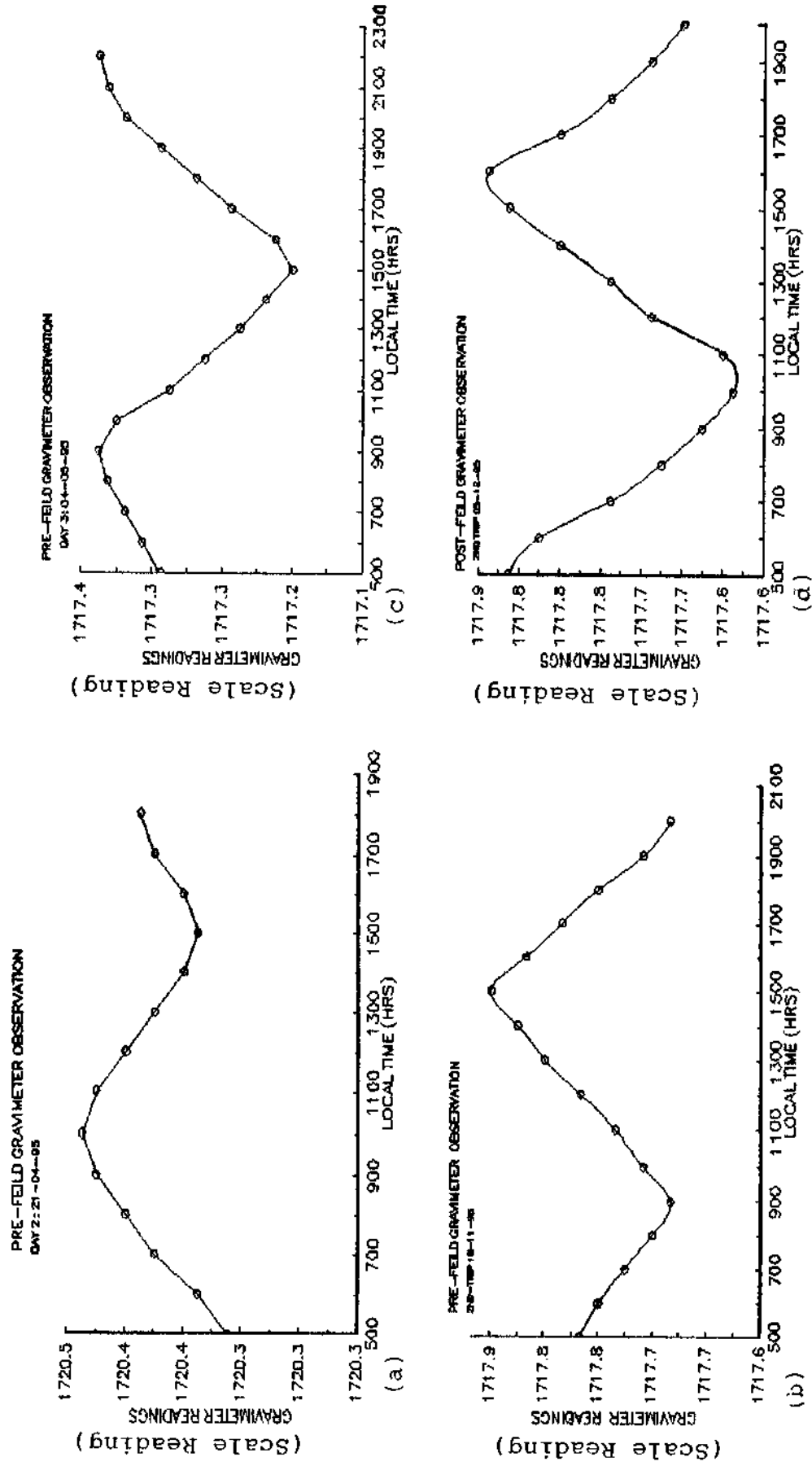


Figure 3.2: LaCoste-Romberg Gravimeter Drift Curves

time limit of about three hours. Since a linear drift is assumed in the computation of the drift rate, readings within loops in the field were confined to this time 'windows'.

3.2 FIELD WORK

The collection of data from the field was carried out in May and November 1995 (to obtain more readings and to collect rock samples for density determination). With the use of the field map of the survey area and the odometer of the field vehicle, station positions were located. Other features such as road junctions and public wells were used to affirm station positions and establish new base stations. The data collected in the field included gravimeter and altimeter readings as well as the psychrometer readings of wet and dry bulb temperatures. All observed gravity values in the survey were taken relative to the value 978049.641 mGal at the first order gravity network of Nigeria base station (GMSC 9) No. 970974, located at Government Secondary School, Funtua, which is tied to the International Gravity Standardization Net, (IGSN 71) by Osazuwa (1985). The reference station GMSC 9 was also used for elevation reduction. Another national gravity base station, GMSC 4, at the Nigerian College of Aviation Technology, Zaria and in physics department building Ahmadu - Bello University were occasionally used. The three national gravity base stations were used for the calibration of the instruments.

The leap-frog method of observational sequence (Osazuwa, 1985) was adopted with the altimeter and gravimeter readings taken simultaneously. The confinement of readings within loops to the linear portion of the altimeter and gravity meter drift curves which on the average is limited to about three hours, was aimed at having effective control over the instrument drift and the diurnal tidal and pressure variations where these may not be corrected for. Figure 3.3 shows the locations and general distribution of field stations.

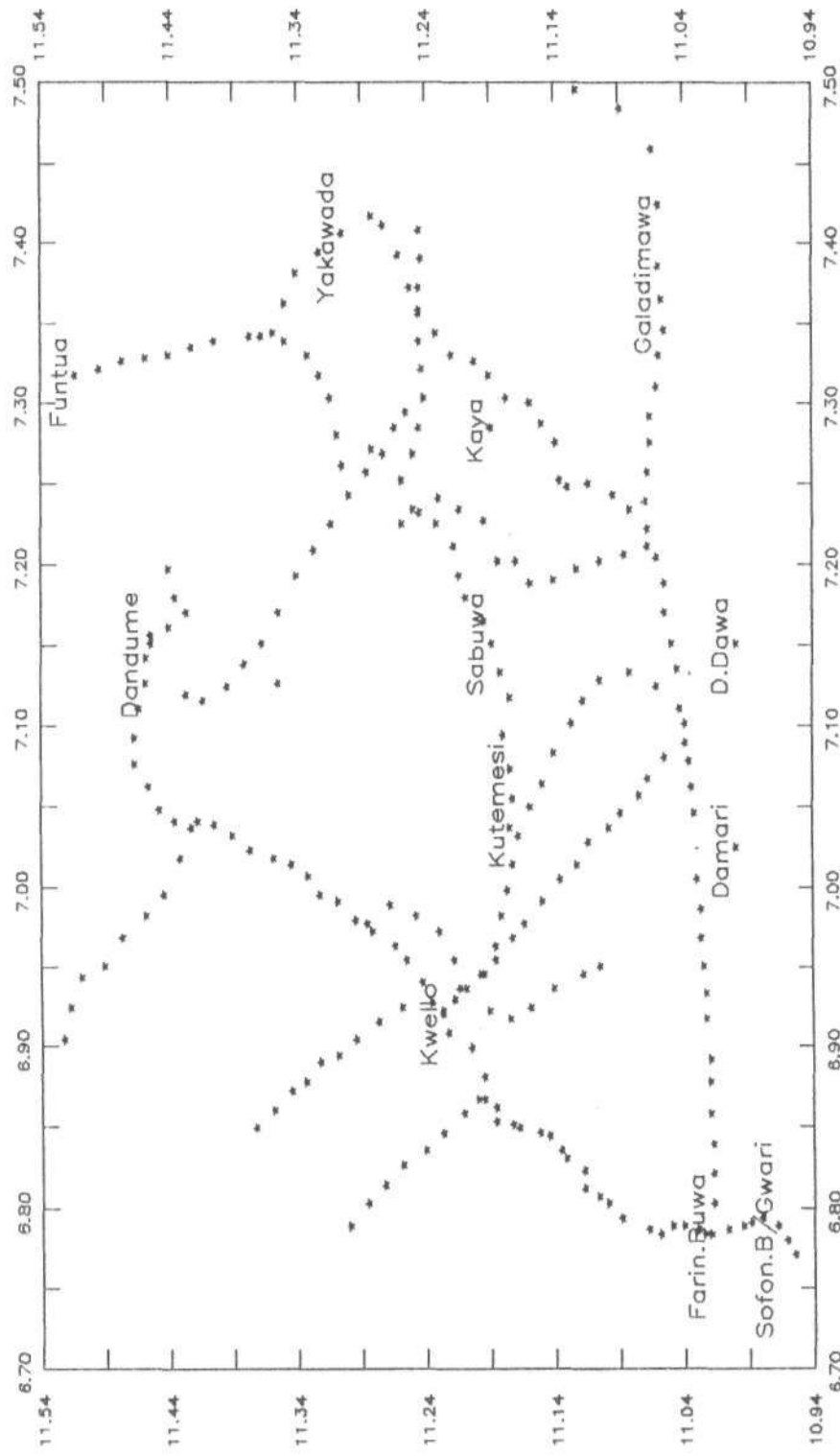


Figure 3.3: Station Distribution Map

Certain precautionary measures taken while handling these equipments in the field included:

- (i) Maintaining the gravimeter constantly on heat by ensuring constant power supply and recharging of the batteries after each days work. This was necessary to avoid spurious readings (Model G446 Manual)
- (ii) The pointers of the altimeters were allowed to settle before taking readings. At the end of each observation, the altimeters were closed tightly to avoid excessive drift during transportation. The beam of the gravimeter was clamped between readings for the same reason.
- (iii) The instruments were shielded from direct sunshine and wind to prevent thermal shock as discovered by Osazuwa and Ajakaiye (1992).
- (iv) The readings were not taken immediately after rainfall. This was to allow for the normalization of the ambient temperature and pressure conditions (Osazuwa, personal communication).
- (v) Care was taken to minimize jerks or mechanical disturbances on the instruments so that they do not suffer undetectable creep (Hamilton and Brule, 1967, Wallace & Tiernan Altimeter Manual).
- (vi) The altimeter was first made to be in a horizontal position before reading was taken to avoid taking erroneous readings at stations.

A total of 267 detailed station were occupied and these were all tied to the main reference base station GMSC 9 at Funtua. On the average, 15 to 25 stations were observed per day depending on the quality of the road, accessibility and weather conditions. Rock sample were collected from outcrops within the area for density determination.

3.3 DATA REDUCTION

The reduction of the field data was done in two phases. The first phase dealt with the humidity corrections applied to the altimeter readings. The second phase involves altimeter drift corrections, conversion of elevation values from feet to meters and gravity data reduction to free air and Bouguer anomalies values by use of a computer program by Osazuwa (1986). The program was modified by Osazuwa to accommodate the revised version of the drift correction based on the Cascade model Osazuwa (1988). The entire computation was carried out with a 386 digital personal computer.

3.3.1 Altimeter Data

The field values recorded from the altimeters for each station were varying. This is explained to be due to the characteristic behaviour of each instrument (Osazuwa, 1992). The absolute elevation for each station was determined for each altimeter using the height of the main reference base, (GMSC 9) at Funtua. The height values obtained correlate well with the values on the topographic map of the area. Drift correction was done separately for each altimeter height value using the cascade drift model (Osazuwa, 1988). The basic principle of the method is that when all observations in a day are tied to the same time origin during a day's work, repeat observations at the same station after drift correction should be equal. The underlying assumption is that drift of the instrument is a linear function of time over a short time interval.

3.3.2 Gravity Data

The gravity data collected were reduced to Bouguer anomaly and free air

anomaly values by use of a fortran 77 computer program written by Osazuwa (1986) and upgraded (modified) by him to suit the observational sequence adopted in the field work of this survey. The program automatically converts the gravity scale readings to their corresponding milligal values. Drift correction, Free - Air and Bouguer anomalies and Bullard term corrections computation were also carried out with the program. Though the program could execute the tidal correction, this was not done since the field observations were strictly made within the selected linear windows of the prefield drift curves. The program uses the Geodetic Reference System 1967 (GRS 67) for the computation of the theoretical (or normal) gravity on the reference ellipsoid. It assumes a value of $2.67 \times 10^3 \text{ kgm}^{-3}$ for the mean density of surface rocks. The density values and the choice of the GRS 67 formula as recommended by Morelli (1971), is to standardize the result of this survey. The standard reduction procedures and basic equations used to obtain the anomalies are as follows:

(a) **Drift Rate:** The cascade model (Osazuwa, 1988) was used to remove the instrumental drift. A linear relationship of drift with time was assumed and the drift rate μ is given by

$$\mu = \frac{(g_2 - g_1) - (g'_2 - g'_1)}{t_2 - t_1} \dots \dots \dots (3.2)$$

were g_1 and g_2 are the absolute gravity values at the terminating stations of the loop, g'_1 and g'_2 are observed gravity values corresponding to g_1 and g_2 at time t_1 and t_2 respectively (Osazuwa, 1988). If the terminating stations are the same station, then equation 3.2 becomes

$$\mu = \frac{-(g'_2 - g'_1)}{t_2 - t_1} \dots \dots \dots (3.3)$$

(b) **Observed Gravity at a Detail Station:** The observed gravity value g_{obs} at a detail station is given by

$$g_{obs} = g_1 + k [(R_1 - R_d) - \mu (t_d - t_1)] \text{ mGal} \dots \dots \dots (3.4)$$

where g_1 is the absolute gravity value at the first base station, k is the meter constant, R_1 and R_d , t_1 and t_d are the readings and time s at the first base station and detail station respectively.

(c) **Theoretical Gravity or Latitude Effect:** The theoretical gravity at a station is given by the GRS 67 formula whose Chebychev approximation form is

$$g_{lat} = 978031.85 (1 + 0.005278895 \sin^2 \phi + 0.000023462 \sin^4 \phi) \text{ mGal}$$

with a maximum error of 0.004 mGal (Dobrin, and Savit 1988) where ϕ is the latitude of the station.

(d) **Free - Air Anomaly:** Correcting the difference between g_{obs} and g_{lat} for the vertical decrease of gravity with increase in elevation, gives the free-air anomaly, $\Delta g_{F.A.}$, which is computed from the expression

$$\Delta g_{F.A.} = g_{obs} - \left(g_{lat} - \frac{dg}{dz} h \right) \dots \dots \dots (3.6)$$

where dg/dz is the vertical gradient of gravity and its value is $0.3086 \text{ mGal m}^{-1}$ (Parasnis, 1962) and h is the station elevation above mean sea level.

(e) **Bouguer Anomaly:** For computation of the Bouguer anomaly, there are just three elements of the earth model:

- (i) The expected increases in gravity with latitude (latitude effect, (g_{lat}));
- (ii) The expected decrease in gravity with increasing elevation above the mean sea level (Free-air effect $(g_{F.A.})$);
- (iii) The expected increase in gravitational attraction due to the mass of rock between sea level and the observation point (Bouguer effect (g_{boug})).

The Bouguer gravity at a point can then be written as:

$$g(B_{grav}) = g(obs) - BC \dots \dots \dots (3.7)$$

$$g(BA) = g(B_{grav}) - g(Theoretical) \dots \dots \dots (3.8)$$

Therefore the Bouguer Anomaly is determined using the expression

$$\Delta g_{B.A} = g_{obs} - g_{lat} + \frac{dg}{dz} h - 2\pi G\rho_c h \dots \dots \dots (3.9)$$

Where ρ_c is the assumed crustal density value of $2.67 \times 10^3 \text{ kgm}^{-3}$ or Bouguer density and G is the universal gravitational constant. The term $2\pi G\rho_c h$, called Bouguer correction is the additional attraction exerted on a unit mass by a slab of rock material of density ρ_c between a station and the reference datum, (in this case the m.s.l) The Bouguer correction mathematically removes the effect of the material between the horizontal plane passing through the station and the reference datum plane. The Bouguer correction, $0.04193\rho_c h \text{ mGal}$ is opposite in sign to the free-air correction and is directly related to it.

Three methods of selection of Bouguer reduction density are documented. The first is to use what could be called traditional or standard density. Most regional maps have traditionally been reduced using a value of $2.67 \times 10^3 \text{ kgm}^{-3}$. The second method determines a Bouguer reduction density that minimizes the correlation between the complete Bouguer anomaly and topography. This method which is widely used in areas of rugged topography (Gerkens, 1989) and which was originally suggested by Nettleton (1939) and also Vajk (1956) could not be used for this survey because the area is relatively flat. The third method is to measure the density of representative rock samples. It is however usually difficult to obtain a suite of rock samples that is truly representative Williams and Finn, (1985). In order to ensure consistency and compatibility with other regional gravity surveys in adjacent areas, the density value of $2.67 \times 10^3 \text{ kgm}^{-3}$ was chosen. Terrain correction was not carried out because the area of study is relatively flat.

3.4 SOURCES OF ERROR IN THE BOUGUER ANOMALY

The computed Bouguer anomaly at each station is usually subject to errors from several sources. These include errors in elevation determination, e_h , errors in terrain effect, e_t , errors in base value, e_b , errors in assumed reduction density, e_p , and errors in station location, e_s . Where stations are on Federal Survey Bench Marks, the height values usually have errors less than 0.03 m and the error in the Bouguer anomaly due to inaccurate elevation determination would be less than 0.006mGal which is insignificant. However a computed error of 0.94 mGal in the Bouguer anomaly due to elevation determination could be expected. Since terrain correction was not carried out, a maximum error of 0.02 mGal would be introduced in

the Bouguer anomaly. Error due to base value is taken as the standard deviation value of 0.13 mGal at the Funtua base station (Osazuwa, 1985).

Other sources of error could arise from mode of observation, non-linear drift of instrument and calibration factor, e_0 . However, Osazuwa (1992) observed that the error in elevation determination could be decreased to less than 1.5 m. This would produce a corresponding error of less than 0.5 mGal in the Bouguer anomaly.

The mean crustal density of $2.67 \times 10^3 \text{ kgm}^{-3}$ was used for the Bouguer correction. The mean density of the most abundant rock types in the area was found to be $2.603 \times 10^3 \text{ kgm}^{-3}$, but this density may not be truly representative of the density of the crust. Therefore there is a density uncertainty of $0.053 \times 10^3 \text{ kgm}^{-3}$ between the assumed and the actual, causing a maximum error of -0.34 mGal.

The map used to obtain the latitudes of stations were on a scale of 1:50,000 and latitudes of stations were determined to the nearest 0.01 seconds. Errors due to inaccurate latitude determination would therefore be about 0.08 mGal. The gravity meter used was a LCR gravimeter which, has a built-in temperature regulatory system and a mechanism for clamping the moving parts during transportation. Therefore the instrument drift which might occur due to shock is minimized. Also since the calibration factor of the instrument does not change perceptibly with time the need for frequent checks of calibration is eliminated (Osazuwa, 1985). The errors in measured gravity values when observations are restricted to the observation time window of 3 hours are negligible and cannot be detected with the gravimeter (Osazuwa, 1992). Murty (1977) gave the total error, (e_T), as

$$e_T = \sqrt{e_h^2 + e_p^2 + e_\phi^2 + e_t^2 + e_b^2 + e_o^2} \dots \dots \dots (3.10)$$

From the analysis above, if the maximum error computed for each of the above sources is assumed, the total cumulative error at each station would be 1.01 mGal. For most stations however, the actual errors would be less than this value since the maximum error in each case is assumed. Murty equally said that in determining the correct contour interval, one should use an interval which is at least two and half times the error, Murty, (1977). A contour interval of 2 mGal was therefore used.

3.5 DENSITY DETERMINATION

In gravity surveying, subsurface geology is investigated on the basis of variations in the earth's gravity field generated by differences of density between subsurface rocks. Gravity anomalies are caused by the lateral heterogeneity of upper crustal density. Because of this therefore, a knowledge of the densities of rock formations in a survey area is very necessary for a meaningful structural interpretation of gravity anomalies.(Grant and West, 1965, Ajakaiye, 1976(b)).

Various authors have published densities of rock types encountered in different parts of the world examples are Ajakaiye (1976(b)), Telford *et al*, (1976) and Dobrin, (1976). As is generally the case, the results published only provides a general overview of rock densities. However, the rock densities and the density contrasts necessary for structural interpretation of gravity anomalies in a particular area may be so small that actual measurements of the densities of fresh rock samples from the area must be carried out.

A total of 229 fresh samples were taken from outcrops along all the traverses during the field work. These fresh samples were collected out from either outcrops or active quarries. The true densities of the rock samples were found using the famous Archimedes principle.

In the laboratory, the samples were weighed in air (W_d) and quickly in water (W_w) using a Mettler balance (Model P515) which has a precision of 0.01 g. These samples were then saturated in water for over 48 hours and were weighed again in air (W_t) and then in water (W_s). The excess water on the saturated samples were wiped off before taking the saturated weights measurements. The dry and saturated densities were then computed using the following formulae.

$$\rho_d = \frac{W_d}{W_d - W_w} \dots \dots \dots (3.11)$$

$$\rho_s = \frac{W_t}{W_t - W_s} \dots \dots \dots (3.12)$$

where ρ_d is the dry density and ρ_s is the saturated density. A digital computer 386 was used for calculating the above densities and their standard deviations. According to Dobrin (1976) and Telford *et al*, (1976), the most likely insitu density of sub-surface rocks lies between the dry and wet densities of the rock. Therefore the average of the dry and saturated densities as measured above was adopted for subsequent interpretation. The results of the densities for the various rock types identified in the area are summarized and shown in Table 3.1. The standard deviation, which are the errors in the density measurements are equally shown. A histogram of each rock type was plotted as shown in Figures 3.4 and Figures 3.5. The true densities for each rock type were grouped into class intervals of 0.03.

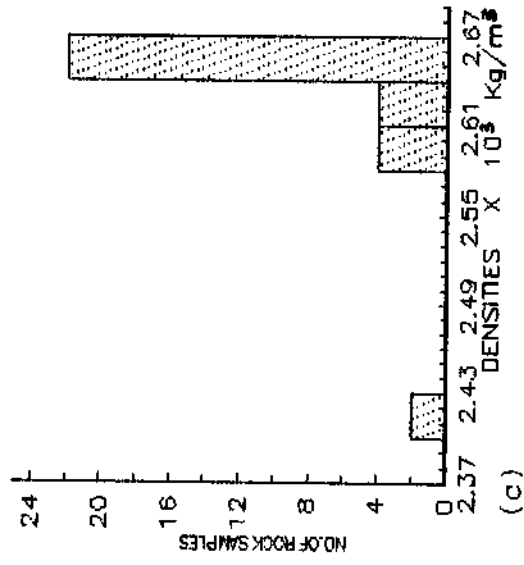
Table 3.1: Summary of Rock Densities

Rock Type	No. of Samples	Range of Densities $\times 10^3 \text{ kgm}^{-3}$	Mean Densities $\times 10^3 \text{ kgm}^{-3}$	Standard Deviation $\times 10^3 \text{ kgm}^{-3}$
Quartz-diorites	40	2.75-2.82	2.79	0.02
Quartzites	32	2.41-2.66	2.63	0.04
Migmatites	16	2.67-2.74	2.70	0.02
Granites	39	2.26-2.72	2.63	0.02
Gneisses	20	2.64-2.74	2.70	0.03
Amphibolites	16	2.67-2.78	2.75	0.03
Schists (Phyllites)	20	2.72-2.81	2.78	0.03
Carbonaceous Schists (Weathered)	36	2.28-2.57	2.43	0.11
Banded Iron Formation	10	3.08-3.33	3.19	0.08

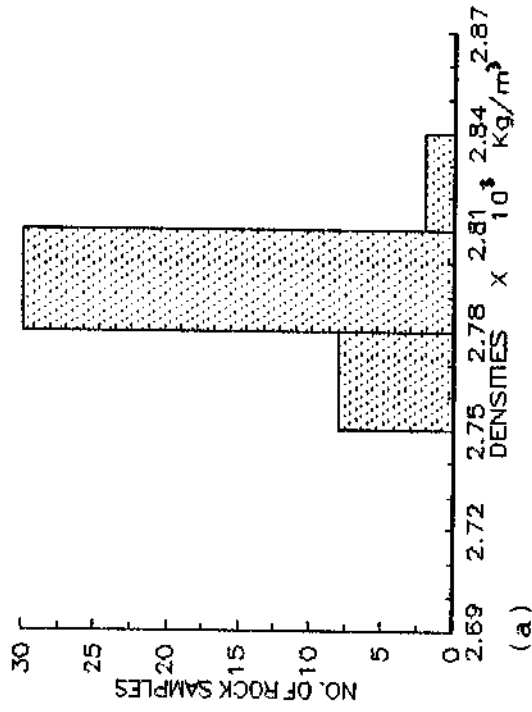
The mean densities for the different rock types ranged from $2.43 \times 10^3 \text{ kgm}^{-3}$ for carbonaceous schists (weathered) to $2.79 \times 10^3 \text{ kgm}^{-3}$ for quartz-diorites and the extreme value of $3.19 \times 10^3 \text{ kgm}^{-3}$ for the banded iron formation. A description of the various histograms is given.

A total of 40 samples for quartz-diorites were obtained and their density distribution is shown in Figure 3.4(a). The calculated mean density for the group is $2.79 \times 10^3 \text{ kgm}^{-3}$ with a standard deviation of $\pm 0.02 \times 10^3 \text{ kgm}^{-3}$. A mean density of $2.70 \times 10^3 \text{ kgm}^{-3} \pm 0.02$ was obtained from a frequency distribution for 16 samples of migmatites, Figure 3.4(b). The distribution is approximately normal. The frequency distribution of the granites, Figure 3.4(d) is seen to be near normal with a mean density of $2.63 \times 10^3 \text{ kgm}^{-3} \pm 0.02$. Although Ajakaiye (1976(b)) suggested that this near normal distribution shows that there exists similar mineralogical contents in granites in

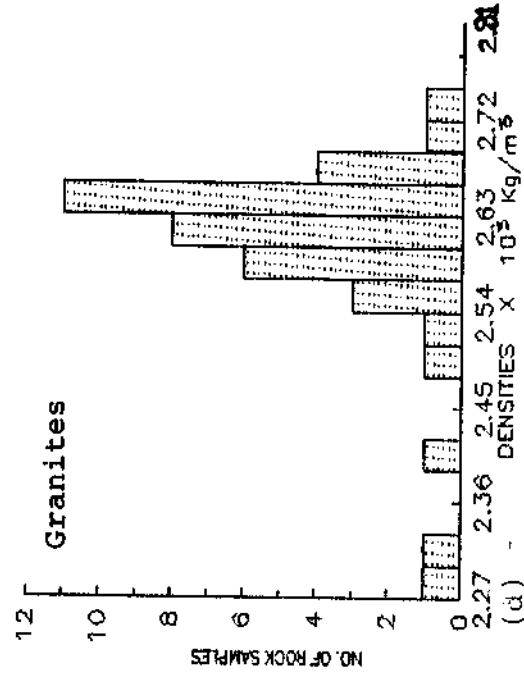
Amphibolites



Quartz-diorites



Granites



Migmatites

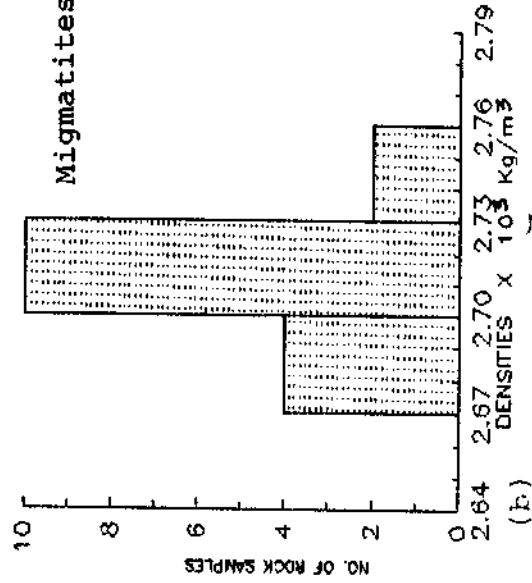


Figure 3.4: Histograms of Rock Densities based on Laboratory Measurements

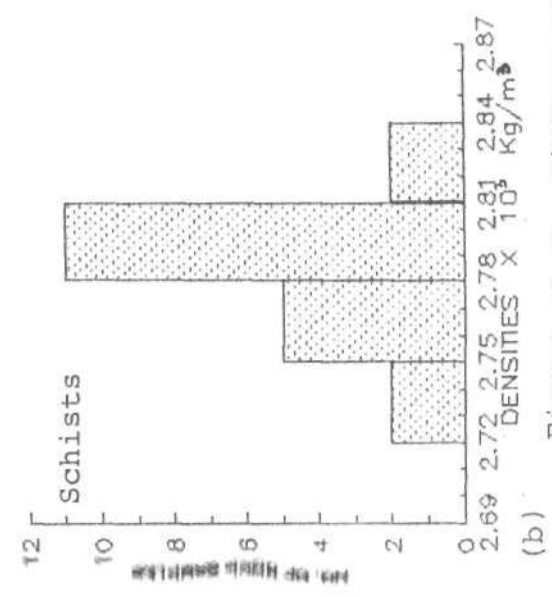
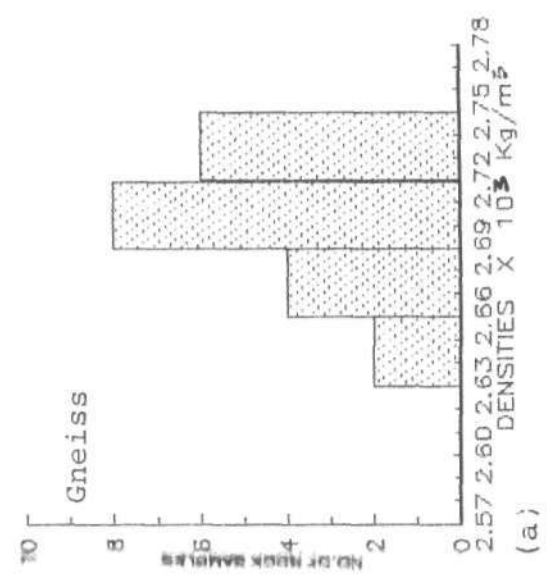
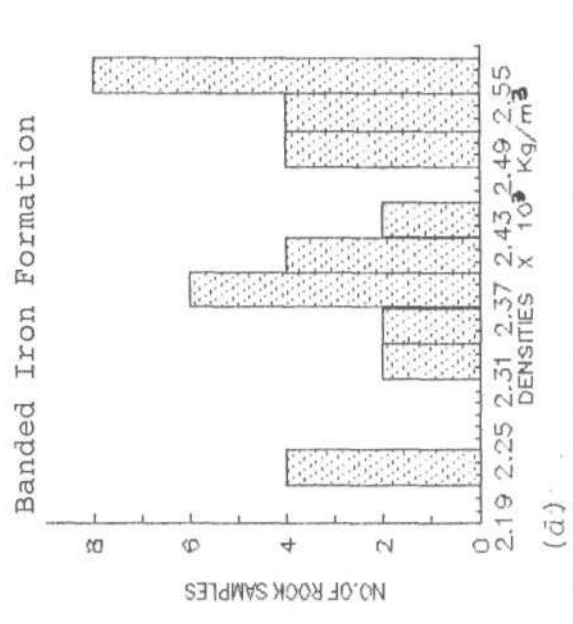
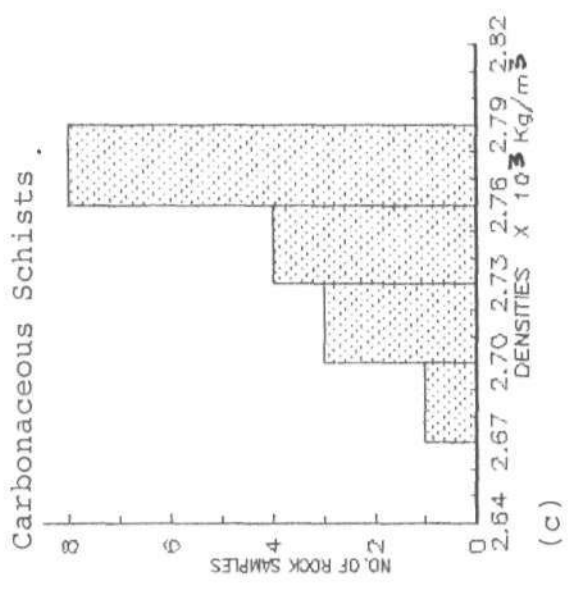


Figure 3.5: Histograms of Rock Densities based on Laboratory Measurements.

the area, Osazuwa (Personal Communication) is of a strong view that if the mineralogical contents of granites are highly variable geochemically, and yet their volumetric properties remain similar, one may still have a near normal frequency distribution if the samples collected are representative. It may therefore be said that the near normal distribution of the granites is an indication of an even spread of the various types of granites in the area. The standard deviation of the mean is $0.02 \times 10^3 \text{ kgm}^{-3}$. The density distribution for the gneisses, shown in Figure 3.5(a), has a mean density of $2.70 \times 10^3 \text{ kgm}^{-3} \pm 0.03 \times 10^3 \text{ kgm}^{-3}$. Its skewness is attributable to the non even spread of the types of gneiss seen in the area. The density distribution for the schists is shown in Figure 3.5(b). The schists has a computed mean density of $2.78 \times 10^3 \text{ kgm}^{-3}$ and a standard deviation of $0.03 \times 10^3 \text{ kgm}^{-3}$. Other rock samples considered are quartzites, Figure 3.4(c), amphibolites, Figure 3.5(c), carbonaceous schists, Figure 3.5(d), and banded iron formations (histogrm not shown due to very few samples) which have mean densities $2.63 \times 10^3 \text{ kgm}^{-3}$, $2.75 \times 10^3 \text{ kgm}^{-3}$, $2.43 \times 10^3 \text{ kgm}^{-3}$ and $3.19 \times 10^3 \text{ kgm}^{-3}$ respectively.

Generally, the observed modes of the density histograms for the metamorphic rocks (e.g quartzites, schists and amphibolites) could be due to the different degrees of metamorphism which gives a general characteristic irregularity in the density behaviour of metamorphic rocks (Ajakaiye, 1976(b)). Grant and West (1965) also pointed out that distinct zoning and chemical differentiation causing irregular density behaviour, could be found in a single rock formation.

3.5.1 DENSITIES ACCEPTABLE FOR MODELS

The mean densities of the various rock units given in Table 3.1, agree with published values for similar rock types from other places (Kearey and Brooks (1984), Ajakaiye (1976(b)), and Telford *et al*, (1976)).

Since the migmatites and gneisses are the dominant rocks of the basement complex in the area the density value of $2.70 \times 10^3 \text{ kgm}^{-3}$ for the basement complex was used in the interpretation. The density values for quartz-diorites, granites, amphibolites and schists, (Table 3.1), were accepted for interpretation since they fall within the acceptable ranges of $(2.75 - 2.99) \times 10^3 \text{ kgm}^{-3}$ for amphibolites and $(2.39 - 2.90) \times 10^3 \text{ kgm}^{-3}$ for schists, (Ajakaiye, 1976(b); Telford *et al* 1976; Kearey and Brooks, 1984 and Dobrin and Savit, 1988).

CHAPTER FOUR

4.0 GRAVITY FIELD DETERMINATION AND MAP PRODUCTION

4.1 GRAVITY FIELD

4.1.1 Introduction

The continuation of the potential field, (gravity or magnetic), enhances the effect of anomalous sources that are of particular interest in the area or reduces those of field variations unrelated to the problem, Tsay (1975). The result of this processing can be an aid to map the subsurface geological structure by interpreting the continued anomaly which has been brought to a suitable elevation above or below the level of original observation.

Many published methods of continuation have been designed by weighting the field values from calculated sets of coefficients (Henderson and Zieth, 1949; Henderson, 1960). These methods require smoothing or averaging the data on the map before continuation is applied. The other methods have been developed which operate directly on the data by using Fourier Transform (Dean, 1958 and Fuller, 1967) and Fourier series (Tsuoboi, 1937). Although the Fourier series method for analysis and interpretation of potential field data has proved very useful, it is inappropriate to apply the method directly and unconditionally (Tsay, 1975), because when the potential field is represented by Fourier series, it implies periodic repetition of the same anomaly. Therefore there exists because of this periodic repetition a discontinuity at the edges of the anomaly which will cause unacceptable errors near edges after continuation. Tsay (1975) proposed two methods of reducing this error as, either (1) to use only the cosine

series, or (2) to add a certain number of constant data to both edges of original data before continuation.

4.1.2 Upward Continuation Field

The transformation of gravity data measured on one surface to some higher surface is called upward continuation. Upward continuation is a filter operation that tends to smooth the original data by attenuation of short wavelength anomalies relative to their long-wavelength counterparts. The upward continuation filter is elegantly simple for the special case of data measured on a flat surface (Dobrin and Savit, 1988). The upward-continuation filter $F_2(k_x, k_y)$ is given by

$$F_2 (K_x, k_y) = e^{-kz} \dots \dots \dots (4.2.1)$$

where $K = \sqrt{(k_x^2 + k_y^2)}$, k_x and k_y are wave numbers with respect to x and y axes respectively, and z is the distance of upward continuation ($z > 0$).

The upward continuation of gravity field on a plane is a process of 2-dimensional numerical filtering. These transformations are linear and can be represented by a convolution process in the space domain of the data with mathematical functions or filters (Bhattacharyya, 1976). The two-dimensional convolution integral is given by (Fuller, 1967)

$$\phi^1 (x, y) = \int_{-\infty}^{\infty} \int_{-\infty}^{\infty} f(\alpha, \beta) \phi (x-\alpha, y-\beta) d\alpha d\beta \dots \dots \dots (4.2.2)$$

where $\Phi(x,y)$ is the input data, $\Phi^1(x,y)$ is the output data and $f(\alpha, \beta)$ is the filtering function.

In order that a filtering function be useful, it must be of a finite extent. If $f(x,y)$ becomes zero for $|x| \geq X$ and $|y| \geq Y$, then equation (4.2.2) may be replaced by

$$\Phi^1(x, y) = \int_{-x}^x \int_{-y}^y f(\alpha, \beta) \Phi(x-\alpha, y-\beta) d\alpha d\beta \dots \dots \dots (4.2.3)$$

Convolution in the space domain is equivalent to multiplication in the frequency domain. Thus in order to arrive at the spectrum of the output, the spectrum of the input is multiplied by the spectrum of the filtering function. Denoting the Fourier Transform of a function by the corresponding capital letter, with a frequency argument and taking the Fourier Transform of equation (4.2.3), we have:

$$\Phi^1(f_x, f_y) = F(f_x, f_y) \cdot \Phi(f_x, f_y) \dots \dots \dots (4.2.4)$$

where f_x and f_y are the angular frequencies along the x and y -axes respectively. From the results of potential theory, the upward continuation of a potential field function $\Phi(x,y,0)$ in a source-free region to a height h above the plane, $z = 0$, is given by Fuller, (1967) as

$$\Phi(x, y, h) = \int_{-\infty}^{\infty} \int_{-\infty}^{\infty} \frac{h\Phi(\alpha, \beta, 0) d\alpha d\beta}{2\pi\sqrt{[(x-\alpha)^2 + (y-\beta)^2 + h^2]^{3/2}}} \dots \dots \dots (4.2.5)$$

Comparison of equations (4.2.5) and (4.2.2) and realizing that the convolution integral is commutative allows the recognition of equation (4.2.5) as a two-dimensional convolution and hence a filtering operation. The potential field function $\Phi(x,y,0)$ is operated upon by the filtering function $f_u(x,y,h)$ in order to arrive at $\Phi(x,y,h)$ where

$$f_u(x, y, h) = \frac{h}{2\pi\sqrt{(x^2+y^2+h^2)^3}} \dots \dots \dots (4.2.6)$$

The theoretical frequency response of a true upward continuation operator may be obtained by Fourier Transform of equation (4.2.6) or the solution of the integral

$$F_u(f_x, f_y, h) = \int_{-\infty}^{\infty} \int_{-\infty}^{\infty} \frac{he^{-2\pi i(f_x x + f_y y)}}{2\pi\sqrt{(x^2+y^2+h^2)^3}} dx dy \dots \dots \dots (4.2.7)$$

since the function to be transformed is even with respect to x and y equation (4.2.7) becomes

$$F_u(f_x, f_y, h) = 4 \int_0^{\infty} \int_0^{\infty} \frac{h \cos 2\pi f_x x \cos 2\pi f_y y}{2\pi \sqrt{(x^2 + y^2 + h^2)^3}} dx dy \dots \dots (4.2.8)$$

Equation (4.2.8) reduces to

$$F_u(f_x, f_y, h) = e^{-2\pi h \sqrt{f_x^2 + f_y^2}} \dots \dots \dots (4.2.9)$$

Equation (4.2.9) describes the desired frequency response of an upward continuation operator. Hence, upward continuation can be seen as a very smooth low-pass filter. As with standard low-pass filters, upward continuation often provides perspective concerning the large regional sources beneath a study area (Dobrin and Savit, 1988).

A fortran 77 computer program (developed by Kangolo of the Physics Department, Ahmadu Bello University, Zaria) was used to upward Continue the Bouguer anomalies at various grid units above the reference plane.

4.1.3 Downward Continuation Field

As might be expected, simply changing the sign of z turns equation 4.2.1 into a downward continuation filter which, when applied to gravity data, gets us closer to the sources. Equation (4.2.9) describes the frequency response of an upward continuation operator. To arrive at a similar relation for downward continuation, theoretically we need only recognise that if we upward continue a set of data, a distance h , and then downward continue the same distance h , we should arrive at the same data we started with. Then the following relation must hold in the frequency domain:

$$\Phi(f_x, f_y) = F_d(f_x, f_y) F_u(f_x, f_y, h) \Phi(f_x, f_y) \dots \dots (4.3.1)$$

Substituting equation (4.2.9) into equation (4.3.1), we have, for the desired frequency response of a downward continuation operator (Fuller, 1967).

$$F_d(f_x, f_y, h) = e^{2\pi h \sqrt{f_x^2 + f_y^2}} \dots \dots \dots (4.3.2)$$

Equation 4.3.2 is valid for source - free regions only.

Practically moving the observational surface nearer to the sources is not a well behaved problem (Grant and West, 1965). Wild Oscillations are noticed on data when the data is downward continued into the causative body, because the shortest wavelengths including data noise and numerical round-off errors are amplified

exponentially (Dobrin and Savit, 1988). Hence downward continuation is used with extreme caution.

4.1.4 Second Vertical Derivative Field

Second vertical derivatives have been traditionally used to enhance local anomalies obscured by broader regional trends and to aid in the definition of the edges of source bodies (Elkins, 1951; Dobrin and Savit, 1988; Gupta and Ramani, 1982 and Henderson and Zeitz, 1967). A shallow geologic feature of limited lateral extent like a salt dome, will typically have a gravity anomaly with greater curvature than the original field (which originates from deeper sources) on which it is superimposed. The second vertical derivative (which is a measure of the difference of the gravity value at a point relative to its neighbouring points) will be greater over the localized feature than over the more smoothly varying regional trend. Plotting a map of second vertical derivative values will have the effect of making the gravitational anomaly from the local feature stand out more conspicuously. Vertical derivatives can be regarded as types of high-pass filters that enhance anomalies caused by small features while suppressing longer - wavelength regional trend.

The use of the second vertical derivative can best be understood by noting that the gravitational potential field satisfies the Poisson's equation given by

$$\nabla^2 U = 4\pi G\rho \quad \dots\dots\dots (4.4.1)$$

where G is the gravitational constant of the earth and ρ is the density of the causative body and U is the gravity potential. Equation (4.4.1) can be written as:

$$\frac{\partial^2 U}{\partial x^2} + \frac{\partial^2 U}{\partial y^2} + \frac{\partial^2 U}{\partial z^2} = 4\pi G\rho \quad \dots \dots \dots (4.4.2)$$

Differentiating both sides of equation (4.4.2) with respect to z, we have:

$$\frac{\partial}{\partial z} \left(\frac{\partial^2 U}{\partial x^2} + \frac{\partial^2 U}{\partial y^2} + \frac{\partial^2 U}{\partial z^2} \right) = 0 \quad \dots \dots \dots (4.4.3)$$

$$\frac{\partial^2}{\partial x^2} \left(\frac{\partial U}{\partial z} \right) + \frac{\partial^2}{\partial y^2} \left(\frac{\partial U}{\partial z} \right) + \frac{\partial^2}{\partial z^2} \left(\frac{\partial U}{\partial z} \right) = 0 \quad \dots \dots \dots (4.4.4)$$

but $\frac{\partial U}{\partial z} = g$ hence equation (4.4.4) reduces to the laplace equation as:

$$\frac{\partial^2 g}{\partial z^2} + \frac{\partial^2 g}{\partial y^2} + \frac{\partial^2 g}{\partial x^2} = 0 \quad \dots \dots \dots (4.4.5)$$

or

$$\frac{\partial^2 g}{\partial z^2} = - \left(\frac{\partial^2 g}{\partial x^2} + \frac{\partial^2 g}{\partial y^2} \right) \quad \dots \dots \dots (4.4.6)$$

Equation 4.4.6 shows that the second vertical derivative of g with respect to z is linearly dependent on the second vertical derivatives of g with respect to x and y. Thus the second vertical derivative is, in effect, a measure of the curvature (Gupta and Ramani, 1982). Since gravity anomalies due to shallow, localised geologic features have greater curvature than those due to broader regional deep sources, the former will be enhanced on the second vertical derivative map. In addition to enhancing weaker local anomalies, the second vertical derivative can often be used to delineate the contacts of lithologies with contrasting densities. These contacts are reflected by inflection points

in the Bouguer gravity, which, while difficult to locate on the Bouguer map, are accurately traced by the zero contours of the second vertical derivative map (Dobrin and Savit, 1988 and Gupta and Ramani, 1982).

4.2 ANOMALY MAP PRODUCTION

4.2.1 Gridding

In order that the gravity anomaly maps of the area be produced, the point Bouguer anomaly values obtained from the random distribution of the detailed stations in the survey area was transformed to regular grid. This was achieved with the aid of a Fortran 77 computer program (written by Kangolo of physics department). Initially a grid interval of 2 km was used. This gave a total of 1271 interpolated data points from 337 observed random data points, (a matrix of 41 x 31). This grid interval introduced more spurious data on the interpolated data than desired. Finally, a grid mesh of $0.04^\circ \times 0.04^\circ$ (or 4.44 km x 4.44 km), considered best, was used; and this yielded a total of 336 interpolated data points from 337 observed points (a matrix of 21 x 16). The regular grid points superimposed on observed random data points is shown in Figure 4.1. This grid interval cuts down on the number of spurious data points, thus reducing the interpolation error.

4.2.2 Bouguer Anomaly Map

The gridded data was used to produce the Bouguer anomaly map which is shown in Figure 4.2. A contour interval of 2 mGal was used to draw the contour maps of the Bouguer, Free-Air and residual anomalies. This contour interval was chosen bearing in mind that the interval should be at least twice the error in the Bouguer field (Murty, 1977).

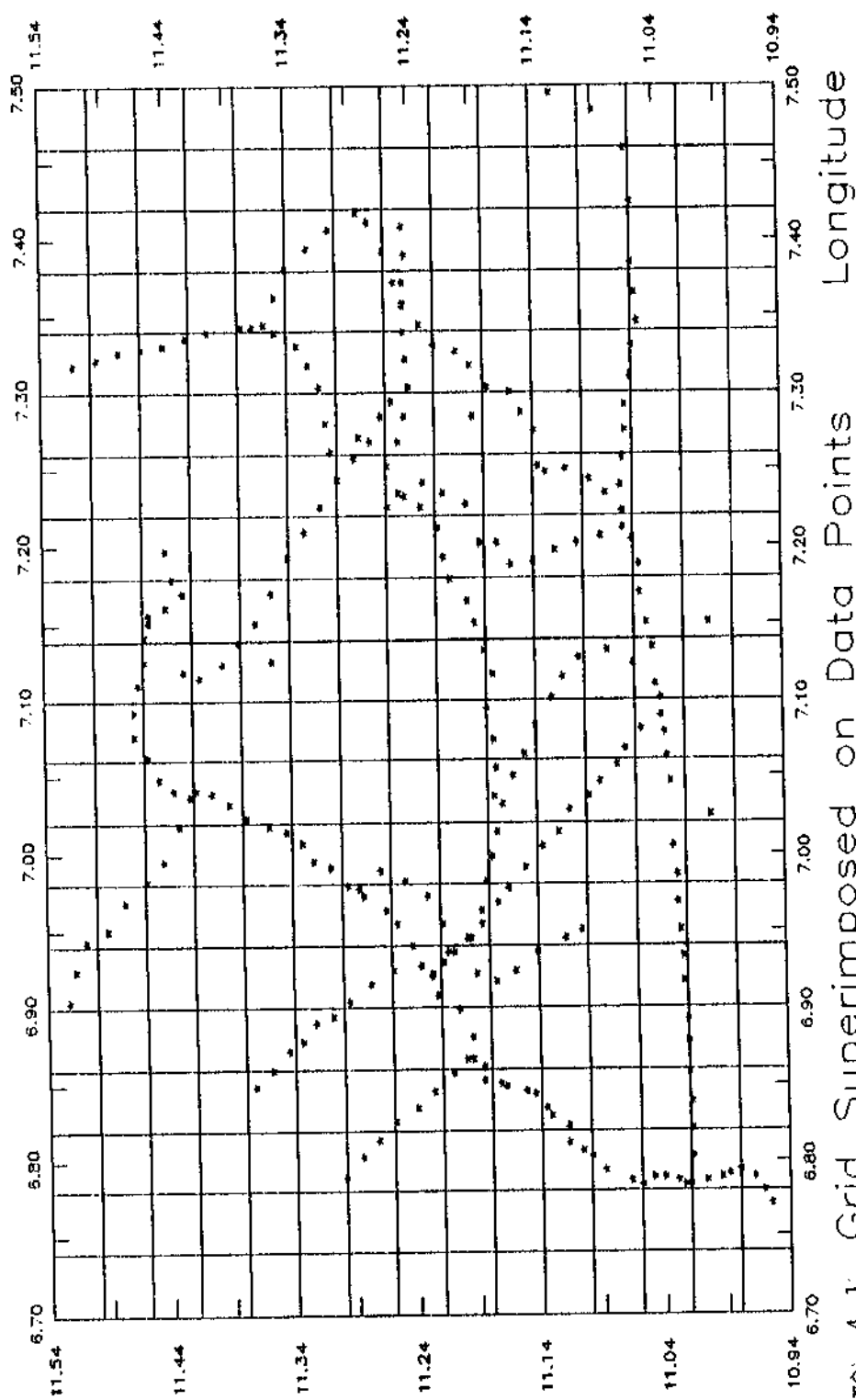


Figure 4.1 Grid Superimposed on Data Points

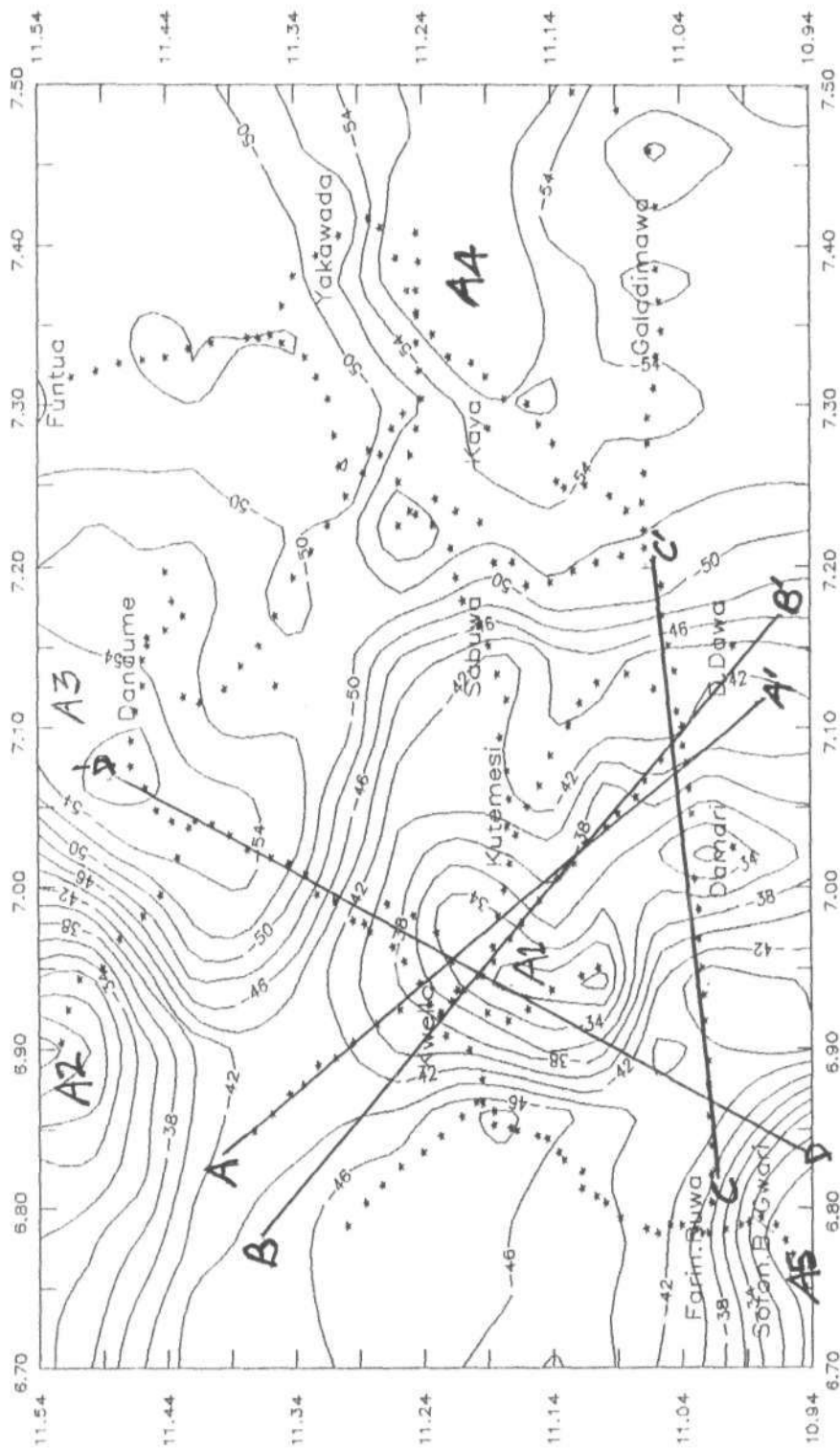


Figure 4.2: Bouguer Anomaly Map of Kwello

4.2.3 Free-Air Anomaly And Topographic Maps

The vertical gradient of gravity is approximately the simple effect of a station at higher elevation being further away from the center of the earth. To a close approximation, the effect is linear and independent of latitude (Nettleton, 1976). The free-air coefficient is 0.3086 mGal/m. It is called free-air because the theoretical anomaly is calculated as if the gravity measurement were made at the elevation of the station without taking into account the attraction of material between that elevation and mean sea level; that is, as if the gravity measuring instrument were suspended freely in the air. The free-air anomaly map which represents the difference between the free-air gravity and the theoretical gravity is shown in Figure 4.3.

In order to investigate the relationship between the free-air anomaly and heights, a plot of the observed height of the area in the field was carried out. The height values were first gridded as discussed in section 4.2.1 and contoured. The resulting map of the observed elevation of the area is shown in Figure 4.4. The relationship between the free-air anomaly and the topography of the survey area is explained in section 5.2.2.

4.2.4 THE REGIONAL ANOMALY FIELD

The picture which Bouguer gravity map presents is usually one that shows the superposition of disturbances of noticeably different orders of size. The larger features generally show up as trends which continue smoothly over very considerable areas and they are caused by deeper heterogeneity in the earth's crust. Super imposed on these trends but frequently camouflaged by them lie the smaller and shallower local disturbances which are generally secondary in size but primary in importance (Grant and West, 1965). The regional anomalies are usually of long wavelength and show a gradual

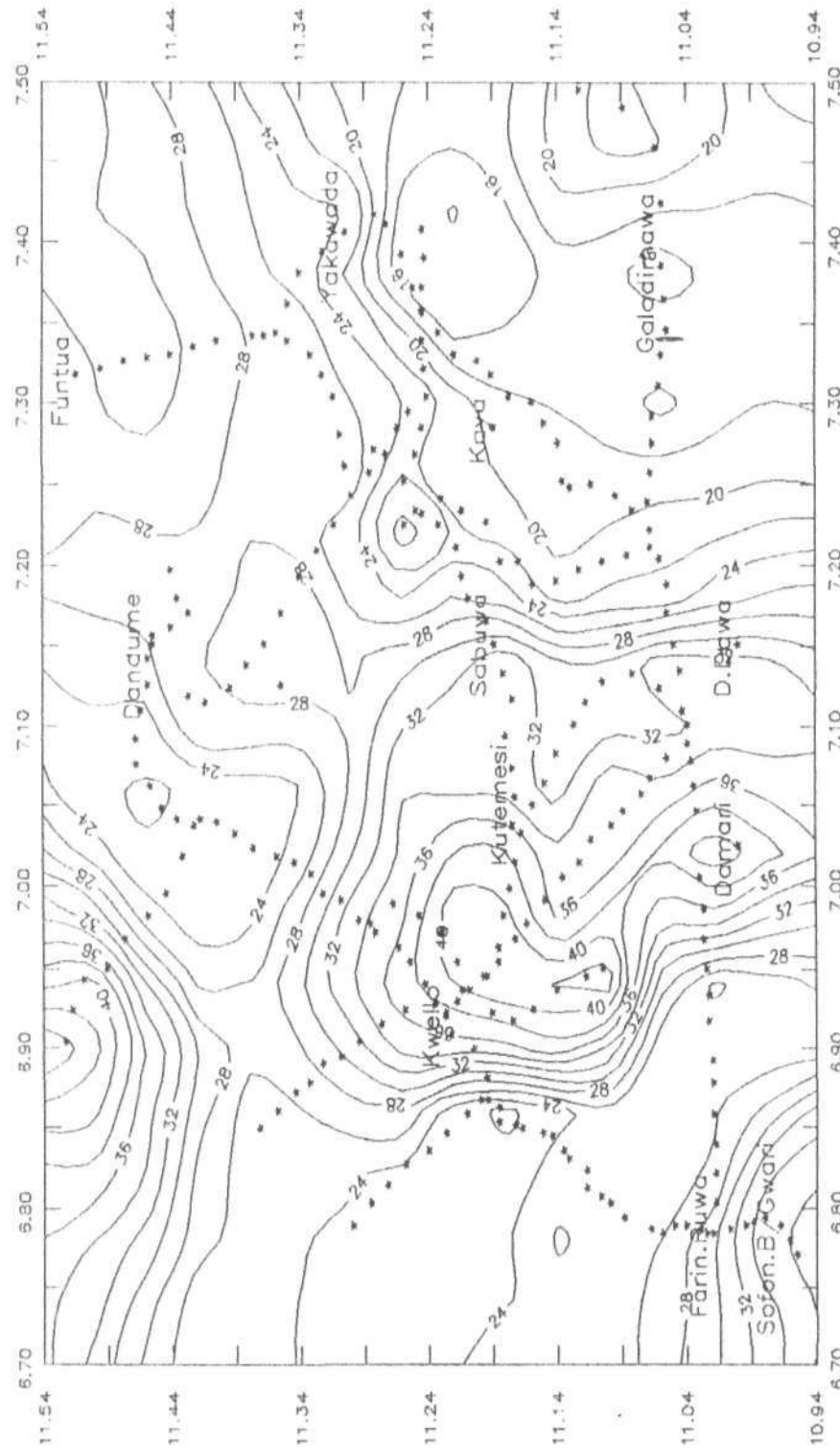


Figure 4.3: Free-Air Anomaly of Kwello

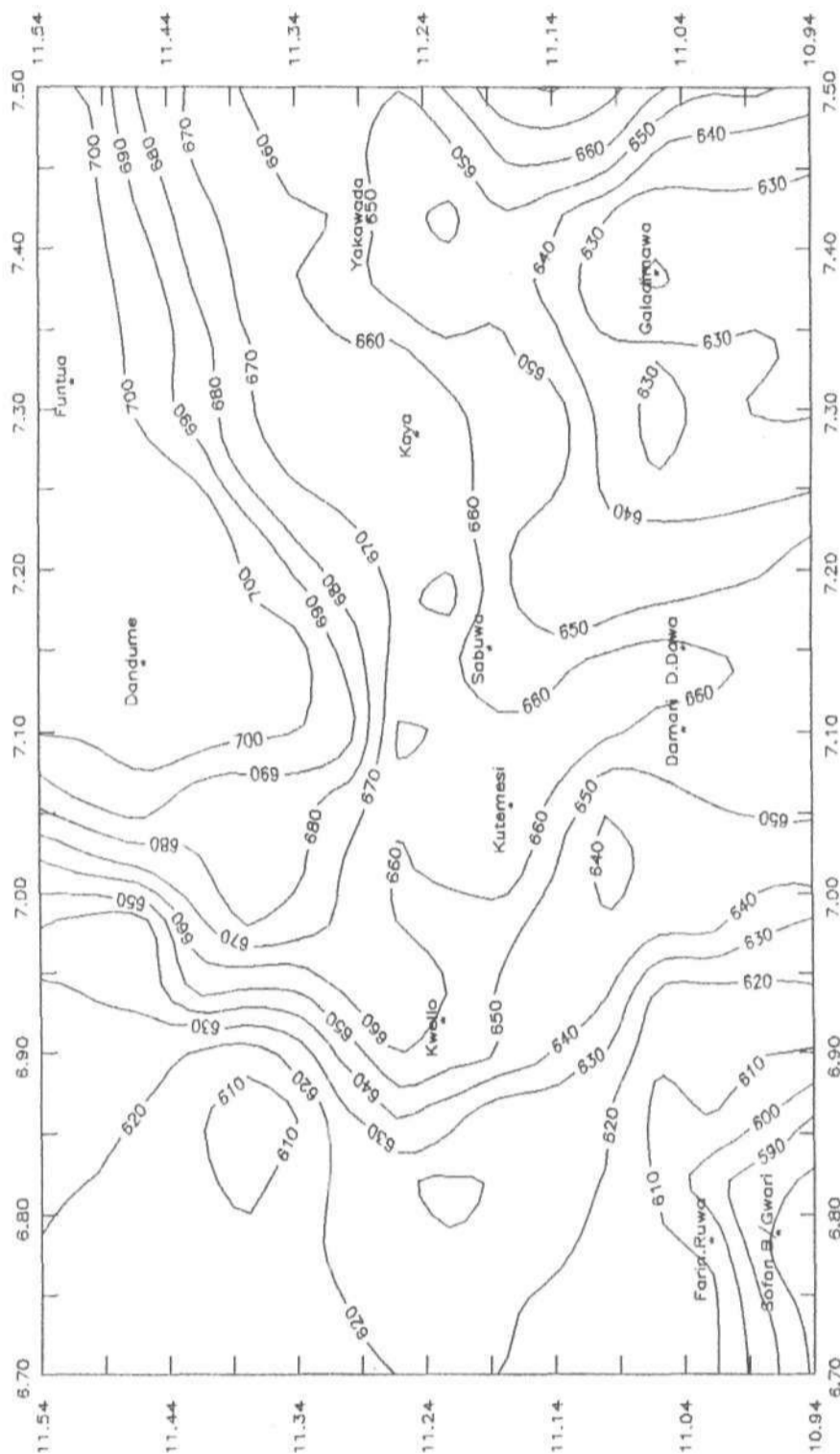


Figure 4.4: Contour map of Observed Elevation in the Study Area.

change in value while the residual anomalies which are due to local effects may show large variations.

No unique determination of the regional effect is possible although several graphical and mathematical methods have been developed by various authors for the regional and residual separation (Nettleton, 1954; Gupta and Ramani, 1980; etc), thus leading to inherent ambiguity. Each method has its merits and demerits. While the graphical method depends on the judgement of the operator, the mathematical methods depend on assumptions or empirical steps in the mathematical derivations of the numerical factors or coefficients used in the calculation.

The first order polynomial surface fitting was used for estimating the regional effect. This was first done using the data upward continued to 2.0 grid units (8.88 km). The regional effect for each case was calculated using a computer program which is based on the robust statistics. Its advantage lies in the fact that it computes a regional that is less affected by the variations of the residual field. Kearey and Brooks, (1984), observed that the upward continuation methods are employed in gravity interpretation to determine the form of regional gravity field over a study area since the regional field is assumed to originate from relatively deep-seated structures. The regional maps obtained from the two sets of data (Figures 4.5 and 4.6) are similar. They both show a similar North-South regional trend having an East-West gradients of 0.18/km and 0.13/km respectively. The regional obtained from the upward-continued field was accepted though it does not have a significant variation with the one from the observed data.

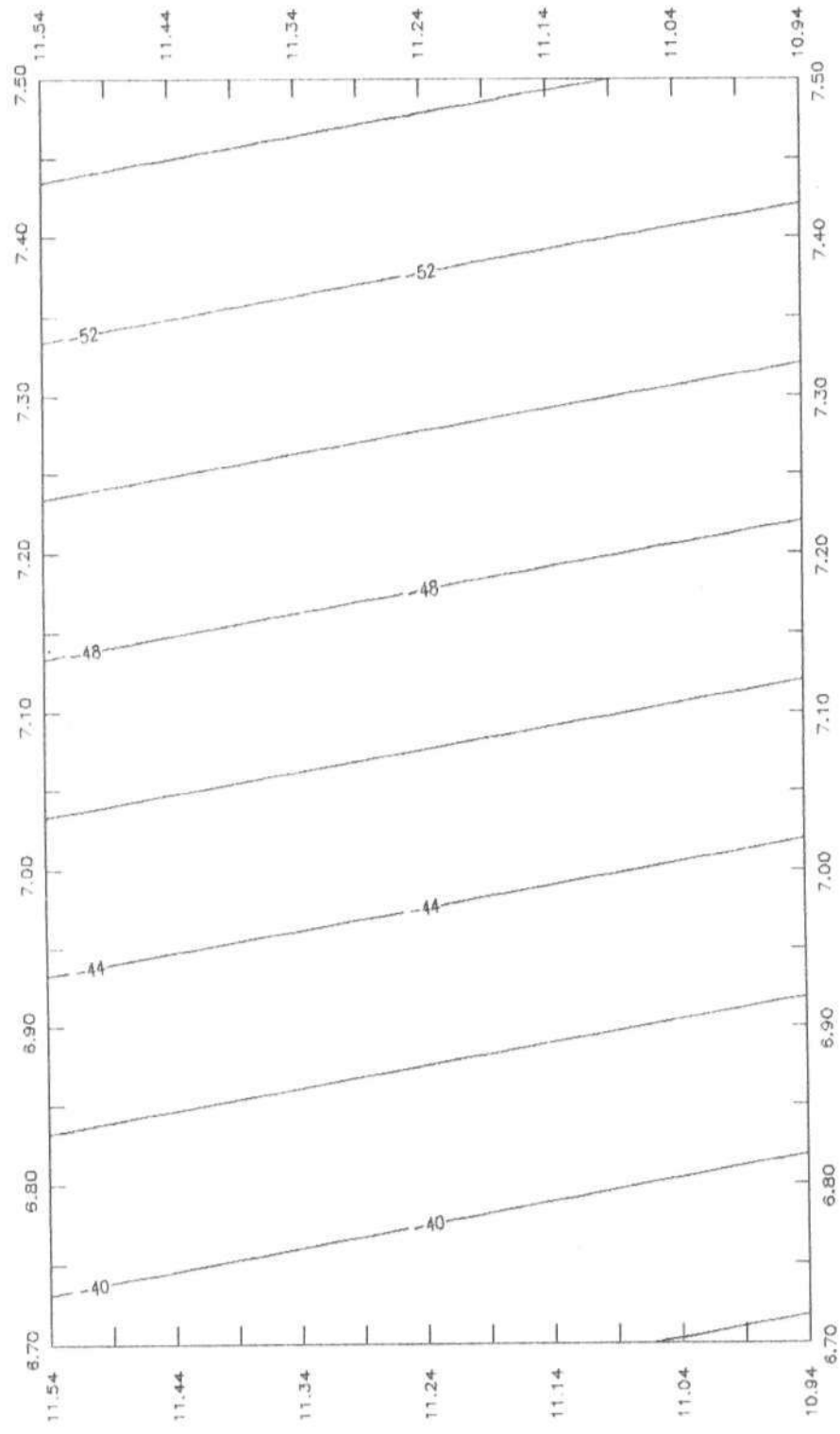


Figure 4.5: Regional Anomaly Of Kwello

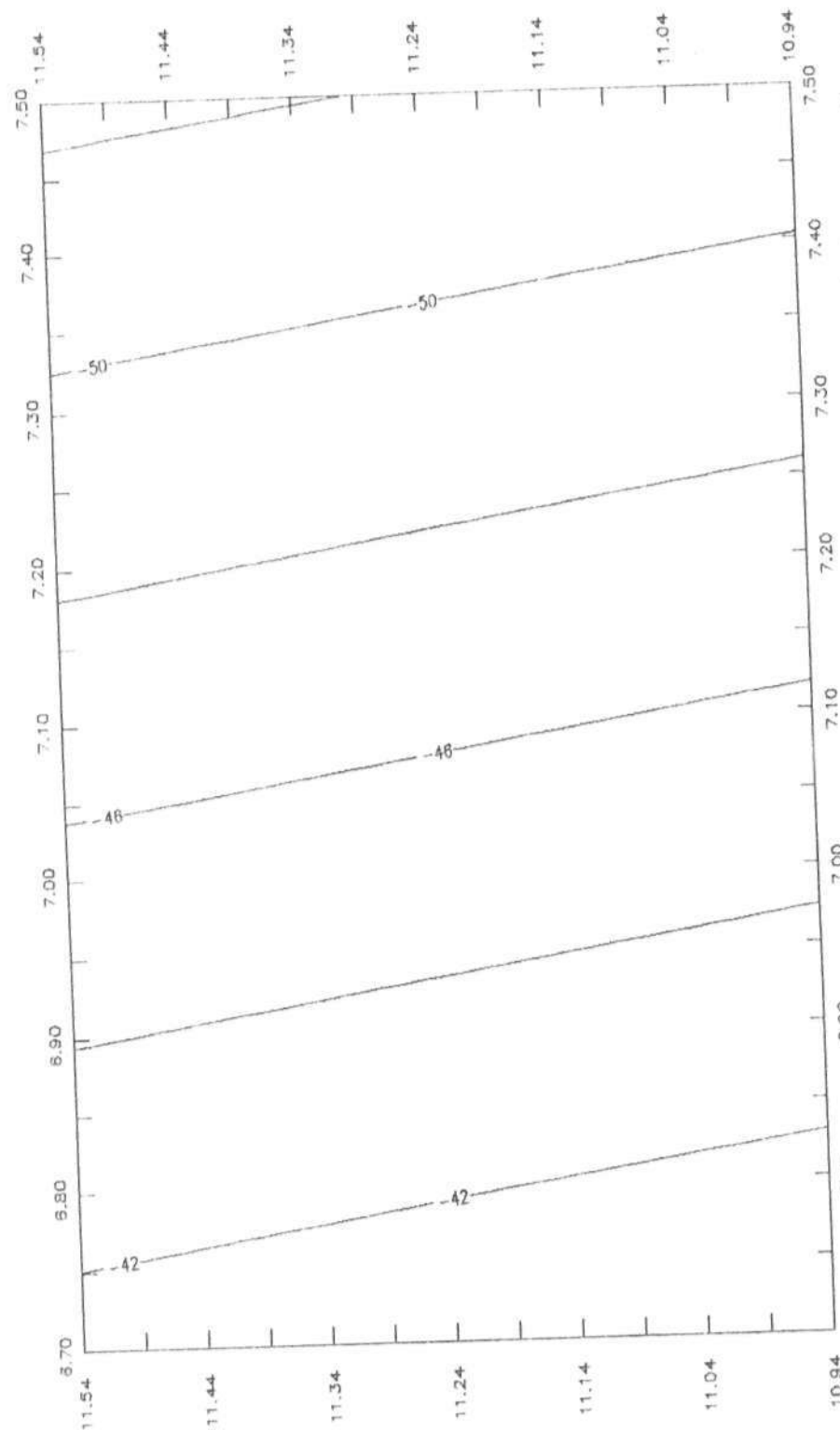


Figure 4.6: Regional Anomaly Of Kwello (From upward continued data)

This is because the regional trend is best estimated using the values in the less anomalous (distorted) area, which is achieved by the filtering process of the upward continuation. However, the residual field used in the modelling is obtained from observed data points since the upward continued data is already interpolated and has some errors introduced to it due to interpolation, and in other to have all the required parameters of the data points for the modelling program (e.g station elevation). The regional maps, (Figures 4.5 and 4.6), correlate very well with those of the survey carried out by Gandu *et al* (1986) in an adjacent area, which has a similar N-S regional trend. The relatively low gradient of the trend (0.13/km) suggests that the causative body is of deep origin. The regional anomaly showed a total change of 16 in a distance of 90km.

4.2.5 THE RESIDUAL ANOMALY FIELD

The residual anomaly Δg_{res} , is expressed as

$$\Delta g_{res} = \Delta g_B - \Delta \bar{g} \dots \dots \dots (4.1)$$

where Δg_B is the observed Bouguer anomaly and Δg is the regional effect. The nature of the residual map is dictated by the estimation of the regional effect. The regional anomaly is obtained by subtracting the regional field from the Bouguer anomaly. For each data point, the regional anomaly was computed. This value was then subtracted from the Bouguer anomaly for that point to obtain the residual anomaly. The residual anomalies at all the points were gridded by interpolation as discussed in section 4.2.1 and contoured. The resulting map, (Figure 4.7), describe the gravitational effect of near-surface and local structures.

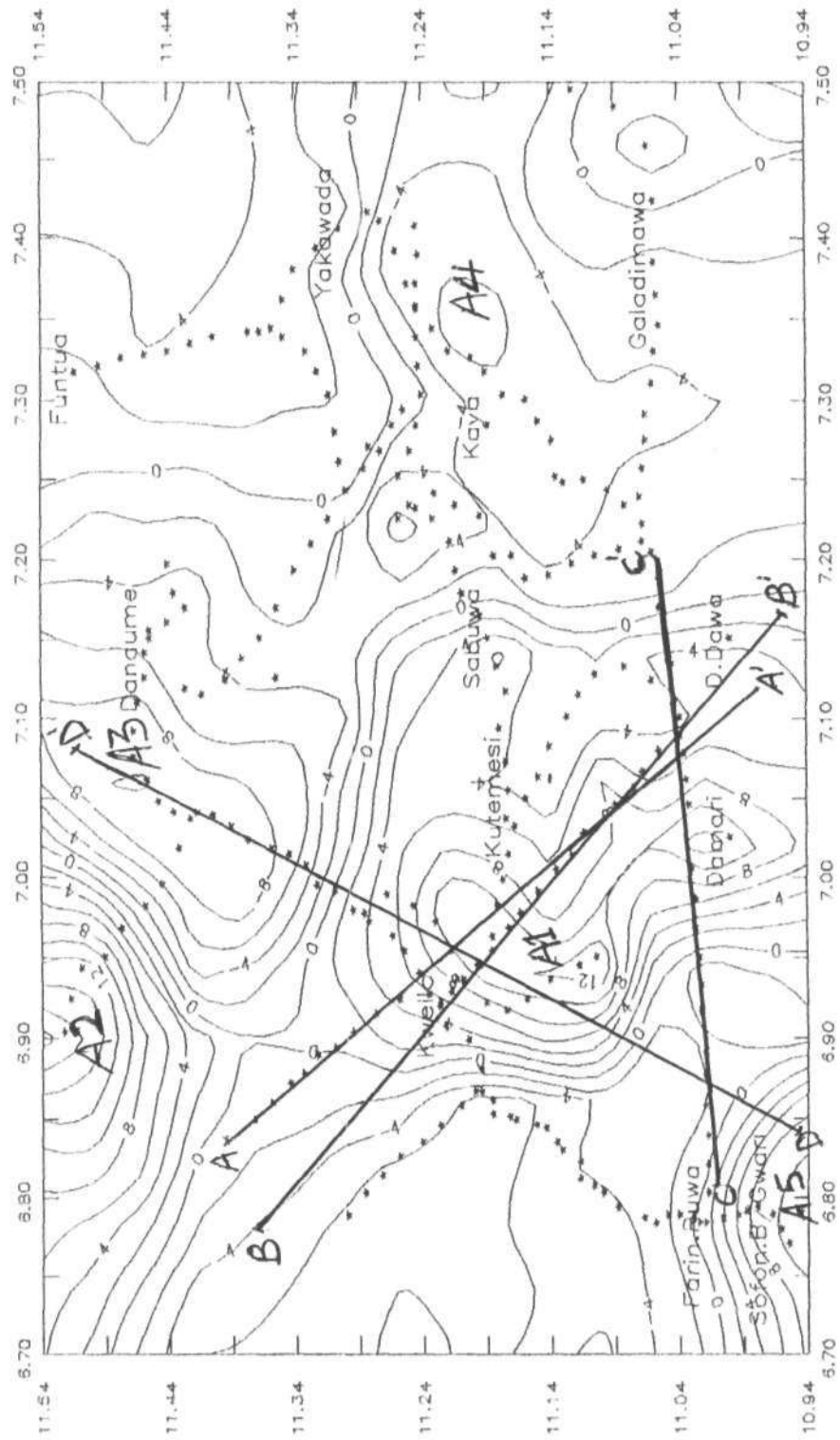


Figure 4.7: Residual Anomaly Of Kweilo

To minimize errors in the residual anomaly values used in the interpretation, the residuals for the interpretation were obtained by taking profiles from the Bouguer map (Figure 4.2), fitting a first order polynomial surface to it, and subtracting the regional obtained from the observed gravity field along the profiles.

CHAPTER FIVE

5.0 INTERPRETATION OF BOUGUER AND RESIDUAL ANOMALIES

5.1 INTRODUCTION

The gravitational field of the earth has a world wide average of 980-Gals with a total variation of about 5.3 Gals from the equator to the poles (Dobrin, 1976). The range of gravity variation in Nigeria is 376.948 mGal, of which that expected in Kwello area is 28.646 mGal (Kano - Katsina difference) (Osazuwa, 1985; Osazuwa and Ajakaiye, 1992). In general, areas underlain by acidic rocks such as granite plutons have gravity lows whereas more mafic rock types show gravity highs.

5.2 QUALITATIVE INTERPRETATION5.2.1 The Bouguer Anomaly Map

Figure 4.2 shows that the survey area is characterized by negative Bouguer values ranging from -30 mGal in the Kwello area to -58 mGal in the eastern part of the area. The major gravity high labelled as 'A1', occurs near Kwello and centered on a schist body (Figure 5.1). Another gravity high labelled 'A2' occurs at the NW-corner. Due to lack of detailed and sufficient field data over the area the gravity high 'A2' is not interpreted. This is the reason also for not interpreting the anomaly at the SW - corner. The dominant trend of the Bouguer field can be seen to be N-S. A major gravity low ranging from -44 mGal to -56 mGal and labelled 'A3', occurs near Dandume area and is centered on a stock of older granites (Figure 5.1). A steep gradient of 1 mGal/km is indicated between 'A1' and 'A3'. The steepness suggests a

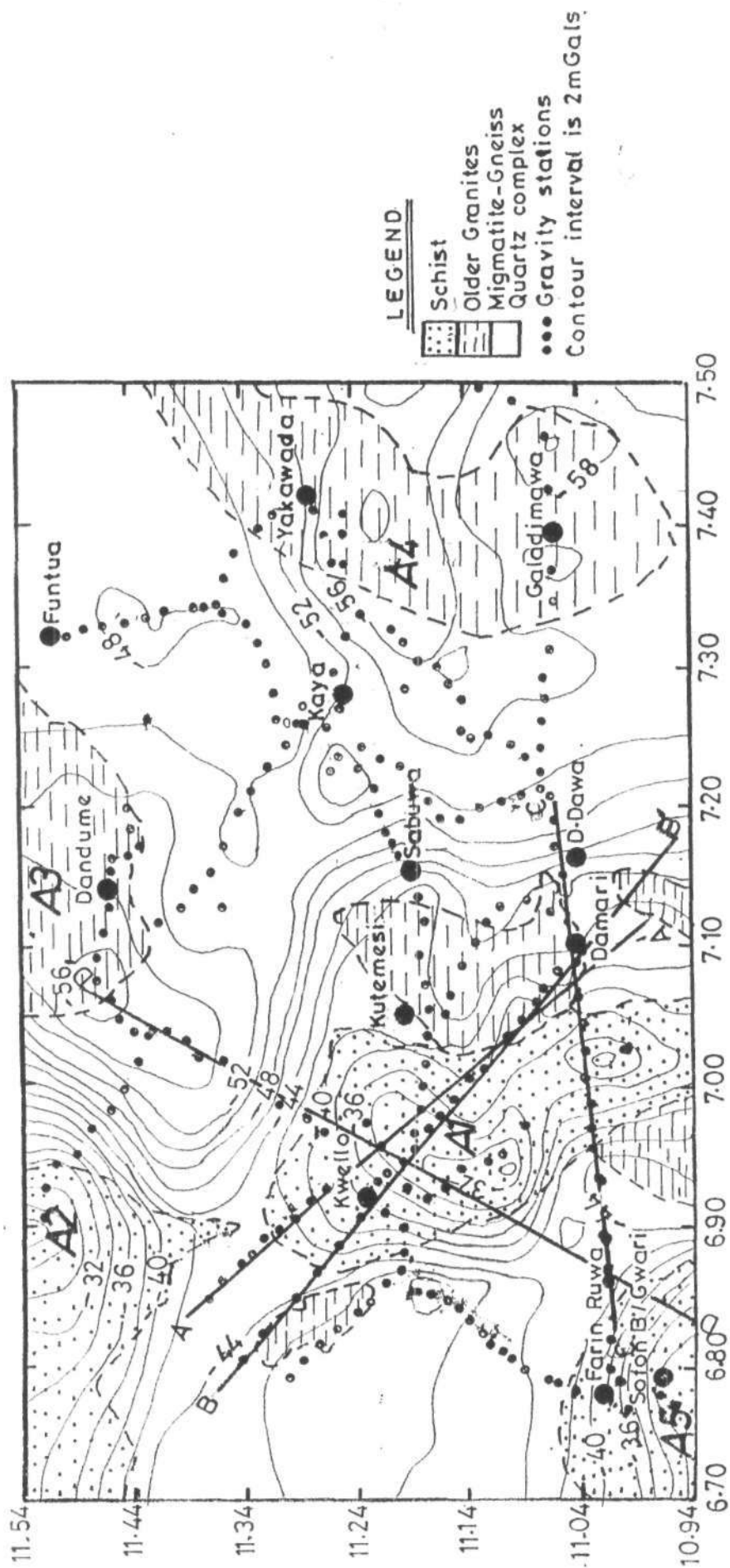


Figure 5.1: Bouguer anomaly of Kwello area superimposed over the geologic map

sharp geologic contact between the bodies or possibly faulting. There is also a NE-SW trend in the eastern part near Yakawada. The different trends together with available geological information suggest that they are heavily influenced by the local geology of the areas.

The Bouguer anomaly map (Figure 4.2) shows a relative gravity high ranging from -30 mGal to -42 mGal in the south west where a schist body is mapped (Figure 5.1) in the Sofon Brinin-Gwari area. The contour pattern in the SW indicates that the centre of this body is beyond the limits of the survey area. The eastern parts of Figure 5.1 shows that the negative contour closures at that part of the map are on granitic intrusion.

The gravity highs could be ascribed to intra - basement igneous intrusions of intermediate to basic composition, while the gravity lows may be caused by acidic granitic intrusions supposedly widespread in the area. Figure 5.1 shows the geological map of the area superimposed over the Bouguer anomaly map. There is a good correlation between the Bouguer field trend and the underlying geologic features.

5.2.2 Free-Air Anomaly Field

The Free-air anomaly map shown in Figure 4.3 is characterized by positive anomalies ranging from 14 mGal to 42 mGal. As the mass between the observation height and the mean sea level is not considered in the computation of the free-air, the anomaly mainly represents the influence of topographic features superposed over the effect of subsurface structures. The free-air anomaly provides a broad assessment of the degree of isostatic compensation of an area (Kearey and Brooks, 1984). The pattern of

the contours suggests that the presence of schists in the area may have influenced the free-air anomalies such that high free-air anomalies are found where there is Bouguer gravity high. According to Gandu *et al* (1986) it was reported from studies in Ghana that there is a substantial increase in the free-air anomalies around gold-manganese province over Bouguer gravity highs. It is clear from Figures 4.3 and 4.4 that low free-air occurs in the areas with high elevation as seen in Dandume area, while high free-air occurs in the area of low elevation as in the Kwello and the SW - corner. Hence the area could be said to have been isostatically compensated.

5.2.3 Residual Anomaly Field

The first order residual anomaly map of the study area obtained is shown in Figure 4.7. The residual map is characterized by both positive and negative anomalies. The first one which is labelled as 'A1' near Kwello has an amplitude of +12 mGal. The second labelled 'A3' near Dandume is a gravity low with values ranging from -2 mGal to -10mGal and the third labelled 'A4' near Kaya is a low with an amplitude of -6 mGal. There is high at the SW-corner of the map around Sofon Brini-Gwari labelled 'A5', but due to lack of sufficient data coverage at the area the anomaly was not interpreted.

The residual anomaly map superimposed over the geologic map of the area is shown in Figure 5.2. The two maps show good correlation with each other. The gravity high around the kwello and Sofon Brini-Gwari areas ('A1' and 'A5' respectively) are directly located over mapped body of schists. The gravity lows around Dandume and Kaya ('A3' and 'A4' respectively) correspond to granite intrusions into a gneissic basement. It is also observed that there is a NW - SE trend in the residual map.

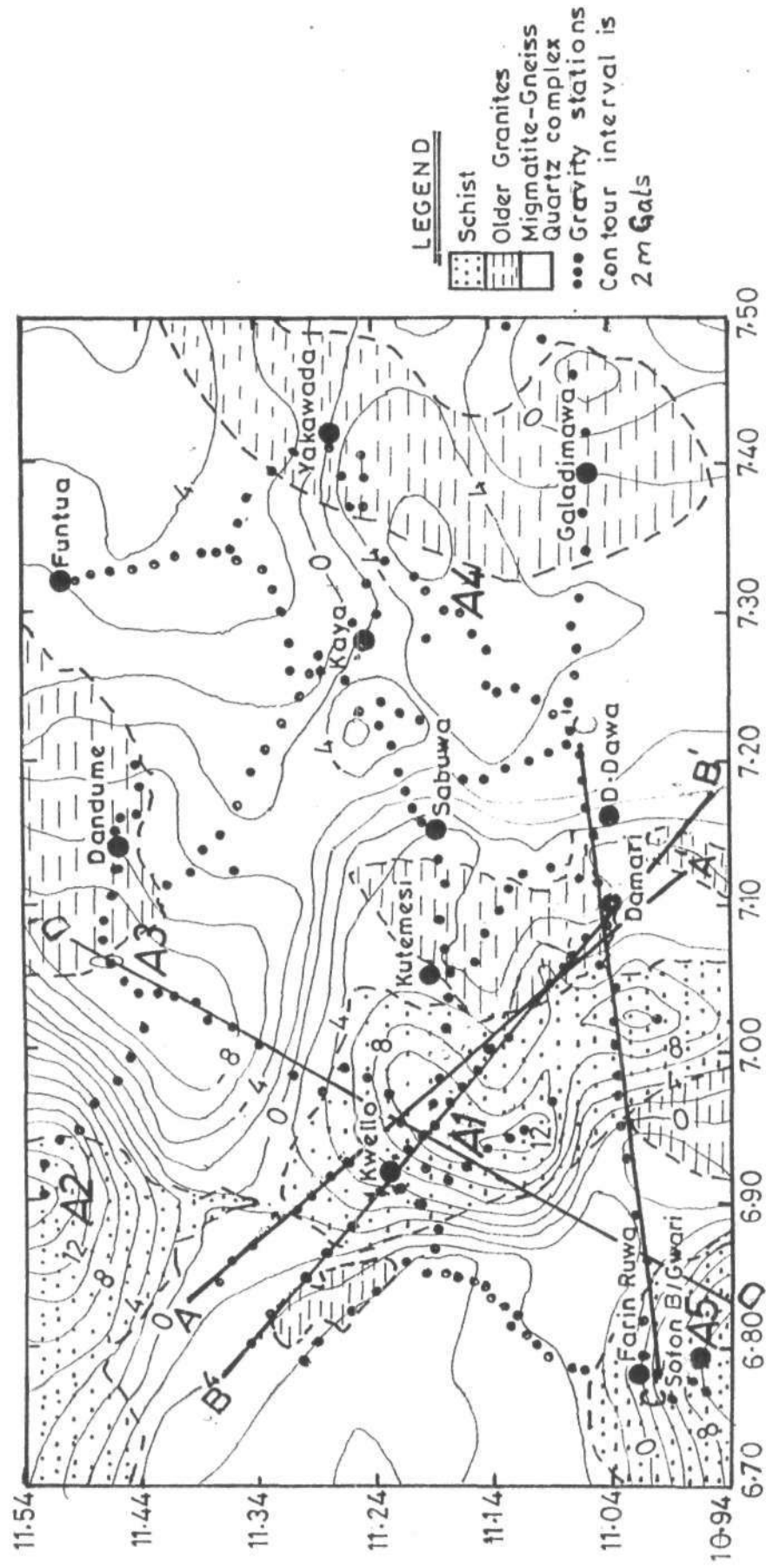


Figure 5.2 : Residual anomaly of Kwello superimposed over the geologic map

5.2.4 The Upward Continuation Field.

The gravity fields obtained at various grid units are shown in Figures 5.3 to 5.8. Notice that the anomalies with shortest wavelengths in the original data are attenuated relative to anomalies with longer dimensions by upward continuation filter. Many of the remaining features are caused by sources of more regional scale and this shows how gravity data would look if they had been measured on the higher surface. It is also observed that anomalies 'A1' and 'A3' (Figure 5.2) almost disappeared at the upward continuation of 1.5 grid units (6.66 km) (Figures 5.5 and 5.6). This roughly provides an estimate of the depths of the causative bodies.

5.2.5 Downward Continuation Field.

Downward continuation is a process by which a measured field from one datum surface is mathematically projected downward to another level surface. In downward continuation an important aspect of the underlying theory is that when the field is continued too close to the depth of the anomalous structure, oscillation sets in due to the instability of the field at that point. Figures 5.9 and 5.10 show the downward continuation fields obtained the original Bouguer gravity data.

Due to the fact that the study area is in the basement complex of NW Nigeria, the downward continuation maps produced (Figures 5.9 and 5.10) have spurious anomalies due to wild oscillations often observed if the field is downward continued into the source region. The oscillation is amplified as the depth of continuation increased (Figure 5.10).

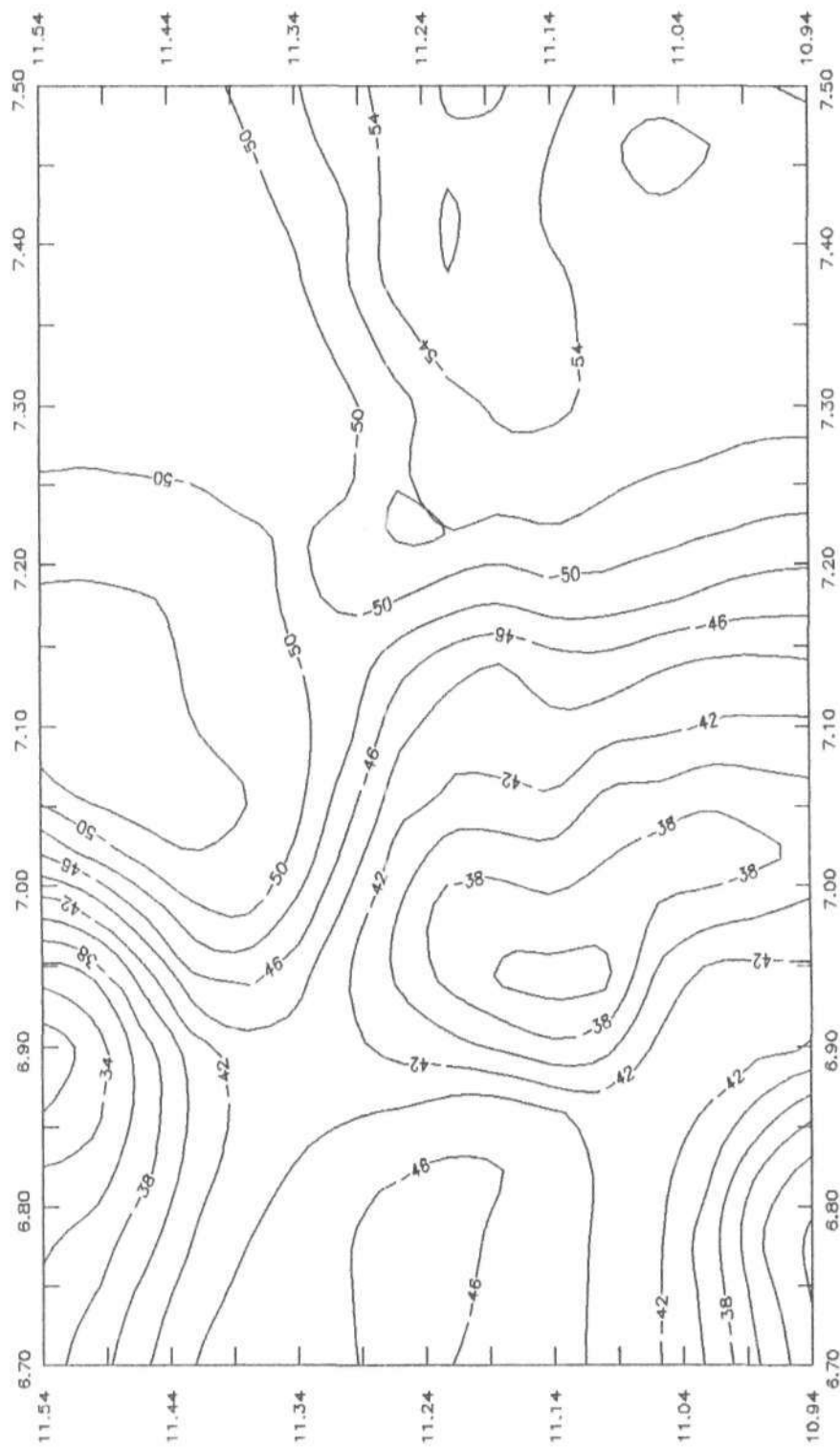


Figure 5.3: Bouguer Anomaly Upward Continued By 0.5 Grid Unit.

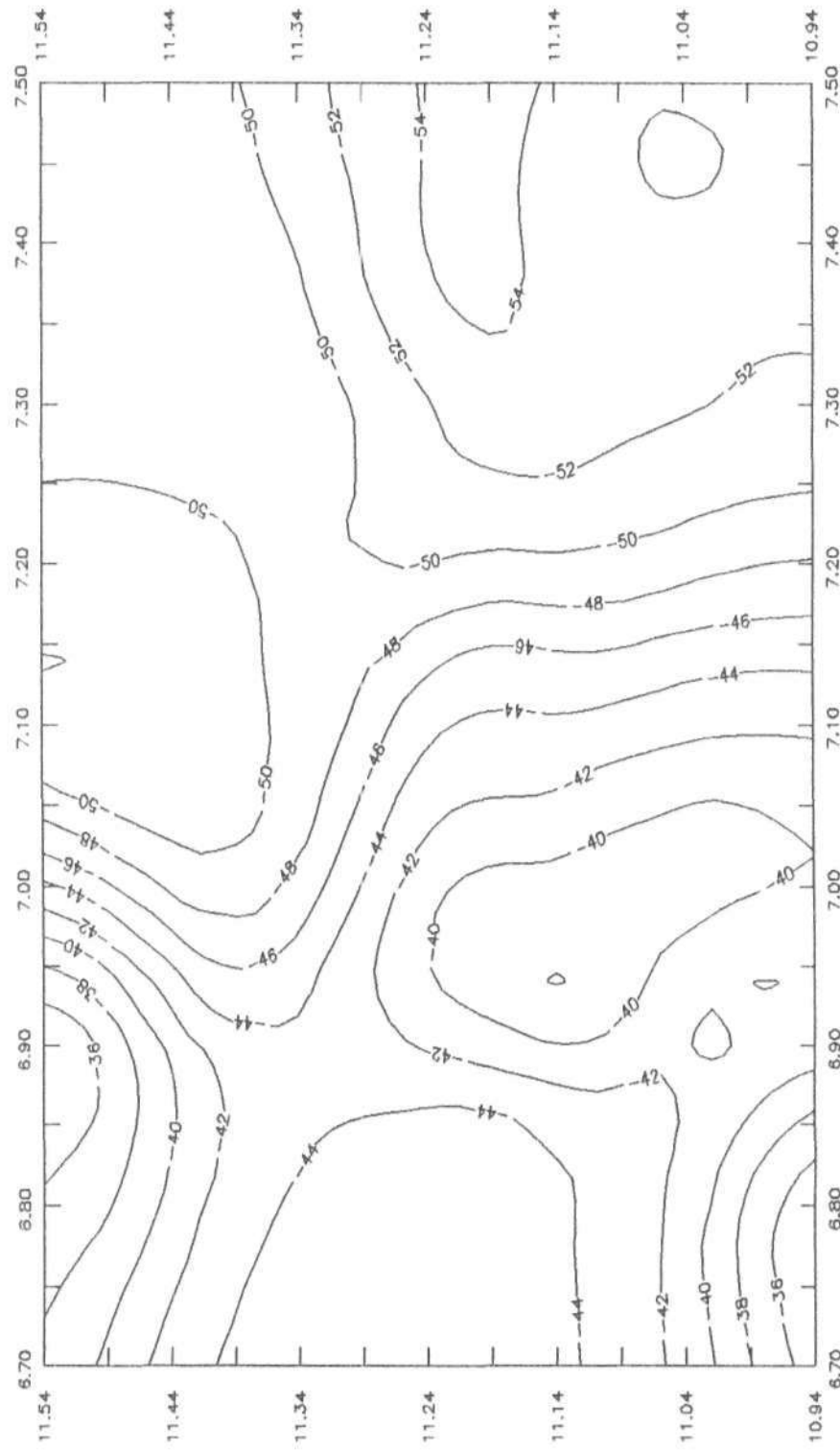


Figure 5.4: Bouguer Anomaly Upward Continued By 1.0 Grid Unit.

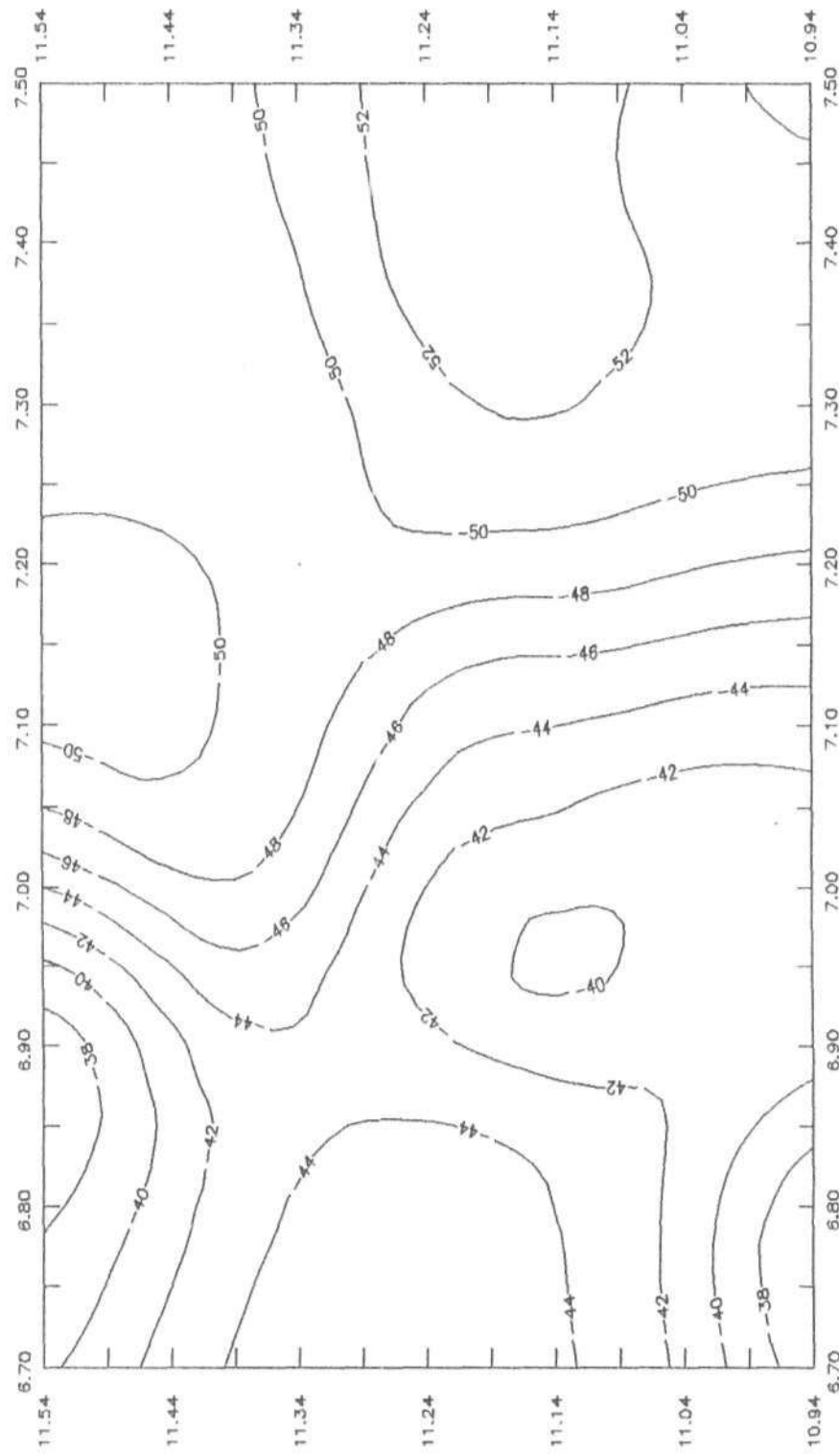


Figure 5.5: Bouguer Anomaly Upward Continued By 1.5 Grid Units.

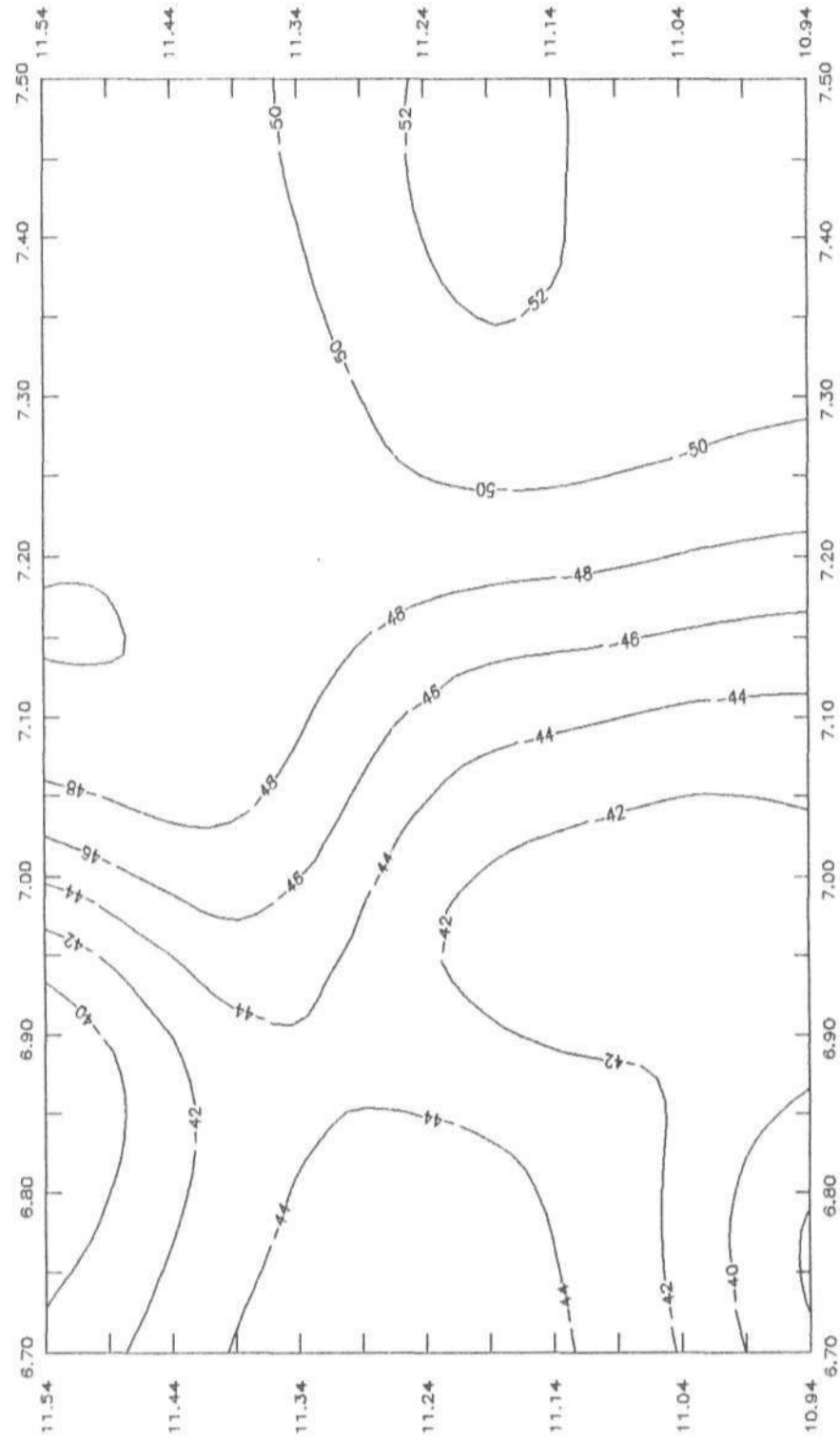


Figure 5.6: Bouguer Anomaly Upward Continued By 2.0 Grid Units.

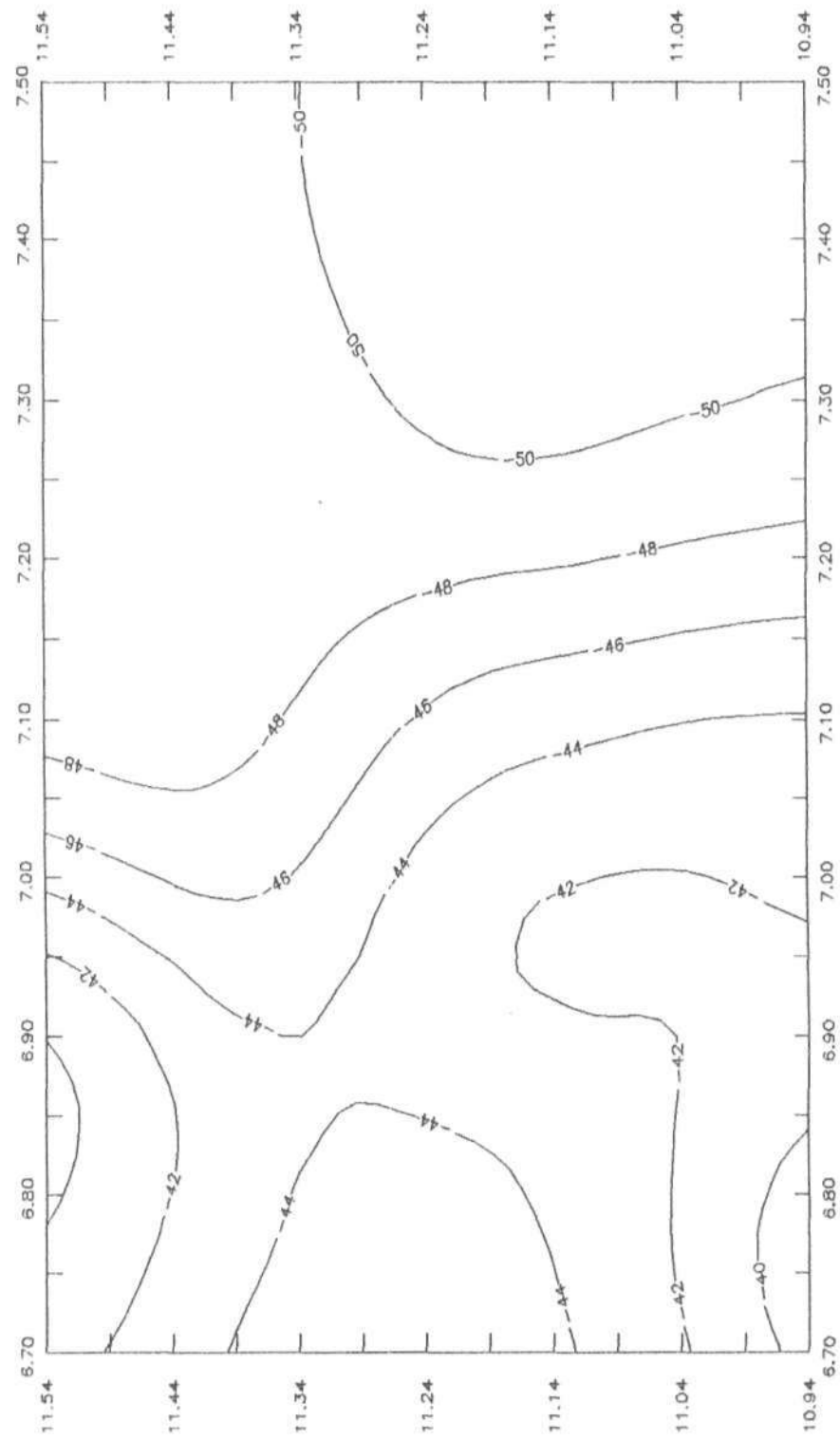


Figure 5.7: Bouguer Anomaly Upward Continued By 2.5 Grid Units.

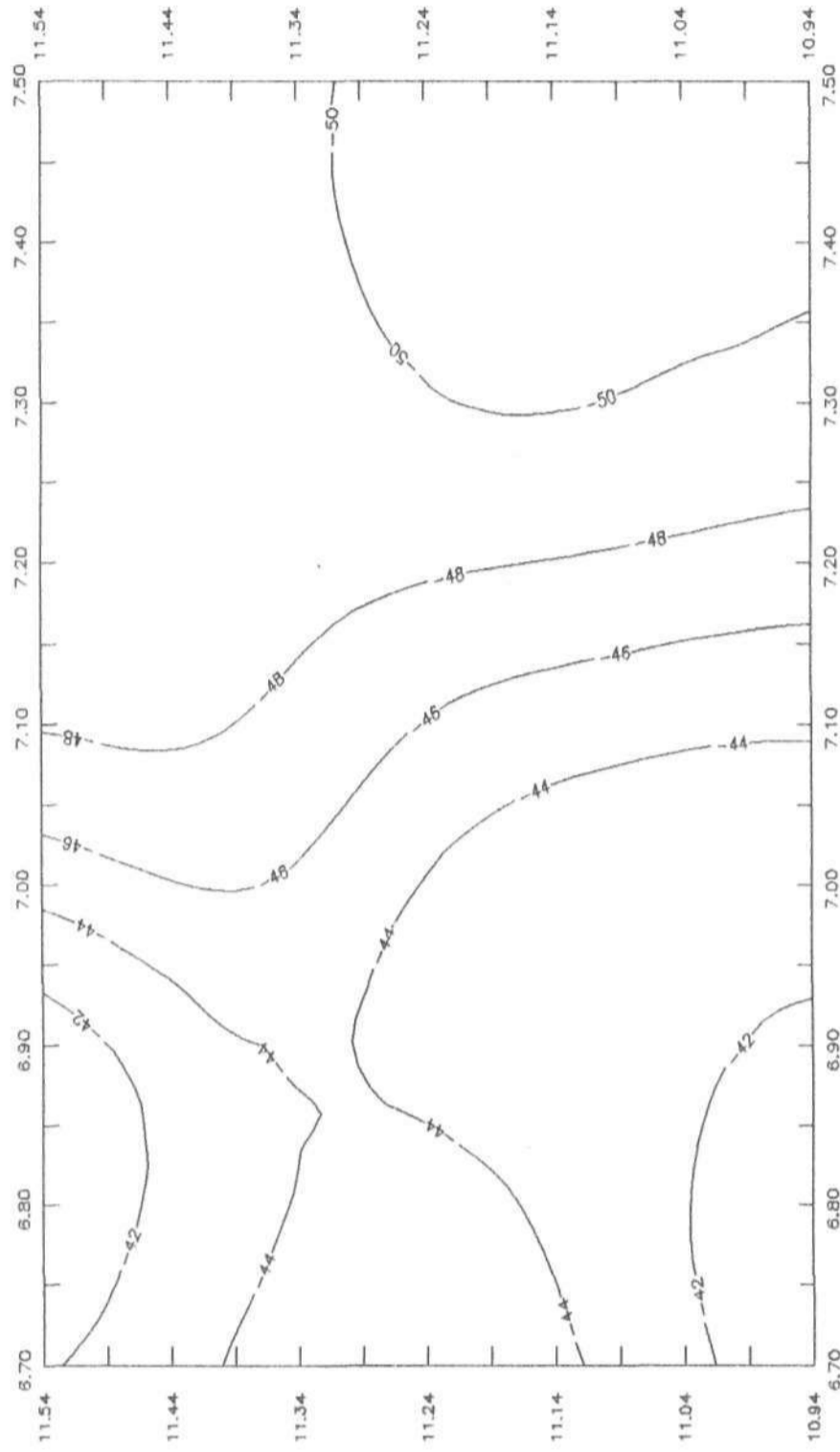


Figure 5.8: Bouguer Anomaly Upward Continued By 3.0 Grid Units.

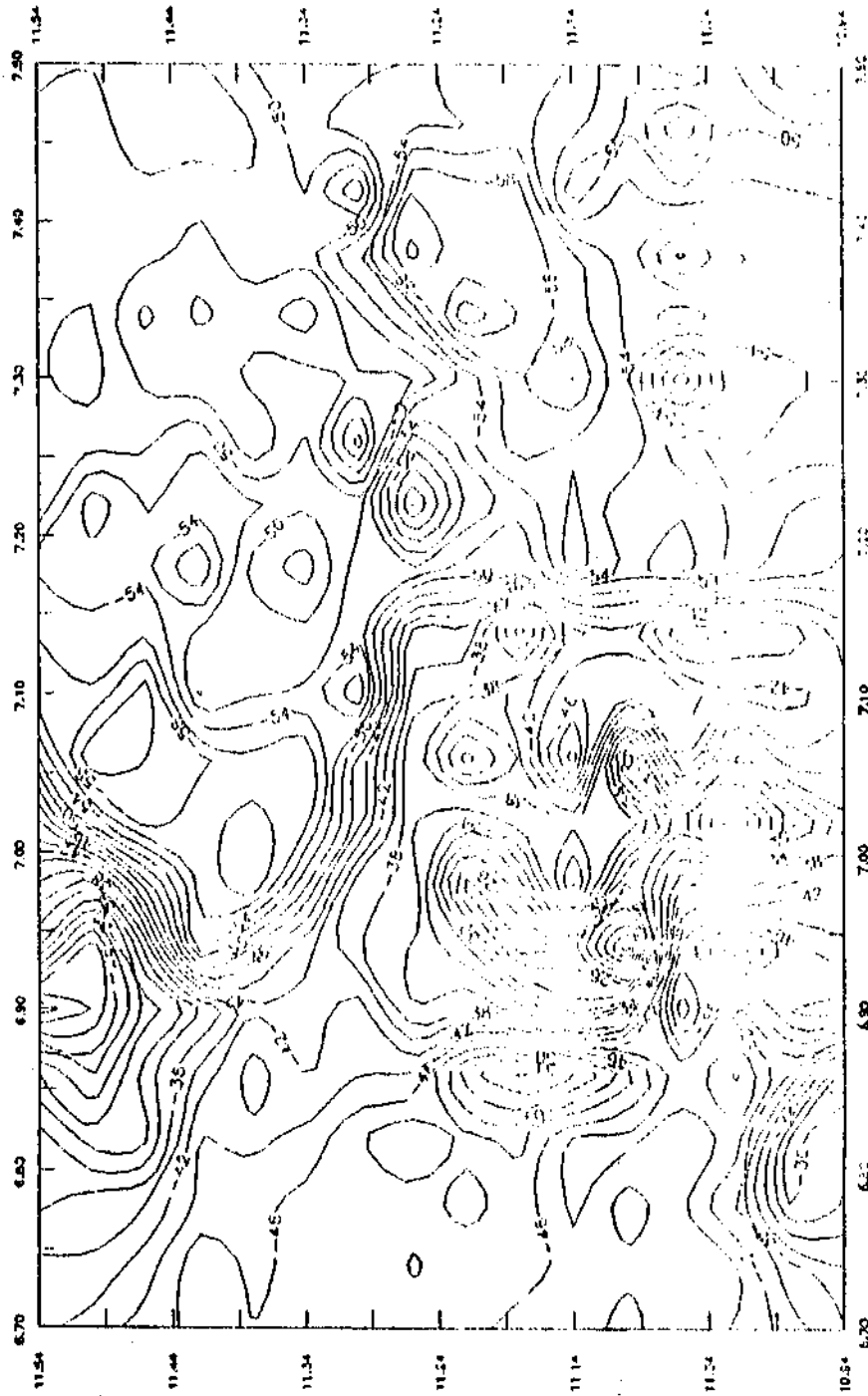


Figure 5.9: Bouguer Anomaly Downward Continued By 0.5 Grid Unit.

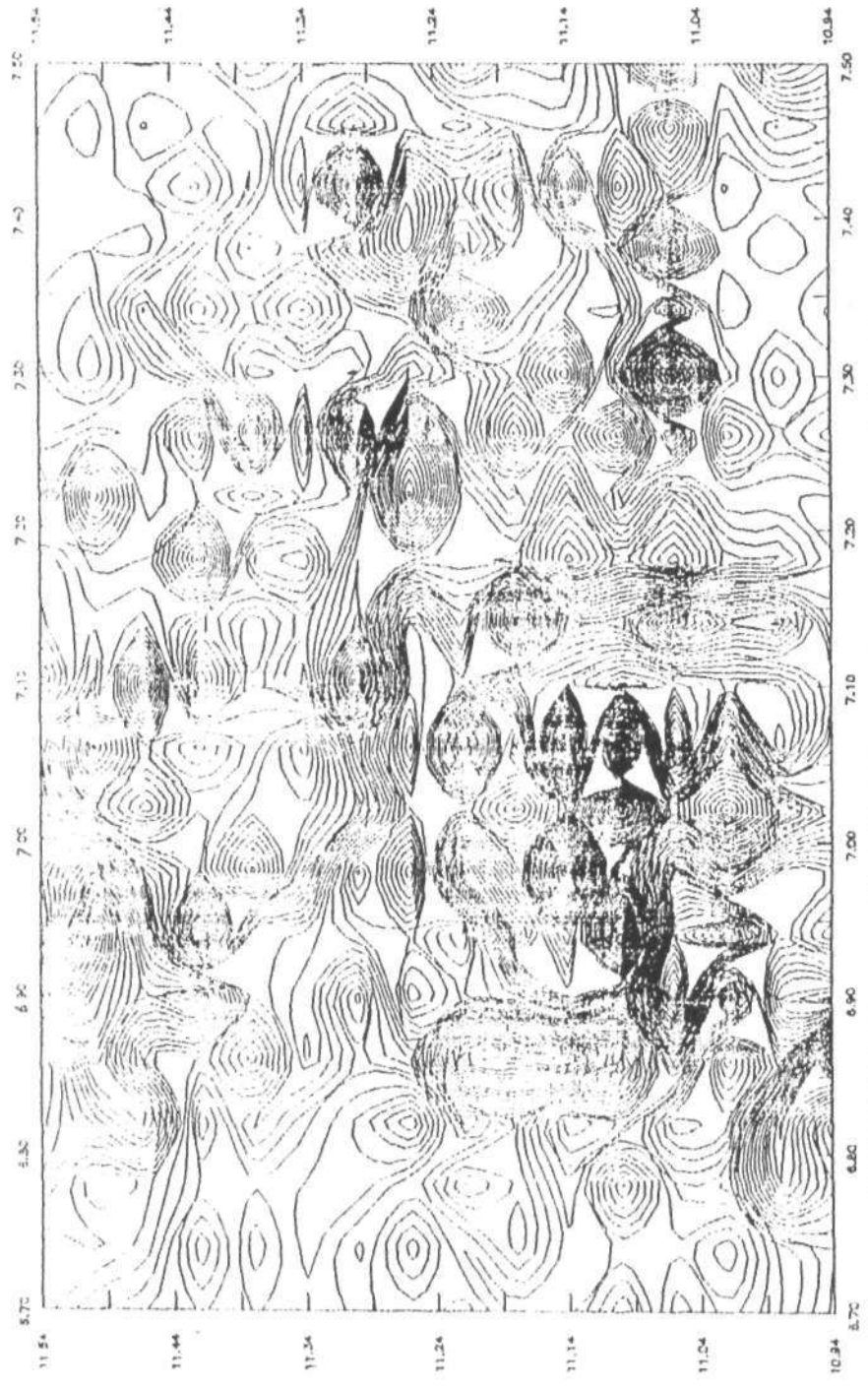


Figure 5.10: Bouguer Anomaly Downward Continued By 1.0 Grid Unit.

5.5.6 Second Vertical Derivative Field.

The second vertical derivative field measures the curvature of a given field. Its usefulness stems from the fact that the effects of nearby structures, even when they are small, are subjected to more abrupt changes and therefore have a greater influence on gravity gradients than on gravity itself. For this reason, the anomalies of shallower structures are enhanced on derivative maps than those of more deeply seated structures.

In addition to enhancing weaker local anomalies, second vertical derivatives are often used to delineate sub-surface contacts of lithologies having contrasting densities. Figure 5.11 shows the map of the second vertical derivative of the Bouguer anomaly. The map contains numerous closures which indicate locations of local features where residual anomalies may be found. The outlines of the anomalous features are often delineated by the zero contours in the map. Figure 5.12 shows the zero contour map of the second vertical derivative.

5.3 QUANTITATIVE INTERPRETATION OF THE RESIDUAL ANOMALIES

In quantitative interpretation of gravity data, a subsurface mass distribution is sought whose gravity effects satisfactorily approximates the observed gravity field measured on the surface. This interpretation cannot be unique. Therefore the gravity data must be constrained by geologic inferences. The gravitational effect of an assumed initial configuration is calculated and compared with the observed profile. Changes are made where necessary on the assumed configuration in order to get a better fit. This process is repeated within geologically reasonable limits until a new structure is obtained whose calculated effect fits the observed profile best. This approach is called forward modelling (Patterson and Reeves, 1985).

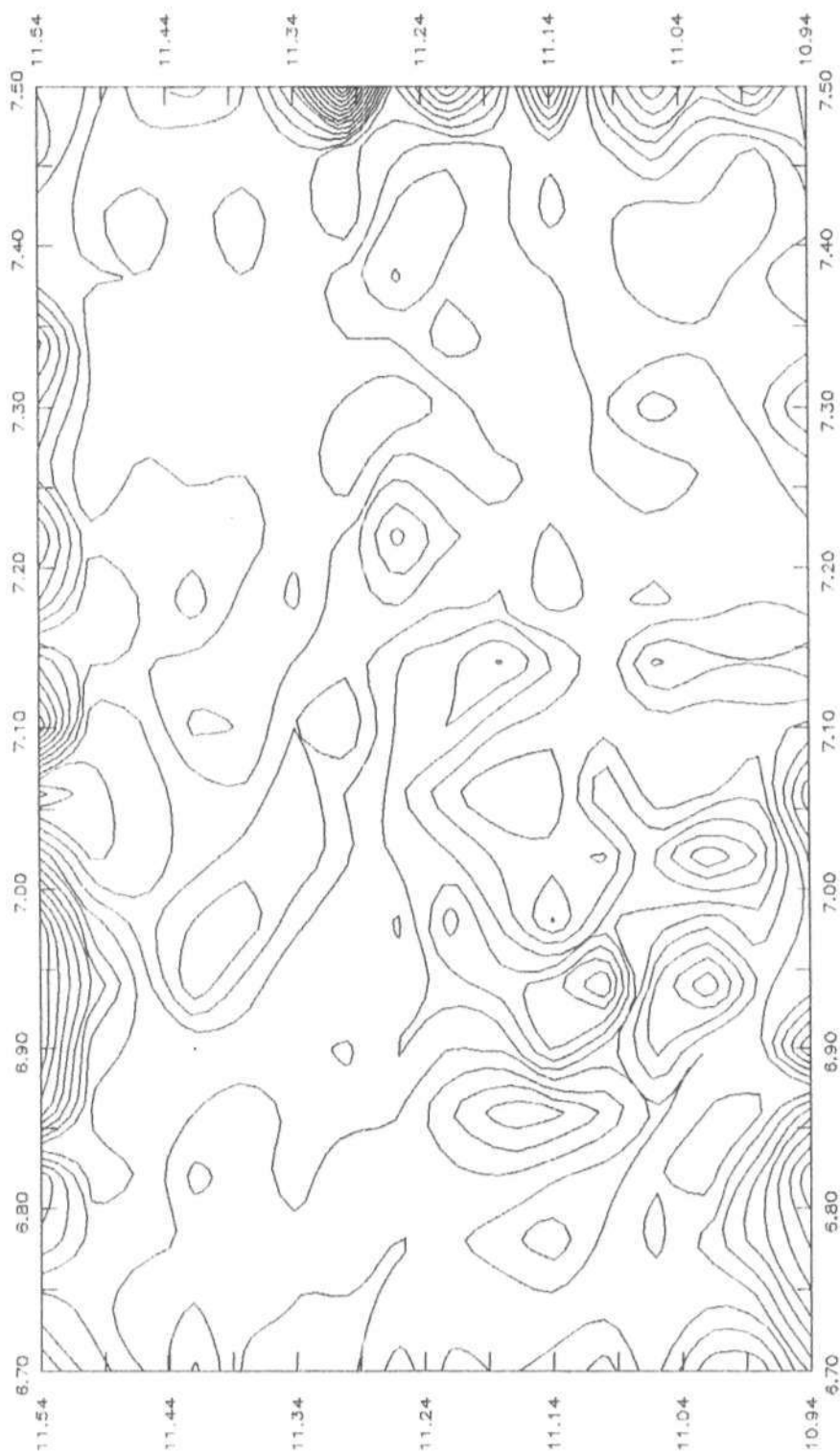


Figure 5.11 Second Vertical Derivative map (General)

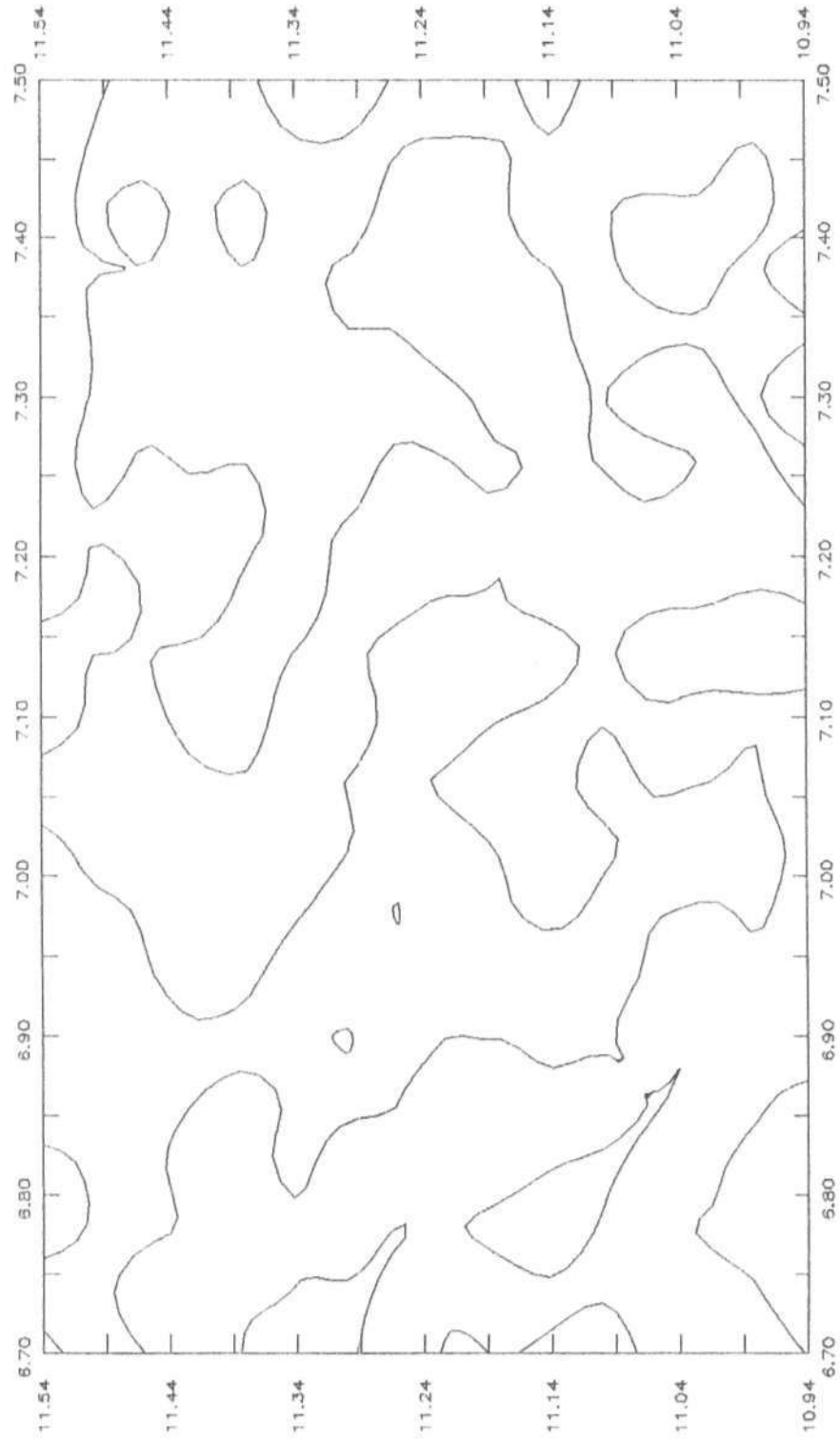


Figure 5.12 Second Vertical Derivative map (Zero Contours)

The coefficients used in calculating the regional trend along the profiles was obtained from considering the entire survey area. There was need, however, to fine tune the regional on each profile since the global mean regional for the area does not necessarily constitute an average along each profile (Osazuwa, Personal Communication). To achieve this, the geology map of the area provided a good control to produce a residual along the profiles which are symmetrical about a vertical or horizontal axis. Four profiles were chosen. Each of the profiles was chosen on the criteria that it crossed the major anomalies in the area and as well as many contour closures, and that it has data points throughout, or almost throughout its length. The Bouguer and regional anomalies and the residual anomalies along the profiles A-A', B-B', C-C', and D-D' are shown in Figures 5.13 - 5.15. A 2½-dimensional gravity/magnetics modelling software based on Talwani *et al* (1959) and Rasmussen and Pederson (1979) was used to model along the profiles (courtesy of Dan Dyrelius, Department of Solid Earth Physics, Uppsala University, Sweden).

5.3.1 Profile A-A'

This profile runs in the NW-SE direction and cuts across granite and schist rocks (Figure 5.2). Several models using various widths and depth estimates of the schist bodies and the granite bodies were considered. Comparing the computed anomalies with the observed, Figures 5.16 and 5.17, show two plausible models which could account for the residual anomalies along the profiles. The models show that the bodies have steeply dipping contacts with the host rock. The first model, Figure 5.16, shows that the schist body (anomaly 'A1') which has outcrops on the surface, extends down to a depth of about 2km. The schist body has inward dipping walls and dips at 60° and 50° on its NW and SE flanks respectively.

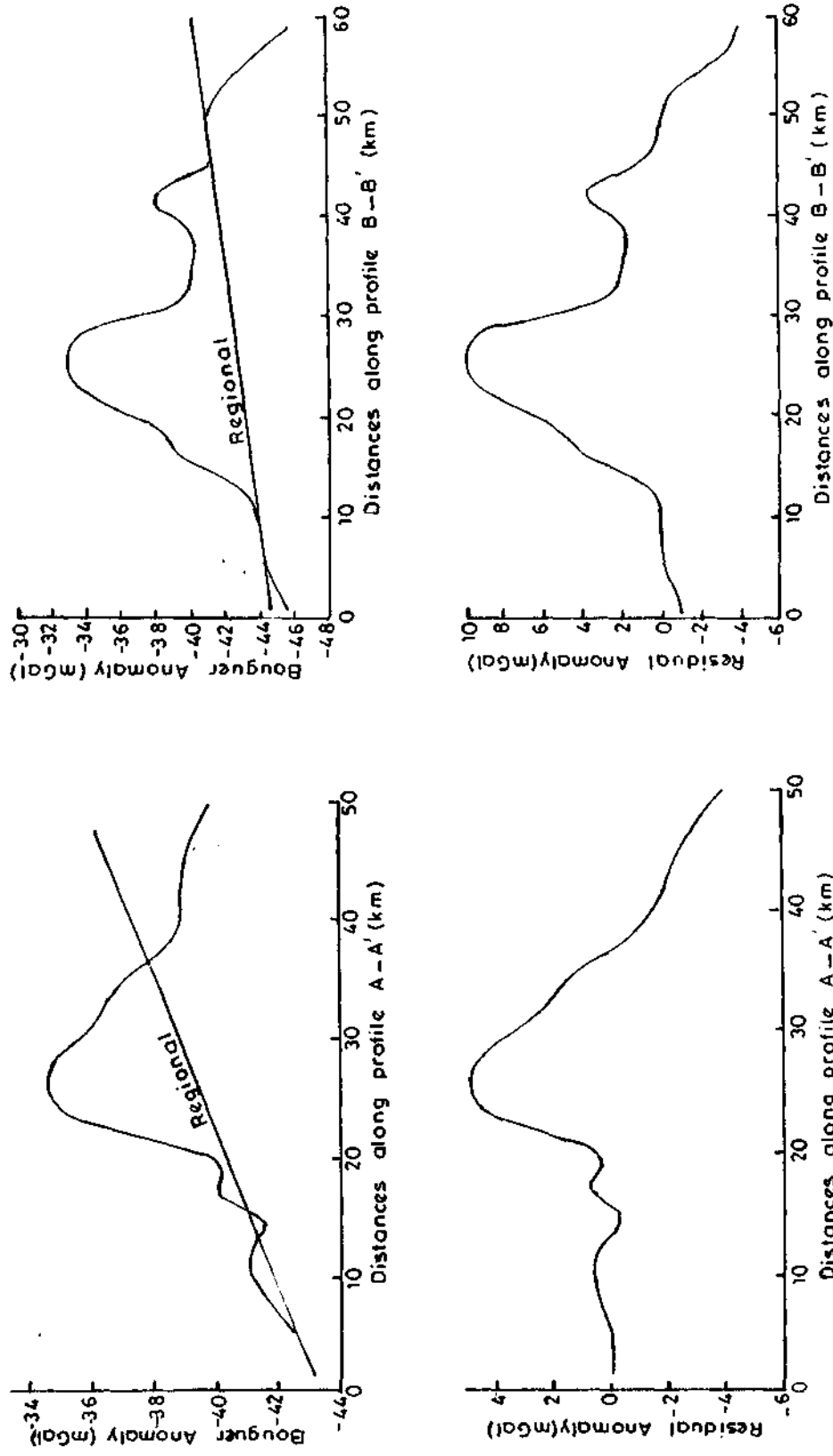


Fig. 5.13: Bouguer, Regional and Residual Anomalies along profiles A-A' and B-B'

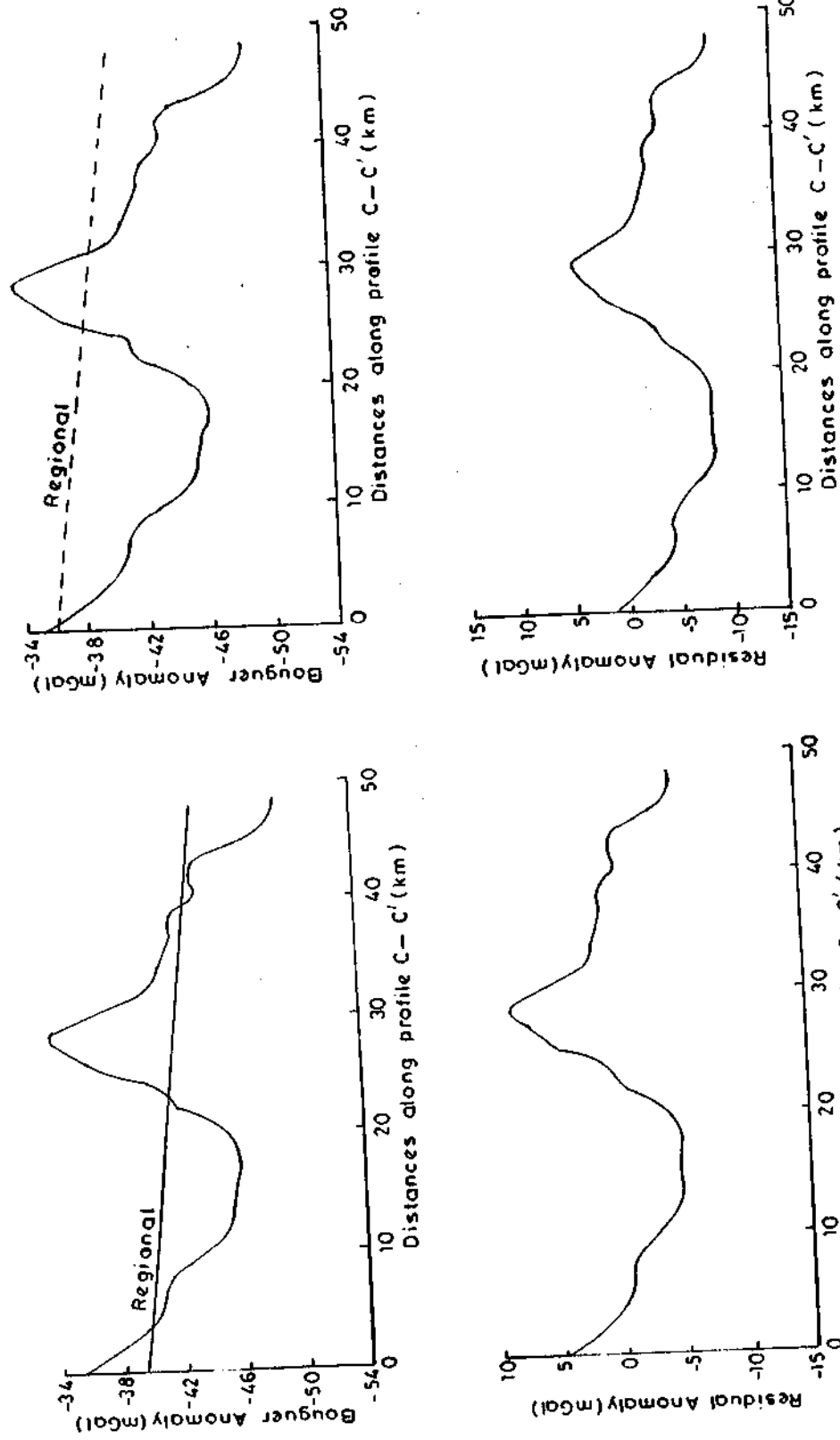


Fig.5.14 ; Bouguer Anomaly, First Regional Field and the corresponding Residual Anomalies along profile C - C'

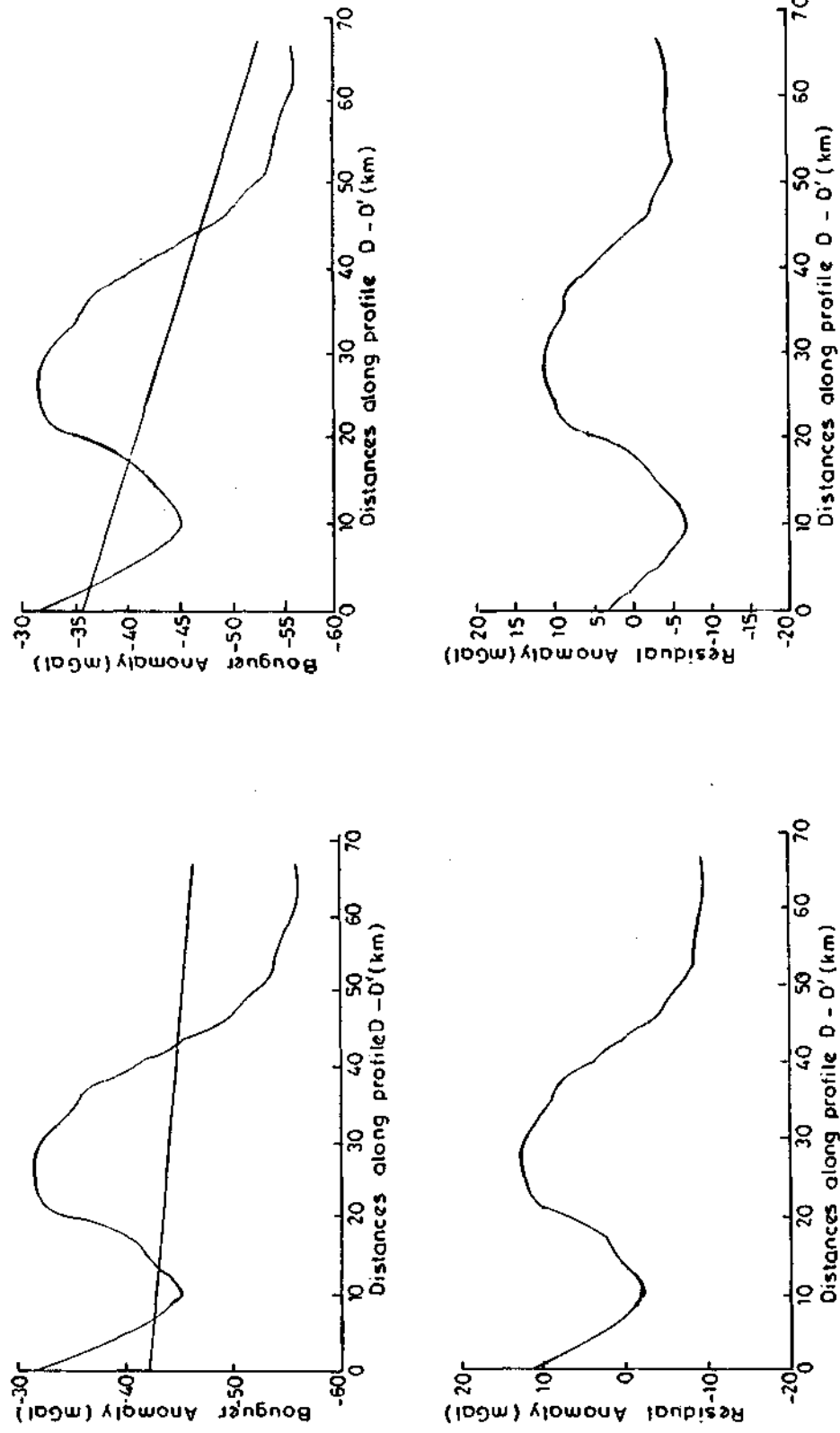


Fig.5.15 : Bouguer Anomaly, Second Regional Field and the corresponding Residual Anomalies along profile D - D'

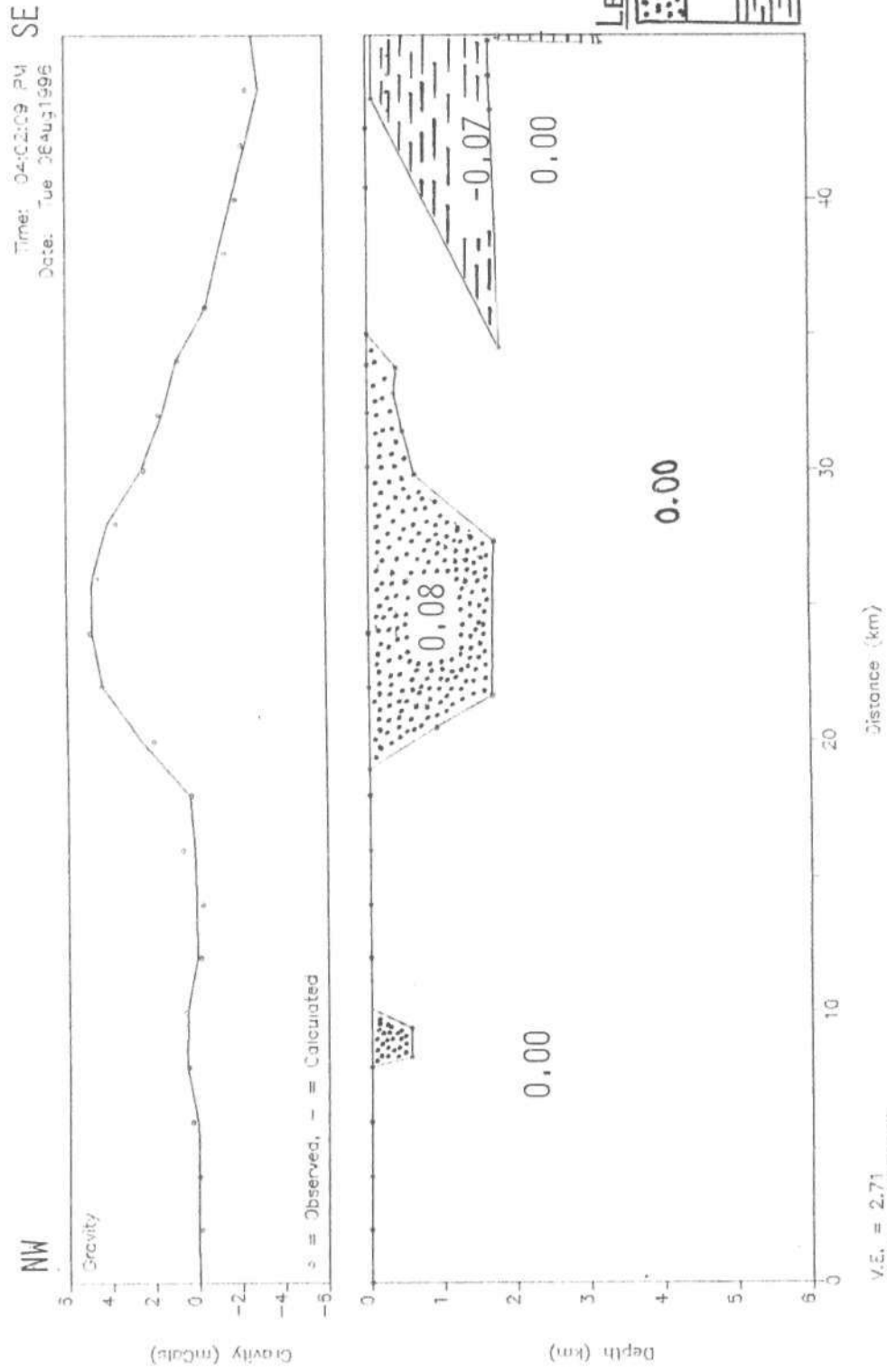


Figure 5.16: 2½-Dimensional Model of Profile A-A' assuming the intrusive granite body is of magmatic origin.

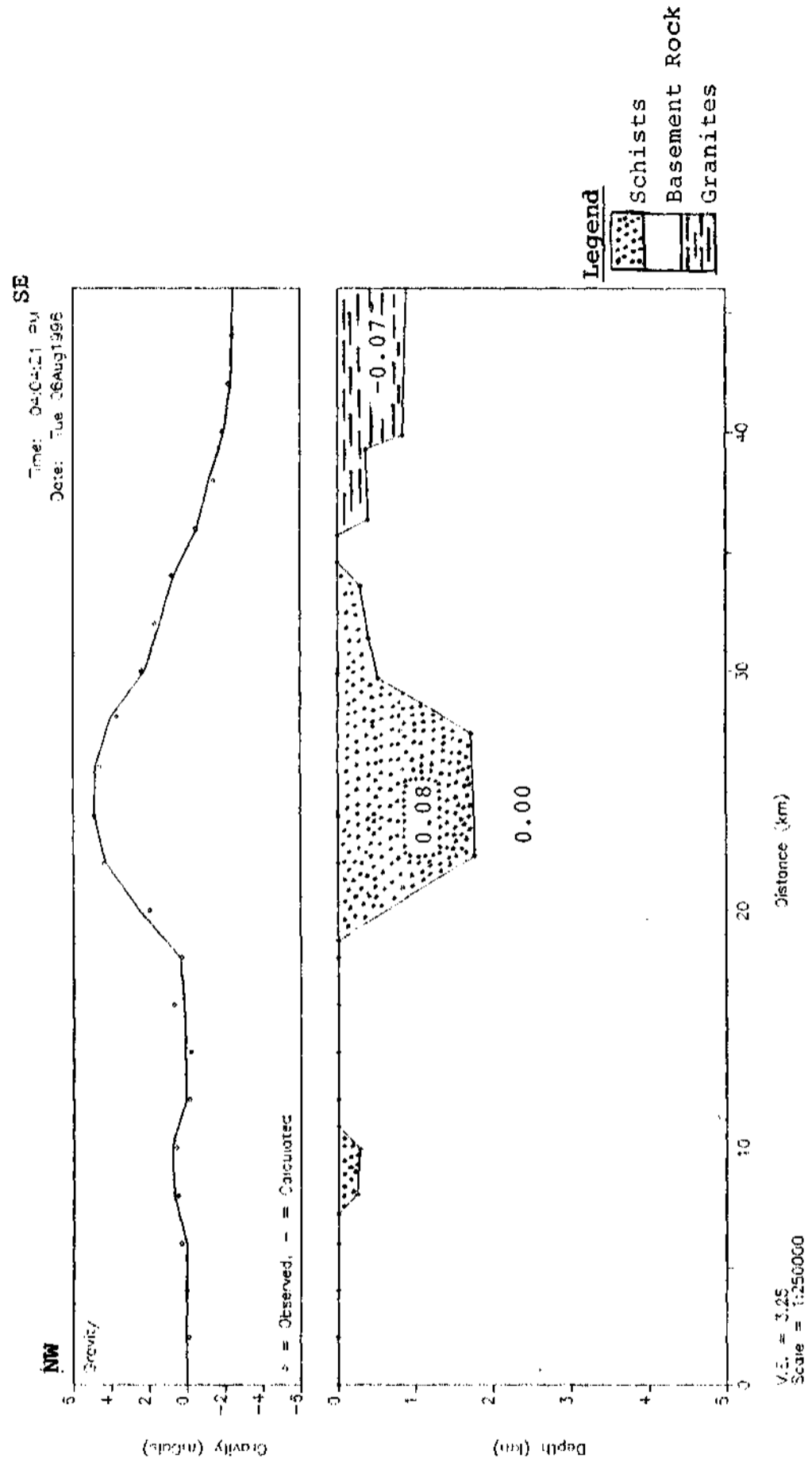


Figure 5.17: 2½-Dimensional Model of Profile A-A' assuming the intrusive granite body evolved through the process of granitization.

This model assumes a magmatic origin for the granite body at the SE corner of the profile. The model suggests that the granitic material may have risen through weak zones of the country rock to a level about 4 km below the surface before spreading out. The maximum depth extent of the granites in the area is 4 km.

The second model, Figure 5.17 shows almost the same lateral and depth extent for the schist body and has the same inward dipping walls with same dip angles of 60° and 50° on the NW and SE flanks respectively. The only difference this model has with the first is that a magmatic origin is assumed for the granite at the SE corner in the first, whereas in the second, (Figure 5.17), granitization process is assumed. The model suggests that the granite body has a maximum depth extent of less than 1 km (precisely 0.91 km). Since there is not likely to be any remnant of magma flow at this rather very shallow depth, granitization process may be responsible for the presence of granites which are observed in the field and on the geological map. In this process various country rocks due to high temperature and pressure are reworked and also due to chemical changes in them to form a rather more acidic and lighter granitic material. The granite body which has an inward dipping wall and dips at 64° also extends beyond the length of this profile.

5.3.2 Profile B-B'

To get a better picture of the relationship between the structure in the area and their depth extents, profile B-B', (Figure 5.2) was chosen. This profile passes through the centre of the anomaly 'A1' and two plausible models obtained are as shown in Figures 5.18 and 5.19.

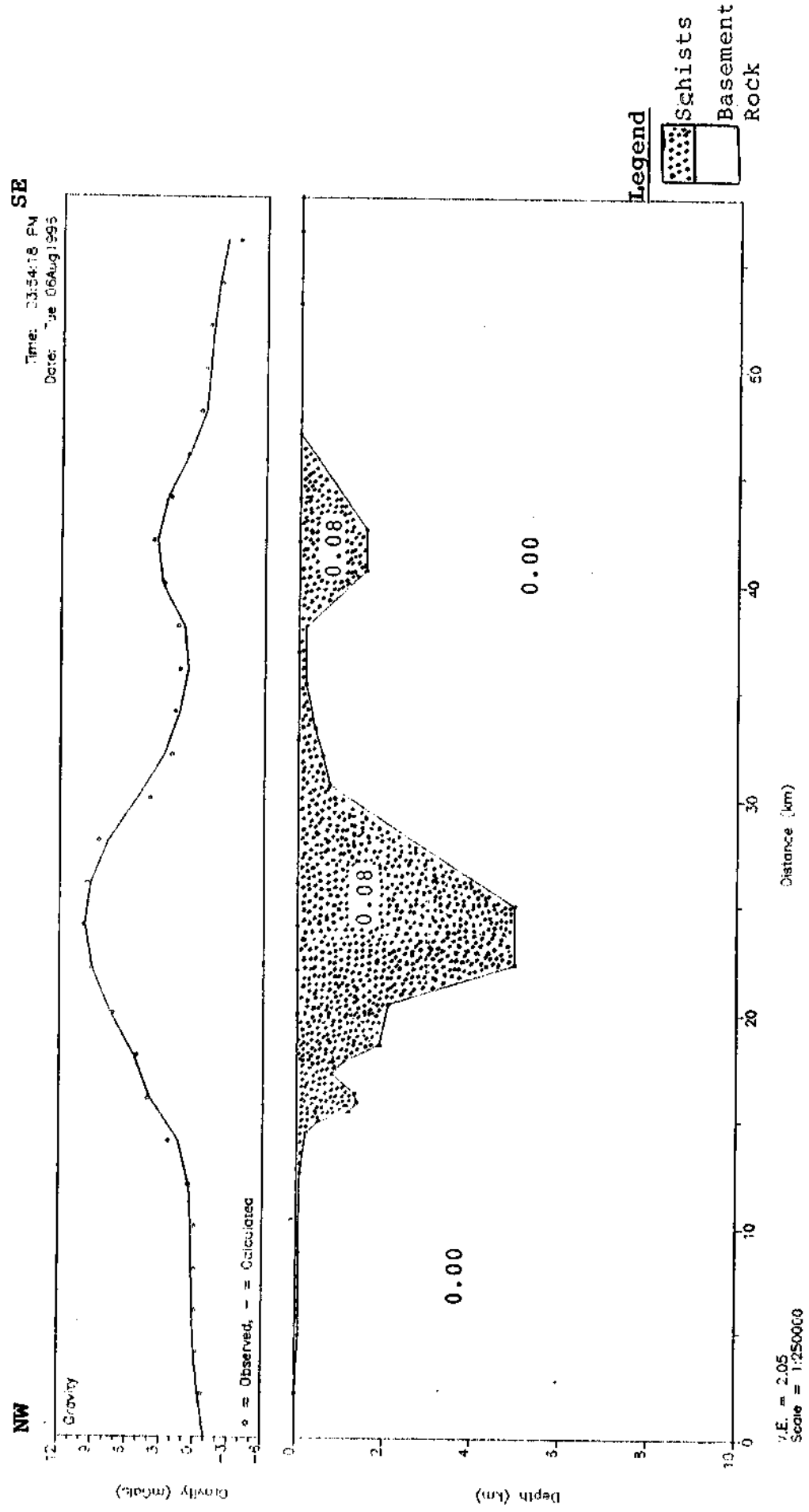


Figure 5.18: 2½-Dimensional Model of Profile B-B' without a compensating granitic body.

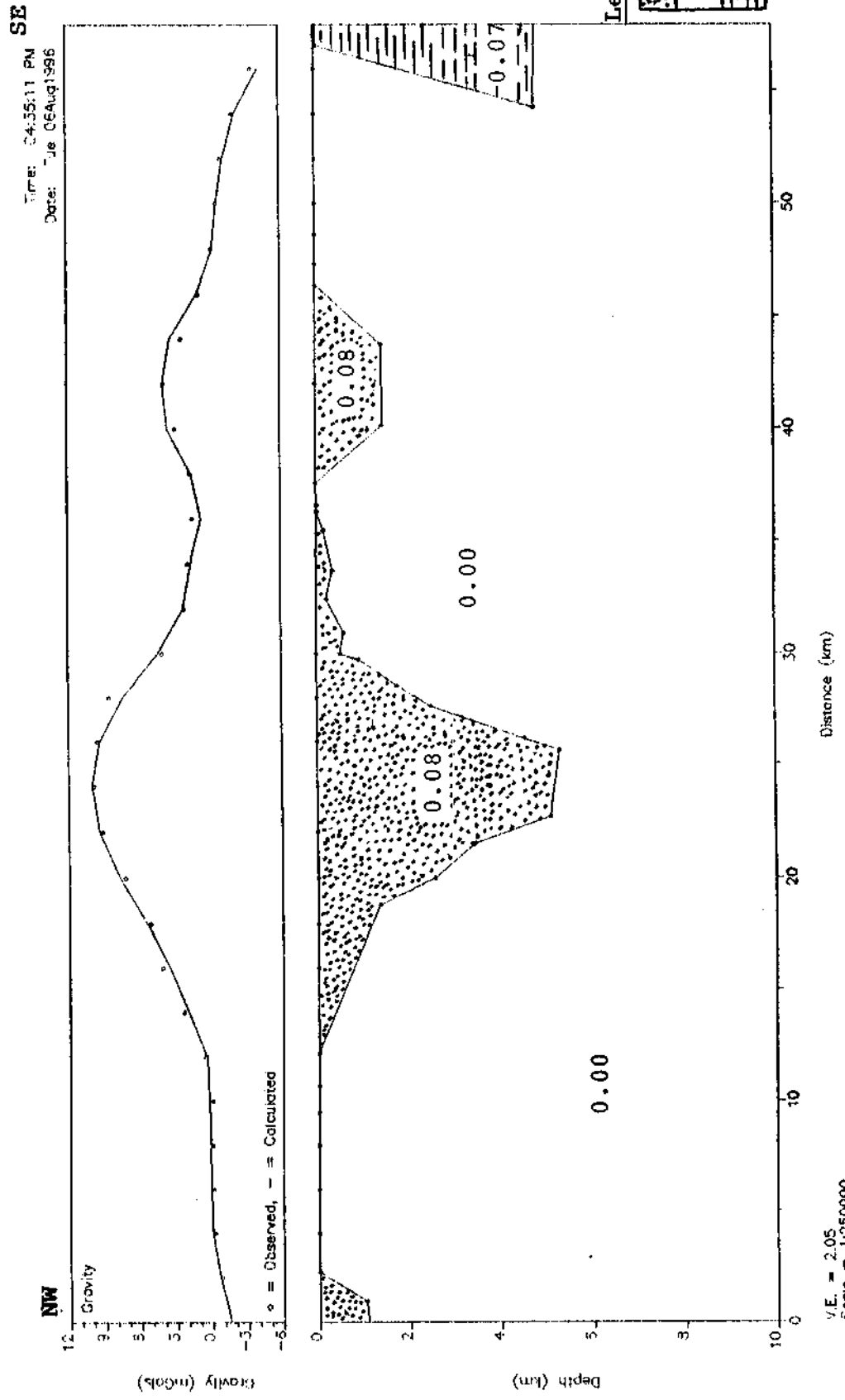


Figure 5.19: 2½-Dimensional Model of Profile B-B' with a compensating granitic body.

The model, Figure 5.18, shows that the body described by anomaly 'A1' is a single elongated schist body which may have been deposited earlier on a sedimentary sub-basin and later folded. The maximum depth of the schist is 5.06 km at about 24 km along the profile. The schist body dips at angle 67° and 55° on the NW and SE flanks respectively. There is a disappearance of the schist between 34 km to 36 km but another schist body, though of a shallower depth of 1.58 km, which dips at 50° and 35° on its NW and SE flanks respectively is also fitted to account for the second gravity high along the profile.

The second model, Figure 5.19, has two separate schist bodies along the profile. The first which falls on anomaly 'A1' has a depth extent of 5.3 km which is about the same with the first model on this profile (Figure 5.18). The first schist body dips at 30° and 60° on NW and SE flanks respectively. A second schist body of shallower depth of 1.46 km dipping at 50° and 48° on its NW and SE flanks respectively accounts for the second gravity high in the observed residual gravity field. The model is equally constrained by an outcropping granite body at about the end of the profile. It assumes the flow of magma from a depth of about 5 km (precisely 4.9 km) through weak zone to the surface where, due to erosion have been exposed at its roof zone. The granite body is also part of the larger granitic intrusion which gives rise to the gravity low as observed in the eastern part of the area (Figure 5.2).

5.3.3 Profile C-C'

This profile runs from the western to the eastern part of the map (Figure 5.2) and cut across schist and granite bodies in the southwest corner. Two possible models which fit the observed residuals reasonably well are shown in Figures 5.20 and 5.21.

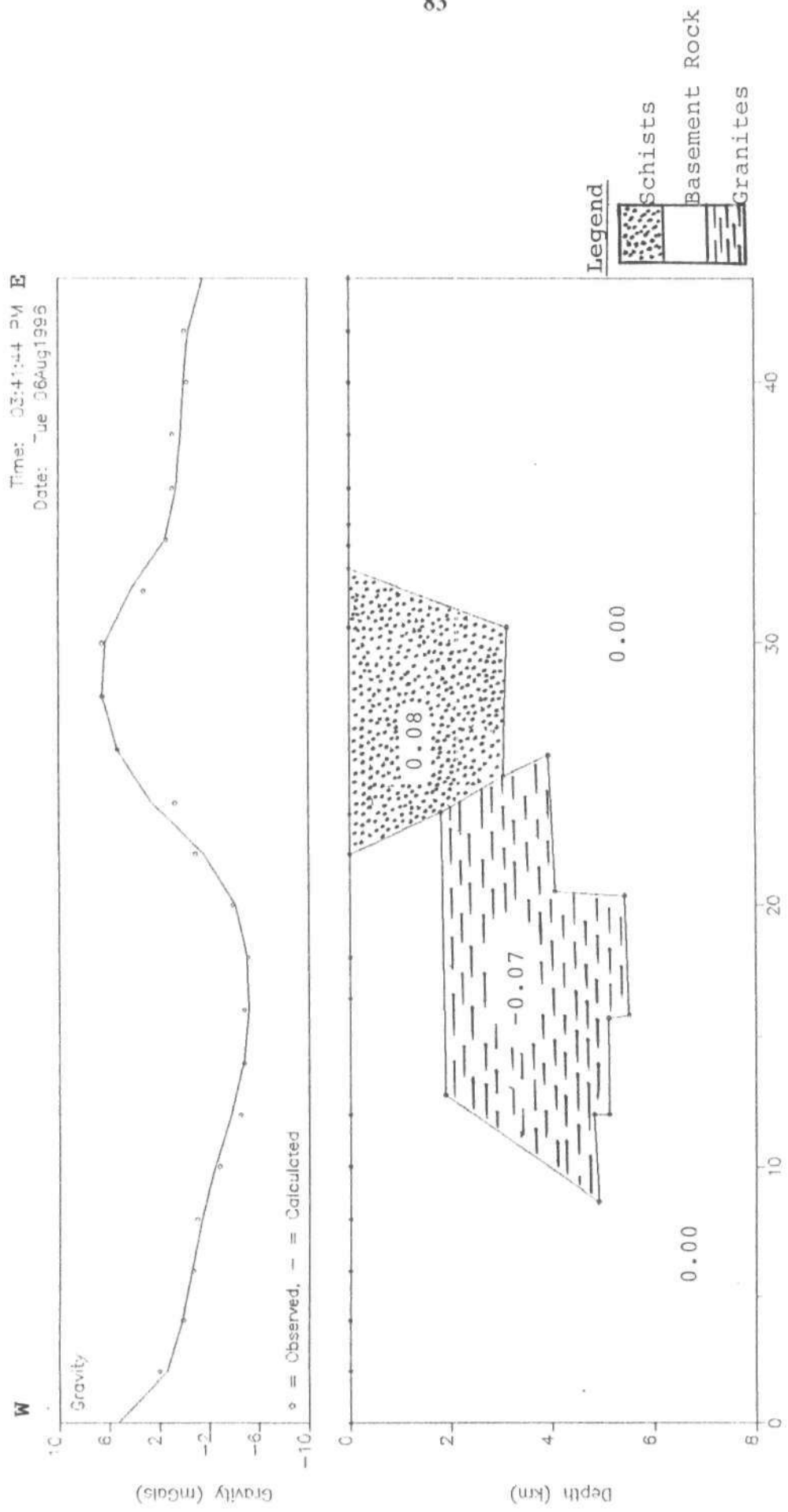


Figure 5.20: 2½-Dimensional Model of Profile C-C'.

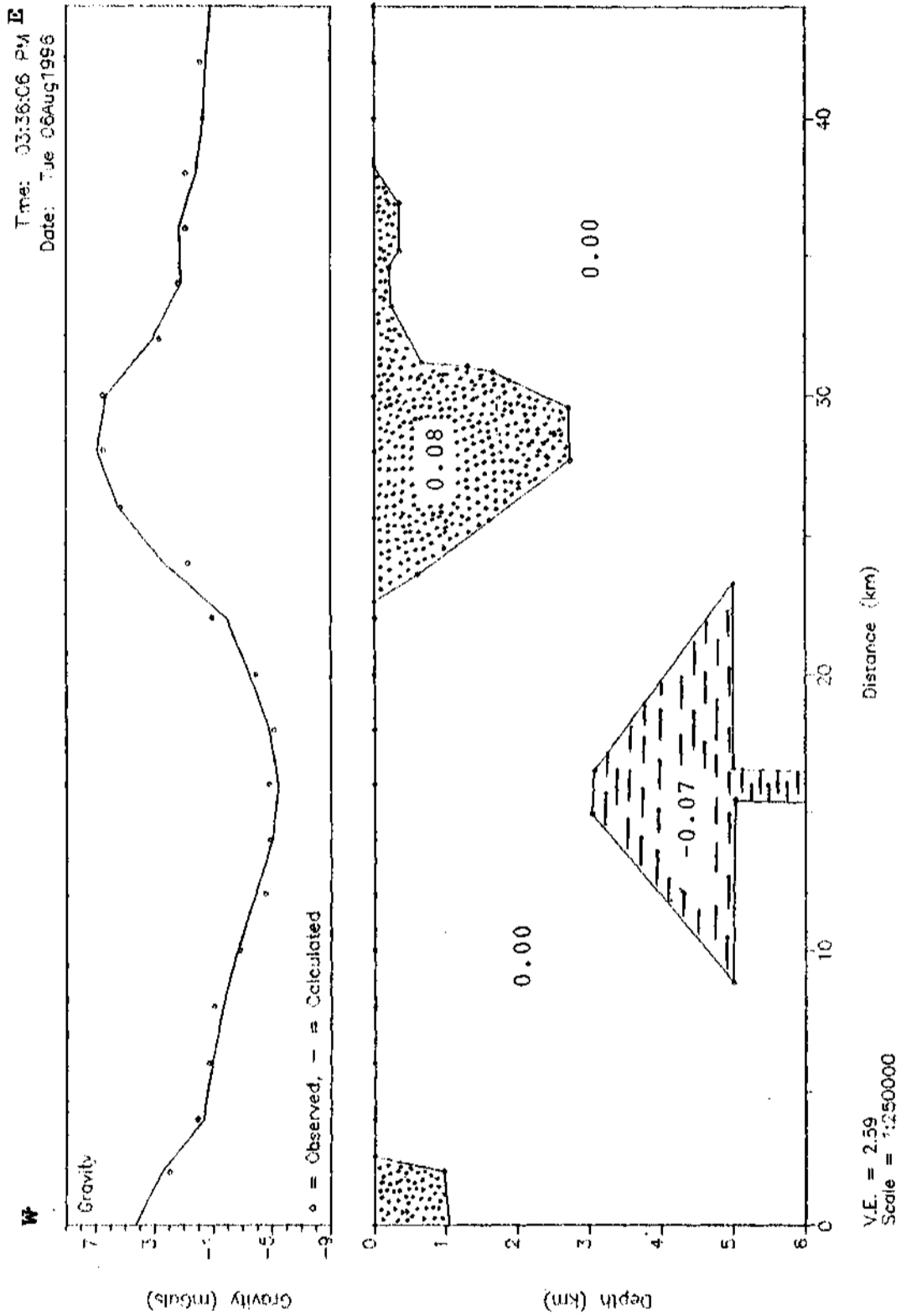


Figure 5.21: 2 1/2-Dimensional Model of Profile C-C' based on the modified regional fit.

The models are similar and both well constrained by available geological information, but differs essentially in the depth extent of the schist and the granites bodies. The residual anomaly obtained from the robust regional gave rise to the model in Figure 5.20 while the revised regional field obtained from geological constraints on the profile gave rise to the second model Figure 5.21. The first model, Figure 5.20, shows the schist body (anomaly 'A1') as a body with a depth extent of 3 km and a lateral extent of about 10 km. The schist body has inward dipping walls which dip at an angle of 63°. Adjacent to this schist body, but not exposed to the surface, is a granitic intrusion at depth. This model assumes magma intrusion from about a depth of 5 to 6 km to a depth of about 2 km. It is about 10 to 15 km in lateral extent. A gravity gradient of up to 1.38 mGal/km over its contact zone with the neighbouring granite body and the high dip angle suggests the probability of faulting.

The second model Figure 5.21 is similar to the first, but its depth extent for schist body is shallower with a maximum of 2.47 km. The body has inward dipping walls of 52° and 35° on the west and east flanks respectively. Like in the first model, Figure 5.20, adjacent and on the west of the schist body is a granitic intrusion though not exposed at its roof zone. The model assumes flow of magma from a depth through a weak zone which gave rise to a root or plug. Magma rises through this plug to a depth of about 5 km before spreading to its present width. The intrusion rises to a depth of about 3 km within the basement rock. This model gave about the same depth of about 3 km for the schist body with other profiles but it does not account for the sharp gravity gradient at the contact zone between the schist and the granite.

5.3.4 Profile D-D'

Again in order to have a better estimate of the depth extent of the structures in the area, a cross profile D-D' was chosen as shown in Figure 5.2. Two possible models believed to fit the observed residuals are shown in Figures 5.22 and 5.23. The models are based on the robust regional and revised the regional. The first model (Figure 5.22) has quartz-diorite rock body which has inward dipping walls and dips at 62° on its NNE flank. This quartz-diorite body has a depth extent of about 2 km and a lateral extent of about 6 km within the area covered by this profile. Adjacent to this body is a granite intrusion, which is assumed to have been emplaced as a result of magmatic activities in the area. The granite has a lateral and depth extent of about 10 km and 4 km respectively. Its walls dip at outwardly at 62° , a shape that is characteristic of granite intrusion through magmatic stopping (Ojo, *Pers. Comm.*). This granite body at the SSW - corner of the profile does not outcrop over the area, but its required to explain the negative anomaly observed there. The gravity gradient of about 2 mGal/km over the contact zones together with high dip angle suggests the possibility of faulting.

Adjacent to the right of this granite is the schist body, (anomaly 'A1' Figure 5.2), with a large lateral extent of about 30 km along this profile and a depth extent of 5.26 km which is similar to the depths obtained from the models along profiles B-B' and A-A'. This schist body has inward dipping walls and dips at angles 45° and 30° on its SSW and NNE flanks respectively. A large granitic body which outcrops towards the end of this profile is adjacent to this schist body. The gradient of about 2 mGal/km at the contact zone of these two rock bodies suggests the possibility of faulting. The granite body has a lateral extent of about 24 km, though only at the area covered by the

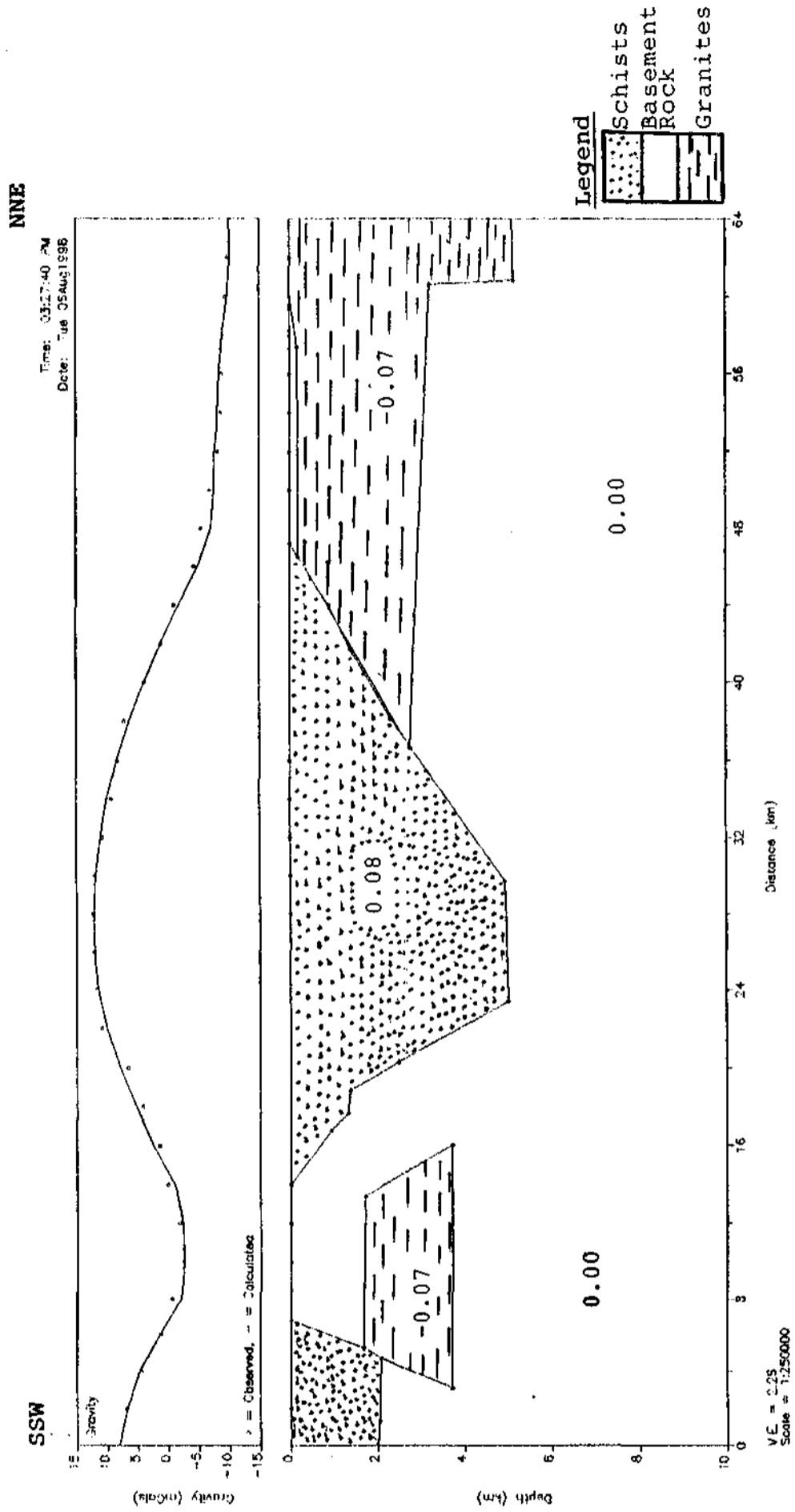


Figure 5.22: 2 1/2-Dimensional Model of Profile D-D'.

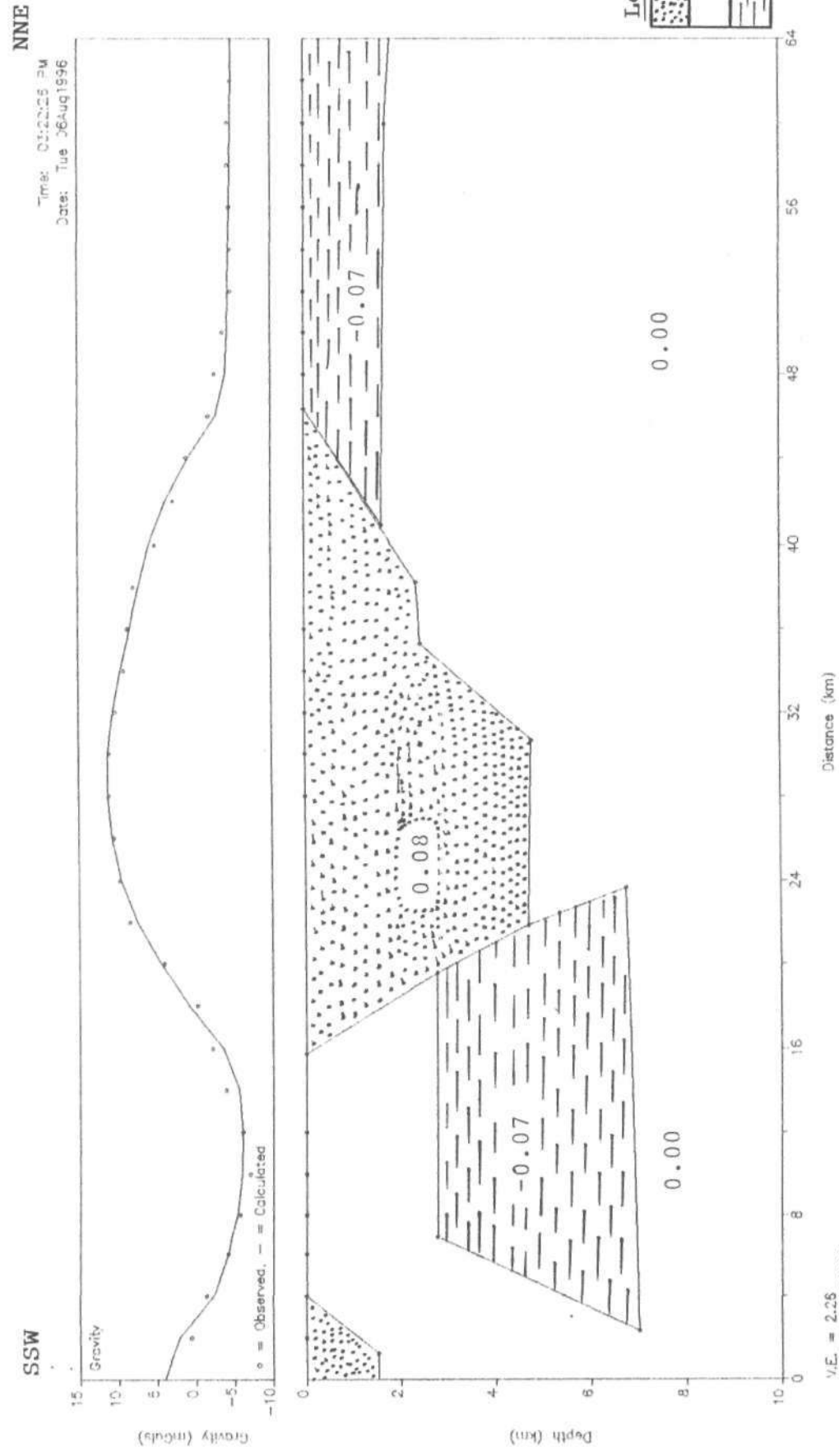


Figure 5.23: 2 1/2-Dimensional Model of Profile D-D' based on the modified regional fit.

profile, and a depth extent of about 5.15 km. The model suggests that the granitic body originates from magmatic emplacement. Its root extends to a depth of about 3.5 km. Due to erosion, the granite body is exposed at its roof zone towards the end of the profile.

The second model, Figure 5.23, is similar to the first, but differs essentially with the granitic intrusions. The depth and lateral extent of the granite body at the SSW end of the profile is larger than that of the first model, precisely 7.12 km and 18 km respectively. The body at the NE corner of the profile, the model suggests, is a part of a large granitic mass whose origin is attributable to granitization process.

CHAPTER SIX

6.0 CONCLUSION

6.1 GENERAL DISCUSSION6.1.1 The Schists

The structural relationship between the different bodies as inferred from the models show that in general, the Older Granite intrusions and Schist Formations in the area have steep contacts with each other and the host Migmatite-gneiss complex. The Schist belts of Northwestern Nigeria are considered to be a continuous sedimentary cover over the migmatite-gneiss complex (Mccurry, 1976). However, Grant, (1978) and Ajibade, (1980) have described different belts (Kushaka and Brinin-Gwari) which have contrasted lithology and concluded that the belts were probably not deposited in the same basin. Grant (1978) also suggested that the belts might be of two different ages, Kibaran (1100 m.y.a) and Pan African (600 m.y.a).

Since the idea of plate tectonics evolved, different geologists in Nigeria have interpreted the schist belts as either ensialic, which involves deposition on the continental crust (Ajibade, 1980 and Turner, 1983) or ensimatic which involves deposition on oceanic crust, proposed by Mccurry (1976). The latter considers that the schist belts were formed as a result of the opening and closing of an ocean comparable to the Red sea. However, Wright (1979) proposed a compromise between an entirely ensialic and entirely ensimatic processes for the schists. He noted that where the serpentinite bodies and calc - alkaline volcanics occur could be taken to be evidence for

an ancient subduction zone, but considers the other Nigerian schist belts to represent former ensialic basins.

The present gravity survey, however, does not show the existence of deep seated mafic materials or any anomalous gravity highs that are usually associated with plate boundaries. This is the case of the Pan African belt east of the West African Craton which is considered to have evolved by ensimatic processes (Burke and Dewey, 1972). In the eastern margin of this craton a gravity survey carried out shows the existence of high positive Bouguer anomalies with amplitudes in the range of +30mGal to +80mGal which is characteristic of essentially ensimatic processes (Caby *et al.*, 1981). Since such high positive anomalies were not observed in this survey, it is concluded that the gravity evidence confirms that the schist belts in the Kwello area evolved in an ensialic environment.

6.1.2 The Granites

Two main hypothesis with regards to the origin of granite masses in the Nigerian Basement Complex have been proposed. These are magmatic emplacement and metasomatic origin whereby sedimentary and metamorphic rocks are reworked to granites by metasomatic migration of material.

Russ (1957) through chemical analysis and examination of petrological features considered the Older Granites of the Nigerian Basement Complex to be of a single magmatic epoch. Oyawoye (1964) suggested that most of the large masses of quartz and quartzdiorites in the Basement Complex originated through potash metasomatism. However, Rahaman (1976), on account of the mode of occurrence of charnockites in

the Ihadan area, and Ajibade (1980), on the basis of field relations in the Zungeru region, suggested a magmatic origin for the Older Granite. Grant (1978), on the basis of geochronological evidence believes that the Older Granite originated through a metasomatic process. These differing opinions are probably the result of regional variations in the tectonism of the Nigerian Basement Complex which could lead to different interpretation of complex textural, mineralogical and physio-chemical field relations (Osazuwa *et al.*, 1992).

Rahaman (1988) is of the opinion that the only valid attempt to classify the Older Granite is the one that is done over short distances. The presence of both positive and negative closures in the Bouguer and the residual anomaly maps, resulting in abrupt changes in gravity gradients over the Older Granite suite does not support a metasomatic origin. The high gradients associated with the contours in some areas, especially at the contacts between anomalies 'A1' and 'A3' with surrounding rocks and the size and shape of the residual anomalies strongly suggest a magmatic origin. Mccurry (1970) suggested that the granite bodies in the Basement Complex of Northern Nigeria may be divided into two groups according to their contact relationship with the surrounding rocks. The first of these groups are the more nearly concordant batholithic sheets in the Zaria area which are exposed nearer their root zones. The granites in this group are also believed to be Syn-tectonic. The second group she suggested are the discordant granites with contact metamorphism and are believed to have a later tectonic origin. The granites in this group are today exposed at their roof zones (Mccurry, 1970) which could be the result of the outcrops observed at the Dandume and Kaya areas (Figure 5.2). According to Mccurry, (1970), discordant contacts demonstrate that most of the Older Granite rocks are intrusives and that 'static' granitization has nowhere been identified. She is

of the opinion that mobility of the Basement Complex gave rise to the movement of dense granitoid facies from lower to higher crustal levels. The geological evidence in support of the view includes the presence of contact metamorphism of the country rock (Russ, 1957; Ajibade, 1980), and the presence of rotated Xenoliths in the granites which suggests movement of the granitic material in semi-plastic condition (Webb, 1972). The contact relationship between the Older Granite and schists also points to the fact that magmatic stopping is the most likely mode of emplacement of the granites.

6.2 SUMMARY OF RESULTS AND CONCLUSION

- (i) The Kwello area is characterized by large negative Bouguer anomalies ranging from -30 mGals to -58 mGals. The area has major N - S and NW - SE trends which appear to correlate with those of the major structures in the area.
- (ii) The results of the density determination of the major rock groups in the area show that the host rocks (Migmatites and Gneisses) have an average density of $2.70 \times 10^3 \text{ kg.m}^{-3}$, the schists have an average density of $2.78 \times 10^3 \text{ kg.m}^{-3}$ while the Older Granite have a comparatively low density of $2.63 \times 10^3 \text{ kg.m}^{-3}$ which confirms the acidic nature (low density) of the Older Granite rocks generally.
- (iii) The area is also characterized by a Bouguer gravity high residual anomaly around the Kwello town and with gravity low residual anomalies at both the Northern and Eastern part of the Kwello town. The Bouguer gravity high residual anomaly is caused by outcropping schist bodies while the Bouguer gravity low residual anomalies are caused by

mapped granitic bodies. Depth estimates obtained from a 2½ - dimensional modelling was 5 km for the schists body and 6km for the granite at the Southwestern part of the area and also about 4-5 km for the granite at the Eastern flanks of the anomaly 'A1' (Figure 5.2).

- (iv) A high (Bouguer anomaly) gradient in some areas between anomalies 'A1' and 'A3' (between longitudes 7.05° and 7.10°) indicate sharp contact and/or possible fault zone. Dips estimate of the subsurface structures in this area range from 60° to 65° for the schist body, and from 48° to 52° for the granite body. Generally the schist bodies are outward dipping while the granite bodies are inward dipping. The fault zone has the same major NW - SE structural trend. The contacts are also highlighted by the zero contours of the second vertical derivative map. The Bouguer and residual maps confirm the existence of the fault in the area which was earlier indicated by Mccurry (1970).

- (v) A magmatic origin for the granites is suggested on the basis of the gravity gradients across the granite bodies. The gravity data also confirms the geological evidence that the schists in the area evolved in an ensialic environment.

6.3 RECOMMENDATION

It is recommended that more detailed geophysical work should be carried out not only in the Kwello area but over the entire schist belt of Nigeria and the Nigerian Basement Complex in general. Emphasis should be on delineation of fault zones which

are possible entrapments of the economic minerals associated with the occurrence of schists. Other geophysical methods such as V.L.F and magnetic methods will be sufficient to complement the gravity method used in this survey in order to determine the size and extent of the structural traps. It is also recommended that an intensive density study of the rocks in the area be carried out and documented for future researchers in the area since the correct density of rocks in the area is an important factor on which the success of any gravity survey lies.

REFERENCES

- Abaa, S.I. (1983) Nature and Origin of Polyphase Pegmatites in the Zaria region of Northern Nigeria Niger J. Sci. Technol.
- Adeniyi, O.O. (1987) Gravity Survey of the Older Granite Plutons in Zaria area of Kaduna State, Nigeria. M.Sc. Thesis, A.B.U. Zaria.
- Adegoke, O.S. (1979) Geology and Engineering Geology of the Federal Capital City Site. Report of the Geological Consultancy Unit, Univ. of Ife, for Federal Capital Development Authority.
- Adekoya, J.A. (1988) Precambrian Iron - Formation of North-Western Nigeria. In Precambrian Geology of Nigeria, a Publication of G.S.N.
- Ajakaiye, D.E. (1976(a)) Gravity Survey over the Nigeria Younger Granite Province. In C.A. Kolgbe (Ed) Geology of Nigeria. Elizabethan Publishing Co.
- Ajakaiye, D.E. (1976(b)) Densities of rocks in the Nigerian Younger Granite Province. Journal of Min. and Geol. (Nigeria) 11: 33 - 43.
- Ajibade, A.C. (1976) Provisional Classification and Correlation of the Schist Belts of Northwestern Nigeria. In Kogbe, C.A. (Ed), Geology of Nigeria. Elizabethan Publishing Co. pp 85-90.
- Ajibade, A.C. (1980) Geotectonic Evolution of the Zungeru Region. Unpublished Ph.D. Thesis, University of Wales, 303pp.
- Ajibade, A.C., and Wright, J.B. (1988) Structural Relationships in the Schist Belts of Northwestern Nigeria. In Precambrian Geology of Nigeria, a Publication of G.S.N.
- Ajibade, A.C., Fitches, W.R, and Wright, J.B. (1979). The Zungeru Mylonites, Nigeria: The Recognition of a Major Tectonic Unit. Rev. Dyn. Geog. Phys. v 21 pp 359 -363.
- Ananaba, S.E. (1983). Evaluation of Remote Sensing Application to Geophysical Studies in Nigeria Unpub. Ph.D Thesis, A.B.U., Zaria.
- Anhaeusser, C.R., Mason R., Viljeon, M.J. and Viljeon, R.P. (1969). A re-appraisal of some Aspects of Precambrian Shield Geology Bull. of Geol. Soc. Amer. Vol 80 pp 2175-2200.
- Bhattacharyya, B.K. (1976). Recursion Filters for Digital Processing of Potential Field Data Geophysics Vol 41 pp 712-726.

- Bott, M.H.P. (1953). Negative Gravity Anomalies over Acid Intrusions and their Relation to the Structure of the Earth's Crust, Geological Magazine, Vol 90, pp 257-267.
- Boyle, R.W. (1979). The Geochemistry of Gold and its Deposits; Geol. Surv. of Canada, Bull. No. 280.
- Burke, K.C. and Dewey, J. (1972). Orogeny In Africa. T.F.J. Dessauvage and A.J. Whiteman (Ed) African Geology Ibadan pp 583 to 608.
- Caby, R., Bertrand, J.M.L. and Block, R. (1981). Pan African Closure and Continental Collision in the Hoggar - Iforas Segment, Central Sahara. In Kroner, A. (Ed) Precambrian Plate - Tectonics Elsevier Scientific Pub. Co. pp 407-431
- Chuku, D.U. (1988). Distribution of Gold Mineralization in the Nigeria Basement Complex in Relation to Orogenic Cycle and Structural Setting. In Precambrian Geol of Nig., a Publication of G.S.N. pp 177 - 194.
- Chukwu-Ike, I.M. (1978). The Regional Tectonic Setting of the North-Western Nigeria Low-grade Metasedimentary Belt. Jour. of Min. and Geol. Vol 15 pp 19 - 22.
- Dallmeyer, R.D. and Lecorche (Ed) (1991). The West African Orogens and Circum-Atlantic Correlatives. Springer-Verlag Berlin Heidelberg.
- Dean, W.C. (1958). Frequency Analysis For Gravity And Magnetic Interpretation: Geophysics 23, pp 97 - 127.
- Dobrin M. (1976). Introduction to Geophysical Prospecting New York McGraw Hill Book Co. 630 pages
- Dobrin M. and Savit, C.H. (1988). Introduction to Geophysical Prospecting New York McGraw Hill Book Co.
- Elkin, T.A. (1951). The Second Derivative Method of Gravity Interpretation. Geophysics, Vol. 16 pp 29 - 50.
- Falconer, J.D. (1911). The Geology and Geography of Northern Nigeria. McMillian and Co. Ltd., London.
- Fuller, B.D. (1967). Two-Dimensional Frequency Analysis and Design of Grid Operators. Mining Geophysics SEG TULSA Vol II pp 658 - 708.
- Gandu, A.H., Ojo, S.B, and Ajakaiye, D.E. (1986). A Gravity Study of the Precambrian Rocks in the Malumfashi Area of Kaduna State Nigeria. Tectonophysics No.126 pp 181 - 194.

Precambrian Geology of Nigeria, a Publication of G.S.N.

- Osazuwa, I.B. (1985). The Establishment of a Primary Gravity Network for Nigeria, Unpublished Ph.D. Thesis, A.B.U., Zaria.
- Osazuwa, I.B. (1986). Unpublished Comprehensive Gravity and Elevation Reduction Program Using Cascade Model.
- Osazuwa, I.B. (1988). Cascade Model For The Removal of Drift From Gravimetric Data. *Survey Review* Vol. 29 No. 228 pp 295 - 302.
- Osazuwa, I.B. (1992). Enhancement of Data Collection Through the Characteristic Behaviour of some Geodetic Instruments. Proceedings of the 1st International Conference on Surveying and Mapping, Tehran, Iran 25th -27th May.
- Osazuwa, I.B., Adeniyi, O.O and Ojo, S.B. (1992). A Gravity Study of the Older Granite Suite in the Zaria Area of Kaduna state Nigeria. *Journal of Mining and Geology*, Vol. 28 No.2.
- Osazuwa, I.B. and Ajakaiye, D.E. (1992). Gravity meter Calibration Ranges in Nigeria. *Journal of African Earth Sciences*, Vol.14 No.4 pp 514 - 525.
- Osazuwa, I.B., Onwuasor, E.O., Azubuike, C.O. and Okafor, B.J.O. (1994). Gravity Map of Kaduna and Katsina States. Publication of the G.S.N.
- Oyawoye, M. O. (1964). The Geology of the Nigeria Basement Complex. *Journal of Nig. Min. Geol and Metall. Soc.* Vol.1 pp 87 - 482.
- Parasnis, D.S. (1962). Principles of Applied Geophysics, Chapman and Hall Ltd. London 176 p.
- Patterson, N.R. and Reeves C.V. (1985). Application of Gravity and Magnetic Surveys, the State of the - art in 1985. *Geophysics*, Vol.50. No.12 pp 2558 - 2594.
- Rahaman, M.A., Oshin, I.O., Ajayi, T.R. and Asubiojo, F.O.I. (1981). Trace Element Geochemistry and Geodetic Setting of Ile-Ife Schist Belt. in Proceedings First Symposium on the Precambrian Geology of Nigeria, Kaduna.
- Rahaman, M.A. (1988). Recent Advances in the Study of the Basement Complex of Nigeria. in Precambrian Geology of Nigeria, a Publication of G.S.N.
- Rahaman, M.A. (1976). Review of the Basement Geology of Southwestern Nigeria. In C.A. Kogbe (Ed) Geology of Nigeria. Elizabethan Publishing Co. pp 41 - 57.
- Rasmussen, R. and Pederson, L.B. (1979). End Correction in Potential Field Modelling. *Geophysical Prospecting*. No. 27 pp.749 - 760.

Wright, J.B. and McCurry, P. (1970). A Reappraisal of some Aspects of Precambrian Shield Geology. Discussion Geol. Soc. Amer. Bull. Vol.81 pp 3491 - 3492.

Wright, J.B. (1979). The Evolution of Northwestern Nigeria A Personal View. A paper presented at the 10th Colloquim on African Geology, Montpellier.